

SECTION 5

ELECTROSTATIC PRECIPITATION

5.1 INTRODUCTION

The electrostatic precipitator (ESP) uses electrical forces to capture either liquid or solid particles from a gas stream. The precipitator is classified as a high-efficiency collector, comparable to the fabric baghouse or gas-atomized (Venturi) scrubber. As such, collection efficiencies higher than 99.5% are possible for most applications.

A prime characteristic separating the ESP from other high efficiency collection methods is that the ESP concentrates its primary energy forces on the particle, rather than on the carrier gas stream. However, the gas stream or process characteristics will generally determine whether the particle will be easily collected or prove difficult to contain by electrical forces.

Even if the ESP is designed for high efficiency based on the gas stream and process characteristics, rapping losses remain the major barrier to achieving the design efficiency (Kubo et al., 1980). Wet ESP's are sometimes used to reduce the rapping losses, but this results in the same wet disposal problem associated with scrubbers.

The three basic steps which take place in an ESP are:

1. Particles are given an electrostatic charge.
2. Particles are removed from the gas under the influence of a strong electrical field and are deposited on a collecting electrode surface.
3. Particles are removed from the electrode surface and deposited in a hopper.

In the past, many industrial precipitators were designed such that the charging and collecting of dust particles takes place in a single stage. This usually involves applying the electrical field between an electrode and a cylindrical pipe or flat plate. The electrode is of such a geometry as to allow the formation of a corona discharge which is responsible for charging the particles.

The use of two-stage ESP's for particle control has gained wide popularity (Surati et al., 1980). Unlike the single-stage or Cottrell type ESP, the two-stage ESP has separate particle charging and collecting sections. The charging process requires a nonuniform field, with saturation charge levels occurring in 0.01 seconds or less. The precipitation of the charged particles takes 1 to 10 seconds and a uniform high voltage field is required for the most efficient separation of the particles from the air stream. Consequently, in single-stage ESP's the corona power is wasted over the major portion of the ionizing electrode.

Electrostatic precipitators are capable of achieving high collection efficiency (greater than 99%) with relatively low pressure drop (usually less than 1.3 cm W.C.). There is no theoretical limit to the particle size which can be collected, although the efficiency generally reaches a minimum between particle diameters of 0.1 to 1.0 μm . This is illustrated in Figure 5.1-1 which presents fractional efficiency for an ESP installed on a pulverized coal-fired boiler.

5.2 GENERAL DESIGN FEATURES

Figure 5.2-1 shows a schematic diagram of a single-stage, wire-plate ESP. Although the details of the construction will vary from one manufacturer to another, the basic features are the same.

Since uniform, low turbulence gas flow is desirable in the collection regions of an ESP, several devices may be employed to achieve good gas flow quality before the gas is treated. Turning or guide vanes are used in the duct prior to the precipitator in order to preserve gas-flow patterns following a sharp turn or sudden transition. This prevents the introduction of undue turbulence into the gas flow. Plenum chambers and/or diffusion screens (plates) are used to achieve reduced turbulence and improved uniformity of the gas flow in expansion turns or transitions prior to the gas treatment regions of the ESP.

The gas entering the treatment regions of the ESP flows through several passage ways (gas passages) formed by plates (collection electrodes) which are parallel to one another as shown in Figure 5.2-2. A series of discharge electrodes is located midway between the plates in each gas passage. High voltage electrical power supplies provide the voltage and current which are needed to separate the particles from the gas stream. The discharge electrodes are held at a high negative potential with the collection electrodes grounded.

An ESP may be both physically and electrically sectionalized. Figure 5.2-3 shows two possible precipitator layouts with the terminology concerning sectionalization (Smith et al., 1977). A chamber is a gas-tight longitudinal subdivision of an ESP. An ESP without any internal dividing wall is a single chamber precipitator. An ESP with one partition is a two-chamber ESP, etc. An electrical field is a physical portion of an ESP that is energized by a single power supply. A bus section is the smallest portion of an ESP which can be deenergized independently. An electrical field may contain two or more bus sections. Electrical fields in the direction of gas flow may be physically separated in order to provide internal access to the ESP.

The material which is collected on the collection and discharge electrodes is removed by mechanical jarring (or rapping). Devices called rappers are used to provide the force necessary to dislodge the collected material from the electrode surfaces. Rappers may provide the rapping force through impact or vibration

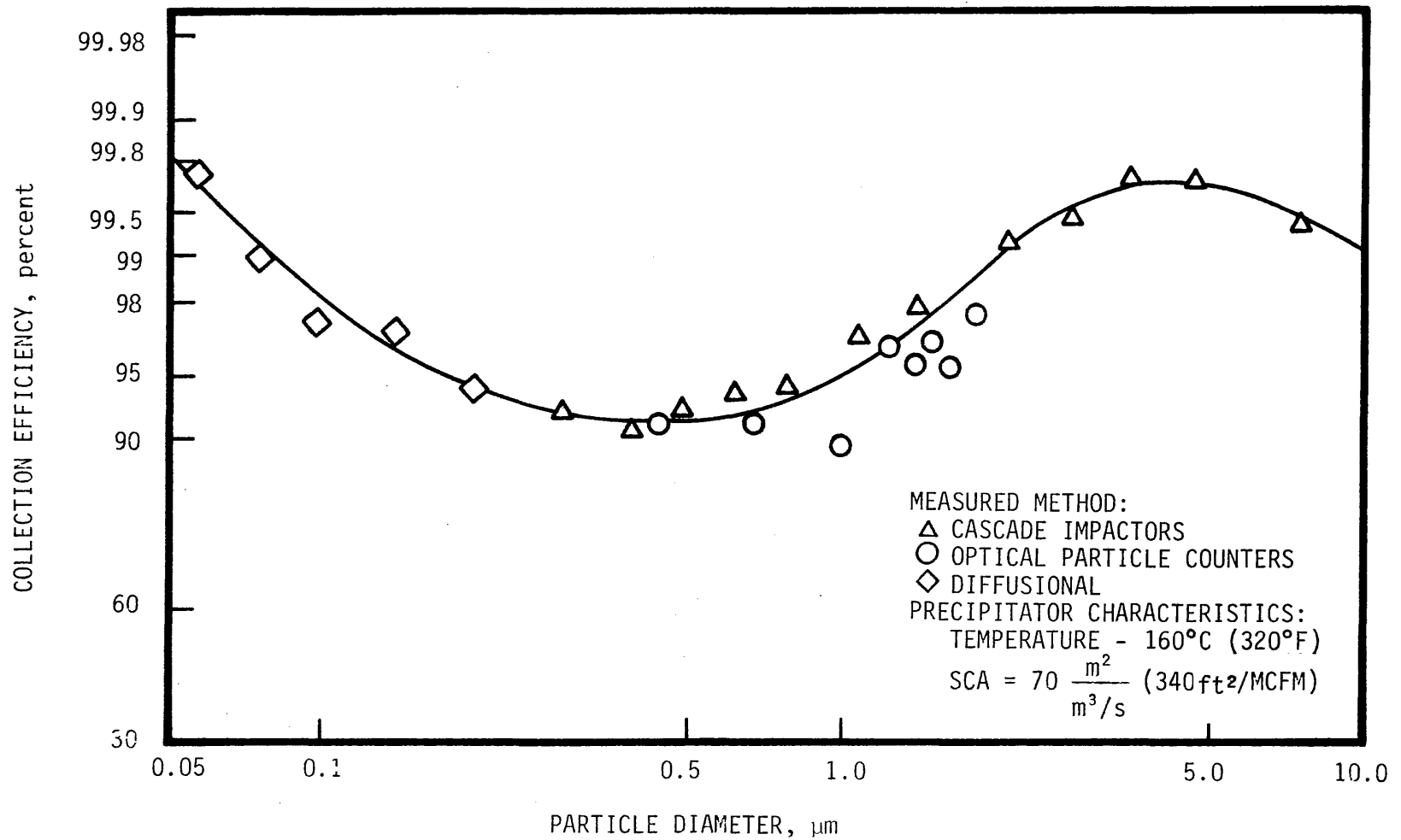


Figure 5.1-1. Fractional efficiencies for a cold-side electrostatic precipitator with the operating parameters as indicated, installed on a pulverized coal boiler.

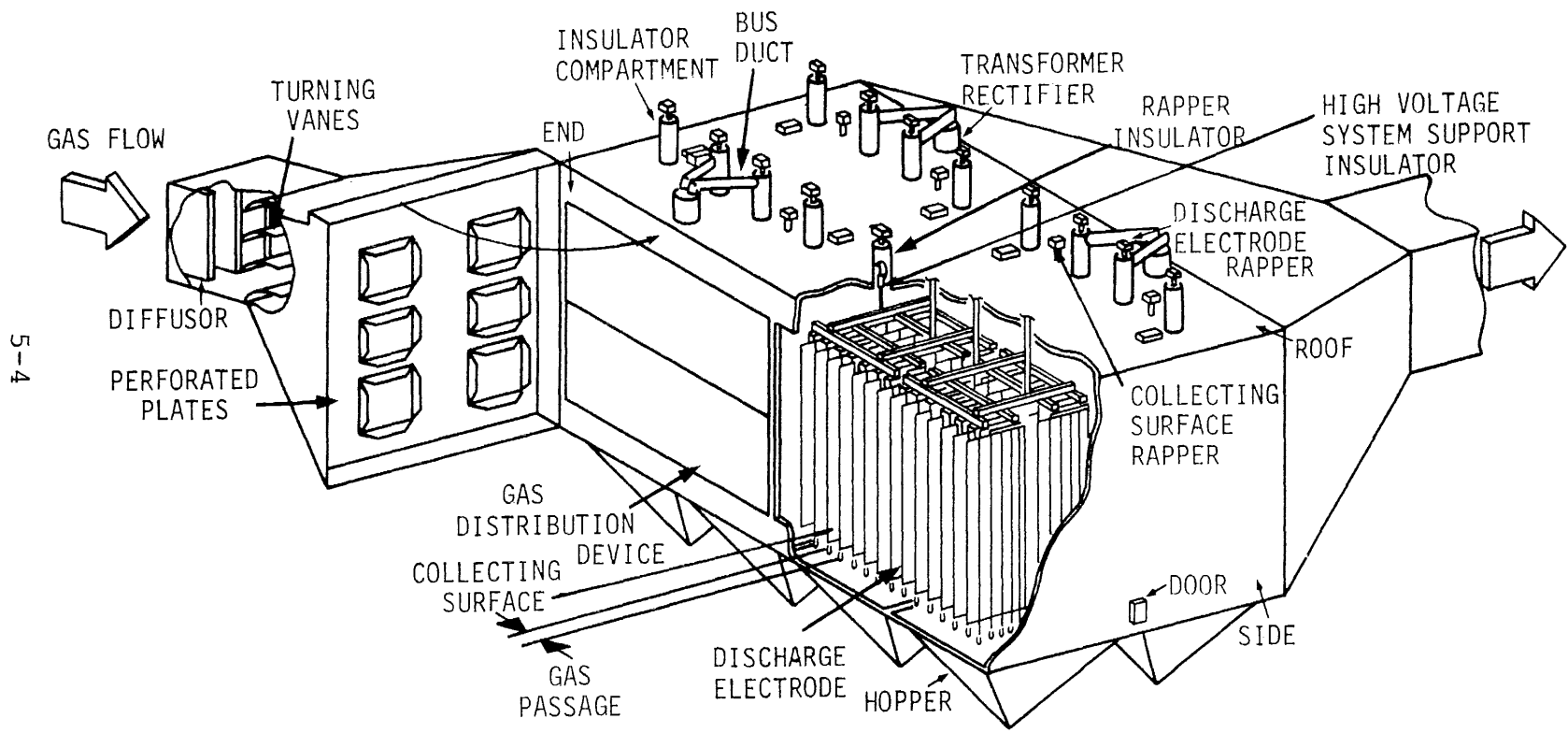


Figure 5.2-1. General precipitator layout and nomenclature.

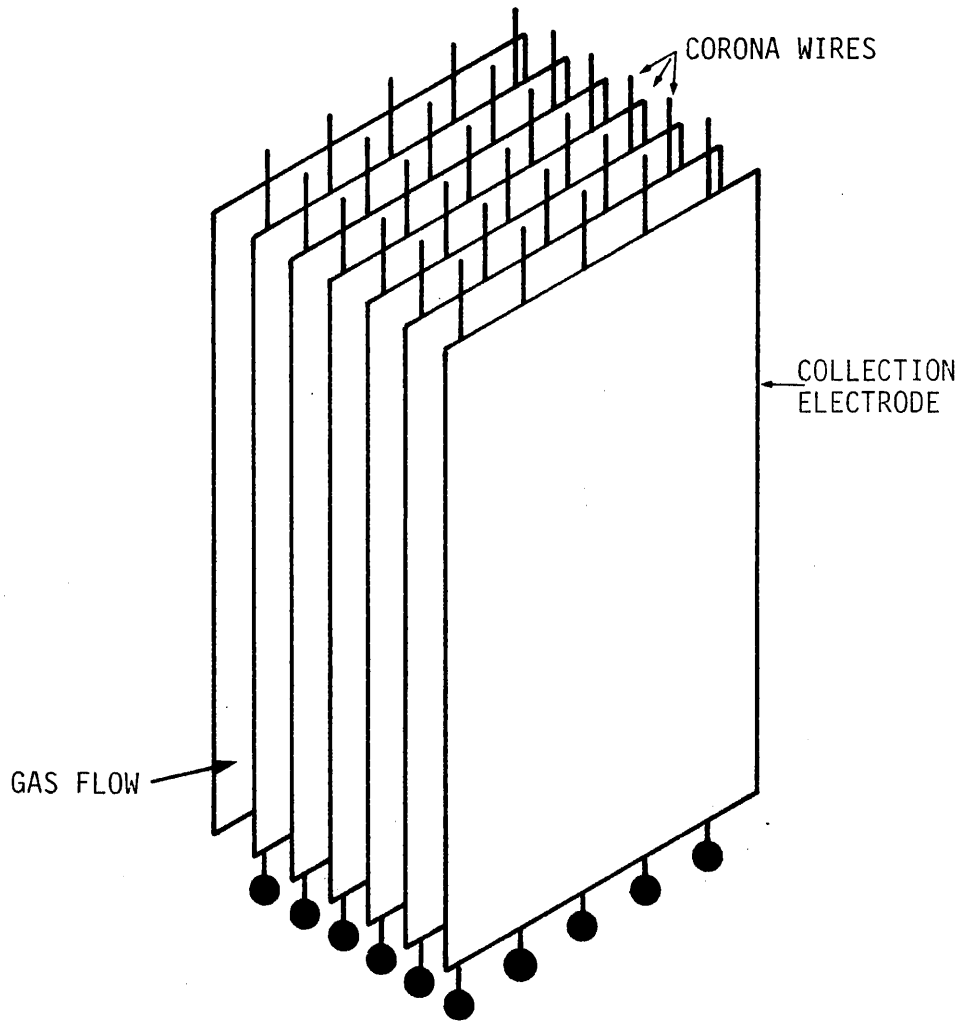


Figure 5.2-2. Parallel plate precipitator.

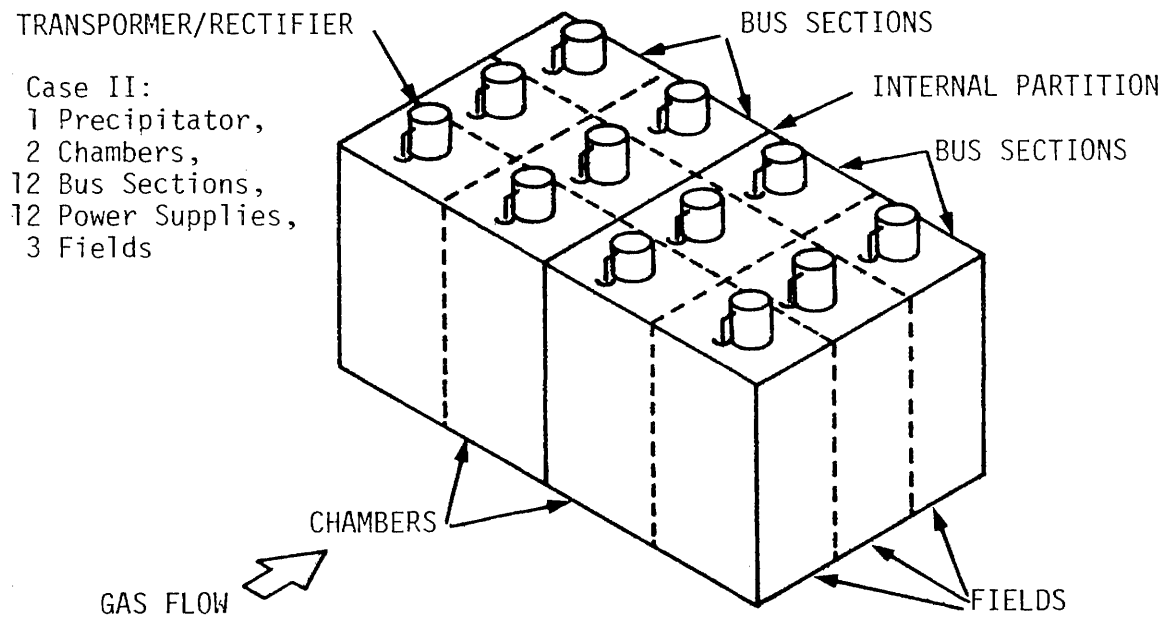
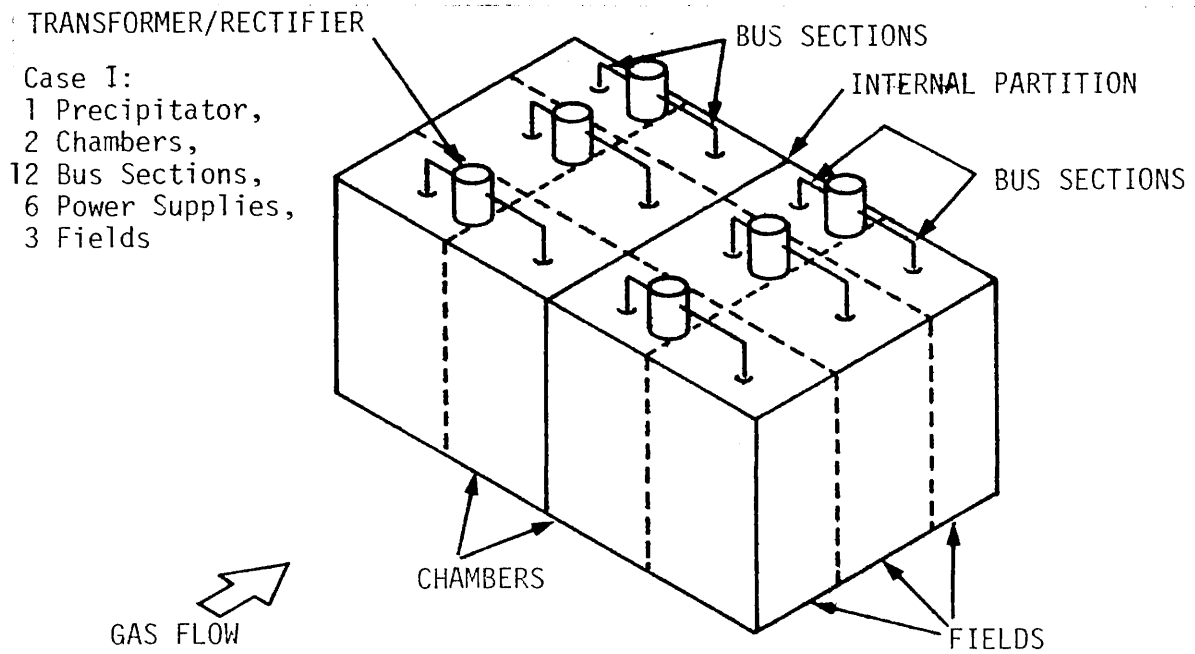


Figure 5.2-3. Typical precipitator electrical arrangements and terminology.

of the electrodes. The material which is dislodged during rapping falls under the influence of gravity into hoppers which are located below the electrified regions. Material collected in the hoppers is transported away from the precipitator in some type of disposal process.

Portions of the gas flowing through an ESP may pass through regions below and above the collection electrodes where treatment will not occur. To minimize this gas sneakage, baffles are located below the collection electrodes to redirect the gas back into the treatment region and to prevent the disturbance of the material collected in the hoppers.

In the two-stage design the ESP consists of a short ionizing section followed by a comparatively longer collecting section as shown in Figure 5.2-4. The ionizing section is typically of the wire and plate design in parallel plate ESP's. In the collection section every other plate is held at ground potential while the remaining plates (electrodes) are held at high potential.

Tubular single-stage ESP's have a large grounded cylinder known as the collecting electrode and, coaxial with it, a high potential wire called the discharge electrode as shown in Figure 5.2-5. In the two-stage design the discharge electrode is in the form of a rod or tube with a sharp needle at the end and is centered in the tube. Various tube geometries have been utilized over the years, the most common being the round and hexagonal. The hexagonal shape is more space efficient than the round shape. The square configuration shown in Figure 5.2-6 is a slight variation of the hexagonal shape and is chosen because of manufacturing ease. The corona is generated on the needle when high voltage is applied to the discharge electrode. The whole length of the rod then acts as a nondischarging electrode still providing the electric field. This arrangement provides a nonuniform electric field in the ionizing section and a uniform electric field in the collecting section.

5.3 ESP FUNDAMENTALS

The electrostatic precipitation process involves several complicated and interrelated physical mechanisms: the creation of a nonuniform electric field and ionic current in a corona discharge; the ionic and electronic charging of particles; and the turbulent transport of charged particles to a collection surface. In many practical applications, the removal of the collected particulate layer from the collection surface presents a serious problem since the removal procedures introduce collected material back into the gas stream and cause a reduction in collection efficiency (McDonald et al., 1980.).

5.3.1 Creation of an Electric Field and Corona Current

The first step in the precipitation process is the creation of an electric field and corona current. This is accomplished by

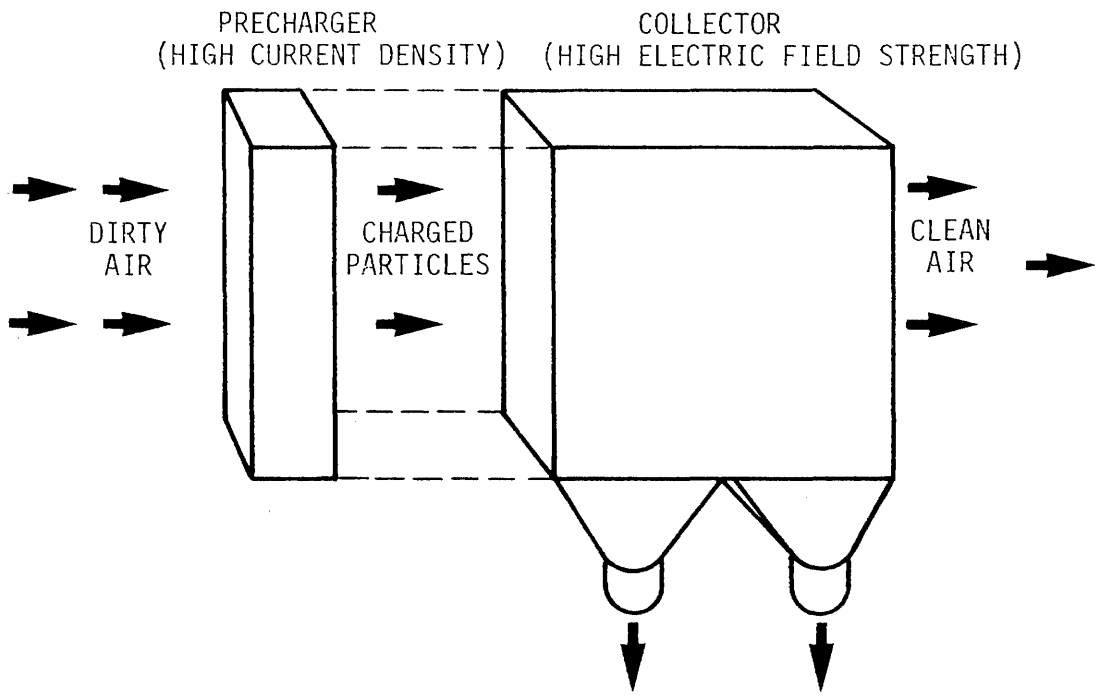


Figure 5.2-4. Two-stage electrostatic precipitator concept.

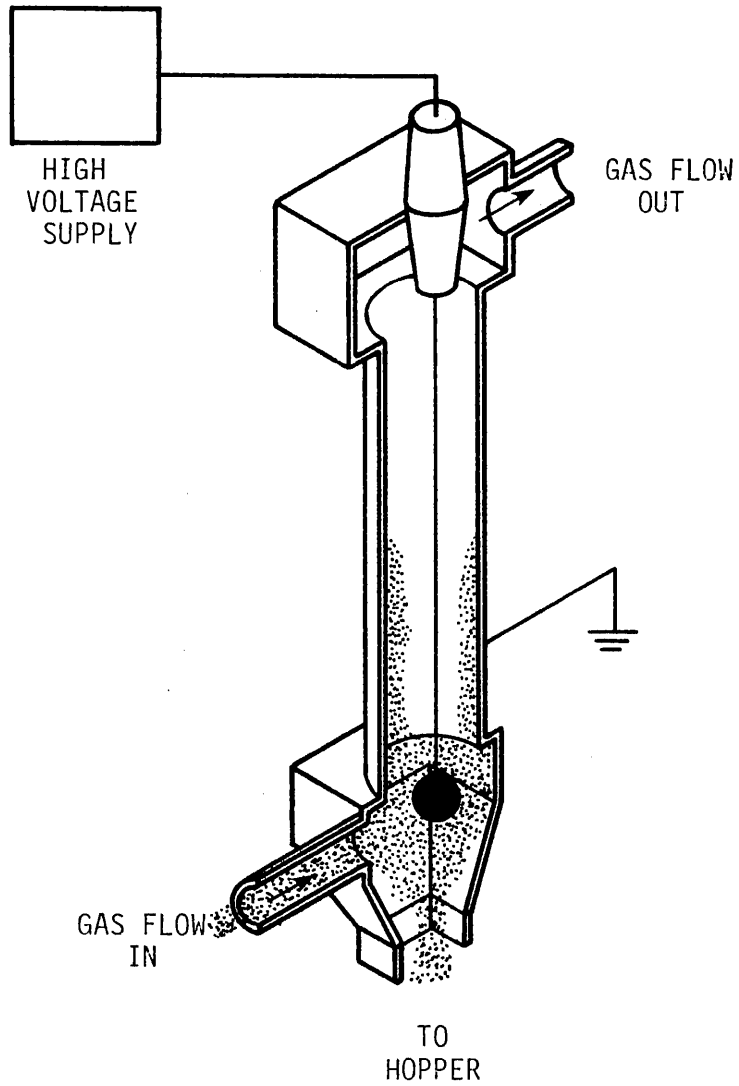
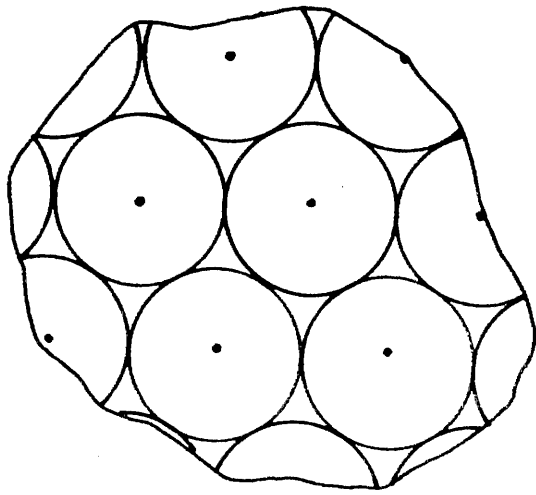
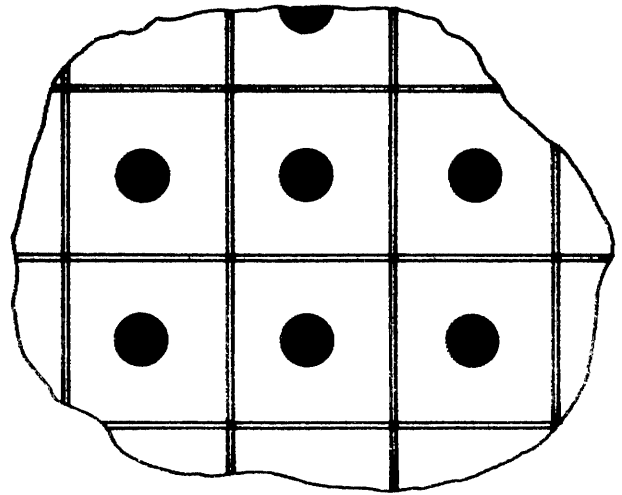


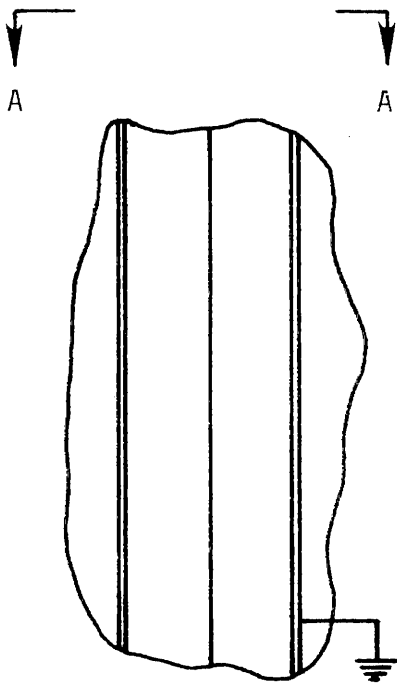
Figure 5.2-5. Tubular precipitator.



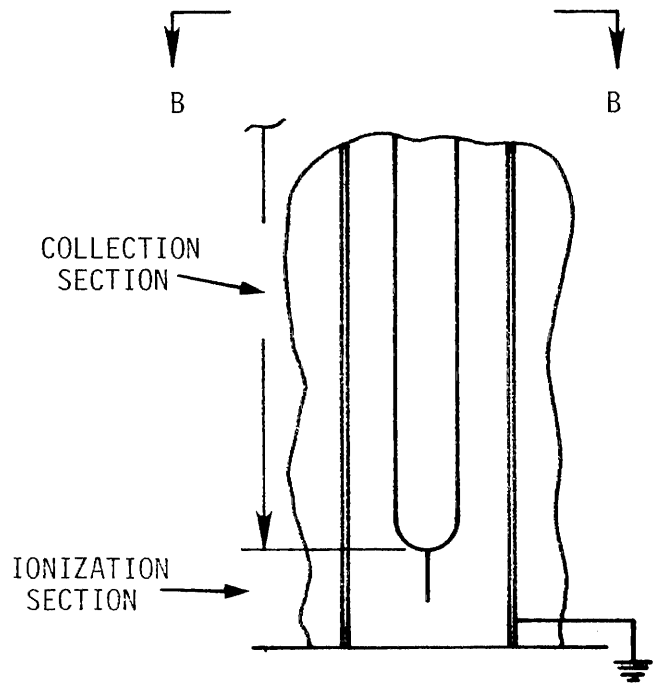
'A-A'



'B-B'



SINGLE-STAGE



TWO-STAGE

Figure 5.2-6. Two-stage tubular ESP.

applying a large potential difference between a small-radius electrode and a much larger radius electrode, where the two electrodes are separated by a region of space containing an insulating gas. For industrial applications, the field is created by applying a large negative potential at the wire electrode and grounding the plates or tubes.

At any applied voltage, an electric field exists in the interelectrode space. For applied voltages less than a value referred to as the "corona starting voltage", a purely electrostatic field is present. At an applied voltage slightly above the corona starting voltage, the gas near the wire electrode breaks down. This incomplete breakdown, called corona, appears in air as a highly active region of glow, extending into the gas a short distance beyond the wire electrode.

The initiation of corona discharge requires the availability of free electrons in the gas region of the intense electric field surrounding the wire electrode. In the case of a negative discharge wire, these free electrons gain energy from the field to produce positive ions and other electrons by collision. The new electrons are in turn accelerated and produce further ionization, thus giving rise to the cumulative process termed an electron avalanche.

The positive ions formed in this process are accelerated toward the wire. By bombarding the negative wire and giving up relatively high energy in the process, the positive ions cause the ejection from the wire surface of secondary electrons necessary for maintaining the discharge. In addition, high frequency radiation originating in the excited gas molecules likewise contributing to the supply of secondary electrons. Electrons of whatever provenance are attracted toward the positive electrode and, as they move into the weaker field away from the wire, tend to form negative ions by attachment to neutral oxygen molecules. These ions, which form a dense unipolar cloud filling most of the interelectrode volume, constitute the only current in the entire space outside the region of corona glow. The effect of this space charge is to retard the further emission of negative charge from the corona and in so doing, limit the ionizing field near the wire and stabilize the discharge. However, as the voltage is progressively increased, complete breakdown of the gas dielectric, that is sparkover, eventually occurs.

Figure 5.3.1-1 is a schematic diagram showing the region near the small-radius electrode where the current-carrying negative ions are formed (McDonald and Sparks, 1977). As those negative ions migrate to the large-radius electrode, they constitute a steady-state charge distribution in the interelectrode space which is referred to as an "ionic space charge". This "ionic space charge" established an electric field which adds to the electrostatic field to give the total electric field. As the applied voltage is increased, more ionizing sequences result and the "ionic space charge" increases. This leads to a higher average electric field and current density in the interelectrode

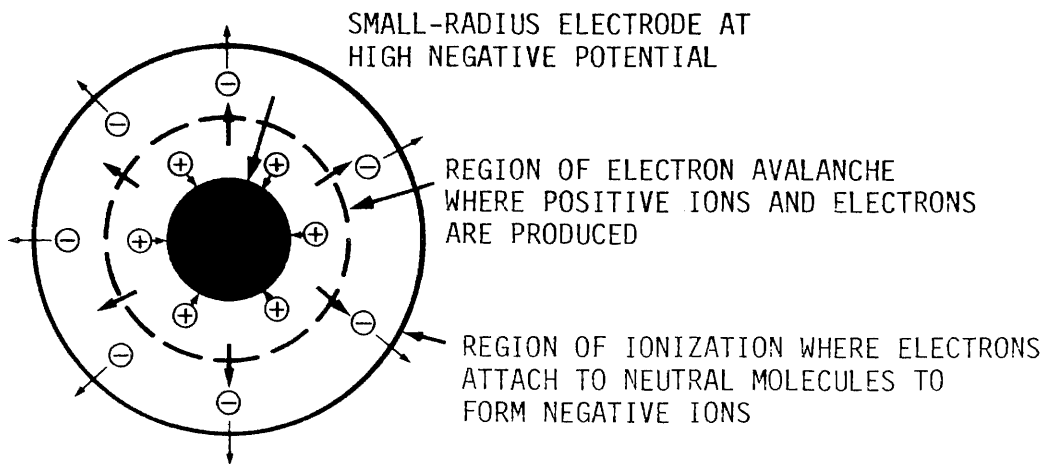


Figure 5.3.1-1. Region near small-radius electrode (McDonald and Sparks, 1977).

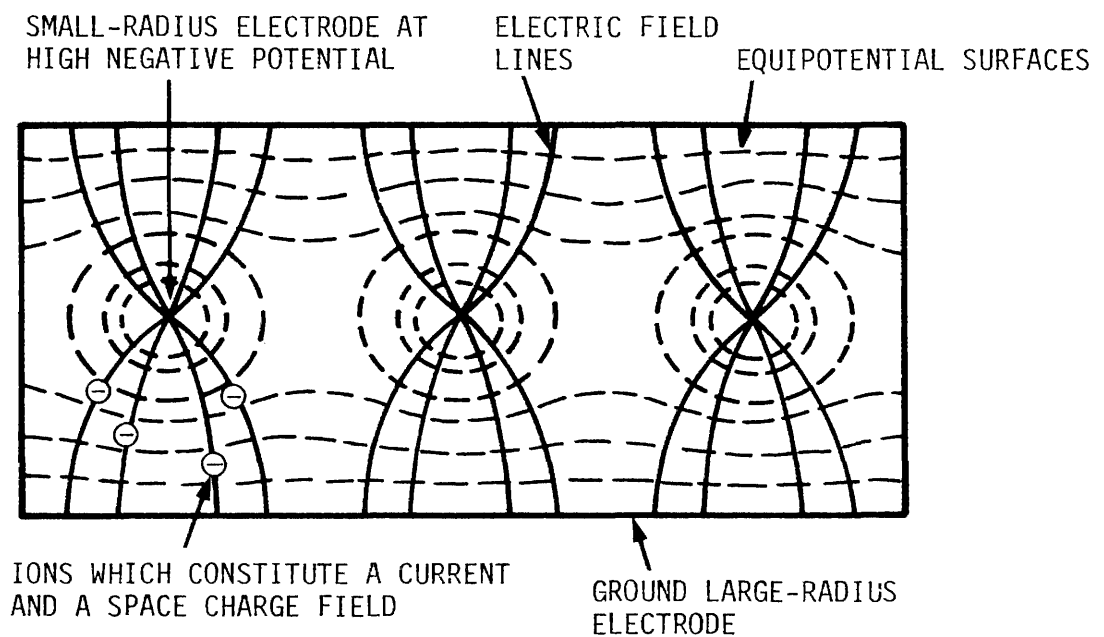


Figure 5.3.1-2. Electric field configuration for wire-plate geometry (McDonald and Sparks, 1977).

space.

Figure 5.3.1-2 gives a qualitative representation of the electric field distribution and equipotential surfaces in a wire-plate geometry (McDonald and Sparks, 1977). Although the electric field is very nonuniform near the wire, it becomes essentially uniform near the collection plates. The current density is very nonuniform throughout the interelectrode space and is maximum along a line from the wire to the plate.

In order to maximize the collection efficiency obtainable from the electrostatic precipitation process, the applied voltage and current density should be as high as possible. In practice, the highest useful values of applied voltage and current density are limited by either electrical breakdown of the gas throughout the interelectrode space or of the gas in the collected particulate layer. High values of applied voltage and current density are desirable because of their beneficial effect on particle charging and particle transport to the collection electrode.

5.3.2 Particle Charging

Once an electric field and current density are established, particle charging can take place. Particle charging is essential to the precipitation process because the electrical force which causes a particle to migrate toward the collection electrode is directly proportional to the charge on the particle. The most significant factors influencing particle charging are particle diameter, applied electric field, current density, and exposure time.

The particle charging process can be attributed mainly to two physical mechanisms, field charging and thermal charging (White, 1963).

(1) At any instant in time and location in space near a particle, the total electric field is the sum of the electric field due to the charge on the particle and the applied electric field. In the field charging mechanism, molecular ions are visualized as drifting along electric field lines. Those ions moving toward the particle along electric field lines which intersect the particle surface impinge upon the particle surface and place charge on the particle.

Figure 5.3.2-1 depicts the field charging mechanism during the time it is effective in charging a particle. In this mechanism, only a limited portion of the particle surface can suffer an impact with an ion and collisions of ions with other portions of the particle surface are neglected. Field charging takes place very rapidly and terminates when sufficient charge (the saturation charge) is accumulated to repel additional ions. Figure 5.3.2-2 depicts the electric field configuration once the particle has attained the saturation charge. In this case, the electric field lines are such that the ions move along them around the particle.

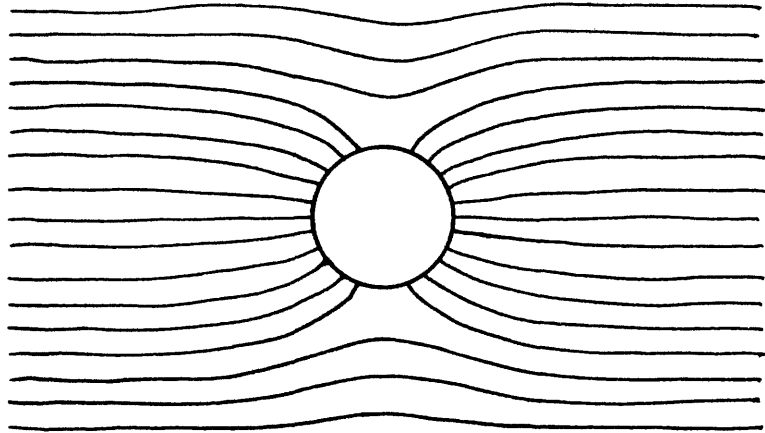


Figure 5.3.2-1. Electric field modified by the Presence of an uncharged conducting particle (Oglesby, et al., 1970).

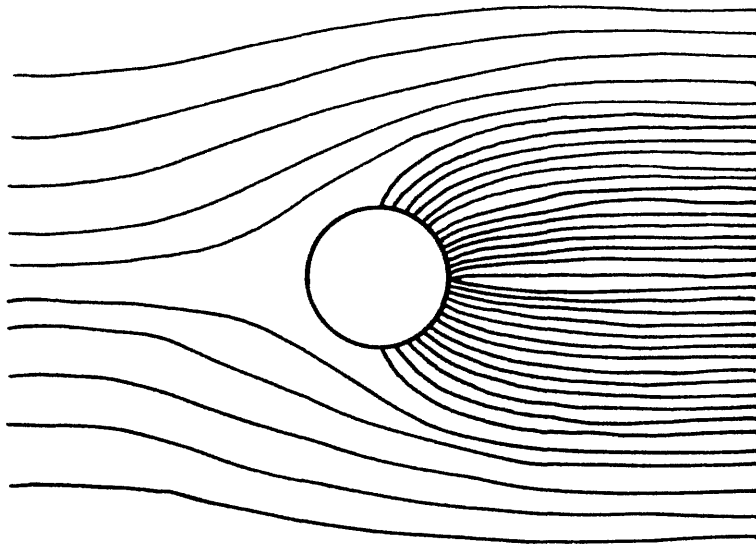


Figure 5.3.2-2. Electric field after particle acquires a saturation charge (Oglesby, et al., 1970).

(2) The thermal charging mechanism depends on collisions between particles and ions which have random motion due to their thermal kinetic energy. In this mechanism, the particle charging rate is determined by the probability of collisions between a particle and ions. If a supply of ions is available, particle charging occurs even in the absence of an applied electric field. Although the charging rate becomes negligible after a long period of time, it never has a zero value as is the case with the field charging mechanism. Charging by this mechanism takes place over the entire surface of the particle and requires a relatively long time to produce a limiting value of charge.

Thermal charging predominates for particle diameters less than $0.1 \mu\text{m}$. Above $2.0 \mu\text{m}$ the field charging mechanism is dominant. The effect of the applied electric field on the thermal charging process must be taken into account for fine particles having diameters between 0.1 and $2.0 \mu\text{m}$. Depending on the applied electric field and to a lesser extent on certain other variables, particles in this size range can acquire values of charge which are 2 to 3 times larger than that predicted from either the field or the thermal charging theories. For these particles, neither field nor thermal charging predominates and both mechanisms must be taken into account simultaneously.

In most cases, particle charging has a noticeable effect on the electrical conditions in a precipitator. The introduction of a significant number of fine particles or a heavy concentration of large particles into an electrostatic precipitator significantly influences the voltage-current characteristic. Qualitatively, the effect is seen by an increased voltage for a given current compared to the particle-free situation. As the particles acquire charge, they must carry part of the current but they are much less mobile than the ions. This results in a lower "effective mobility" for the charge carriers and, in order to obtain a given particle-free current, higher voltages must be applied to increase the drift velocities of the charge carriers and the ion densities.

The charged particles, which move very slowly, establish a particulate space charge in the interelectrode space. The distribution of the particulate space charge results in an electric field distribution which adds to the electric fields due to the electrostatic field and the ionic field to give the total electric field distribution. It is important to consider the space charge resulting from particles because of its influence on the electric field distribution, especially the electric field near the collection plate. The electric field at the plate for a given current is higher in the particle containing case than in the particle-free case. The particulate space charge is a function of position along the length of the precipitator since particle charging and collection are a function of length.

5.3.3 Particle Collection

As the particle-laden gas moves through a precipitator, each charged particle has a component of velocity directed towards the collection electrode. This component of velocity is called the electrical drift velocity, or electrical migration velocity, and results from the electrical and viscous drag forces acting upon a suspended charged particle. For particle sizes of practical interest, the time required for a particle to achieve a steady-state value of electrical migration velocity is negligible.

If the gas flow in a precipitator were laminar, then each charged particle would have a trajectory which could be determined from the velocity of the gas and the electrical migration velocity. In industrial precipitators, laminar flow never occurs and, as in any collection mechanism, the effect of turbulent gas flow must be considered. The turbulence is due to the complex motion of the gas itself, electric wind effects of the corona, and the transfer of momentum to the gas by the movement of the particles. Average gas velocities in most cases are between 0.6 and 2.0 m/sec. Due to eddy formation, electric wind, and other possible effects, the instantaneous velocity of a small volume of gas surrounding a particle could be much higher than the average gas velocity. In contrast, migration velocities for particles smaller than 0.6 μm in diameter are usually less than 0.3 m/sec. Therefore, the motion of these smaller particles tends to be dominated by the turbulent motion of the gas stream. Under these conditions, the paths taken by the particles are random and the determination of the collection efficiency of a given particle becomes the problem of determining the probability that a particle will enter a laminar boundary zone adjacent to the collection electrode in which capture is assured (McDonald and Dean, 1980).

A model has been developed to predict the collection efficiencies of ESP's. The model is discussed in Section 5.6, Engineering Models.

5.4 FACTORS INFLUENCING PERFORMANCE

5.4.1 Electrode Arrangement

The conventional design uses a wire and parallel plate arrangement as shown in Figure 5.2-1. Plates are generally spaced 0.2 to 0.25 m apart. Wider spacing is sometimes used to reduce sparking in wet ESP's. Also, the Japanese have used wide spacing (0.4 m) and higher voltages to reduce the weight and capital cost of their roof-mounted ESP's (Masuda, 1980b).

Wire-in-pipe designs (Figure 5.2-5) are commonly used for applications such as collecting liquid particles or collecting particles at high pressure. In these situations the pipe geometry is more appropriate in the process design. Generally, however, the parallel plate arrangement gives higher gas throughput for a given capital cost and collection efficiency.

5.4.2 Gas Flow

Nonuniformity of the gas flow can cause severe reentrainment and variable residence times in the ESP which decrease the collection efficiency significantly. Reentrainment losses are more significant when light or bulky dusts are being collected, such as from incinerator or pulp mill recovery boilers.

Because of space limitations and other constraints, the flue connections to the precipitator are often contorted, asymmetrical, and generally unfavorable to good gas flow. Guide vanes are used to improve the gas flow pattern especially where the gas flow is changing direction, and to prevent flow separation.

Diffusion screens or perforated plates (diffusers) can be used effectively to reduce turbulence and provide more uniform flow. Typically such screens or plates have about 50% open area.

5.4.3 Electrode Rappers

Collected material must be removed from the precipitator to prevent the buildup of excessively thick layers on the plates and to ensure optimum electrical operating conditions. Material which has been precipitated on the collection plates is usually dislodged by mechanical jarring or vibration of the plates, a process called rapping. The dislodged material falls under the influence of gravity into hoppers located below the plates and is subsequently removed from the precipitator.

Mechanical rappers use either a periodic impact or vibration of the collection electrode which dislodges the dust and permits it to fall into the hopper. Modern practice tends to favor the use of impact rappers for plates and vibrator rappers for corona electrodes. To prevent excessive reentrainment, the rapping intensity and frequency must be adjusted carefully. Most ESP's are separated into a number of sections so that only a small portion of the precipitator is being rapped at any given time. Typically the rapping frequency is once every few minutes.

In a well designed, high efficiency ESP, particle reentrainment strongly affects the overall collection efficiency. Reentrainment losses in each section can be 20% or greater. Therefore, the net effect on overall performance can be high, even with several independent sections in series. Wet ESP's with irrigated collection electrodes are used to reduce reentrainment losses, but this results in the same wet disposal problem associated with scrubbers.

5.4.4 Electrical System

The power supply to a precipitator consists of three sections: the voltage control system, the transformer which steps up the line voltage, and the rectifier which converts alternating to direct current. Automatic voltage control is used in all large modern installations. Required voltages vary from about 10

to 80 kV depending on the precipitator geometry and the specific application. The optimum voltage is just less than that required to cause sparking.

The discharge current ranges from a few up to several hundred milliamps. The corona current density (current per unit collector area) should be kept as high as possible without sparking in order to maximize the particle collection rate. In practice, the current density is limited by many factors, including the effects of baffles in the flow path, the corona electrode geometry, and pulsating currents supplied by the rectifier sets. High resistivity fly ash and poor electrode alignment can further limit the current densities.

5.4.5 Sectionalization

ESP performance improves with the degree of sectionalization. Small areas have less electrode area for sparking to occur. Electrode alignment and spacing are more accurate for smaller sections. Smaller rectifier sets are more stable under sparking conditions and the sparks are less intense and damaging to performance. In general, small corona sections can operate at voltages 5 to 10 kV higher than large sections.

5.4.6 Gas Properties

The composition, temperature, and pressure of the gas can affect the ESP performance very significantly. The gas composition will have a very strong effect on the space charge (and current flow) which can be maintained with a negative corona. Higher space charge (less current) allows a higher operating voltage, and thus stronger precipitating force, without excessive sparking.

Changes in gas temperature and pressure cause changes in the gas density and hence the mean free path of gas molecules. This alters the voltage required to initiate the corona. In general, the corona starting voltage will be higher in a denser gas.

Temperature also influences the mobility of the charge carriers. Mobility increases with temperature. For this reason sparking occurs at lower voltages when higher temperatures are encountered.

5.4.7 Particle Properties

The size and concentration of particles will have an effect on ESP performance. Particle diameter affects the total charge the particle can acquire, and therefore the migration velocity and collection efficiency. The dielectric constant of the particle also will have some effect on the level of charge attained.

As long as there are plenty of free ions to charge the particles and to carry the corona current, more particles will result in a larger space charge. If there are too many particles

relative to free ions, however, the particles will become the principal charge carriers and cause a slower flow of current from the corona. This will decrease particle charge, migration velocity, and collection efficiency through what is called corona suppression. This may occur when controlling fine mist or metallurgical fumes where large number concentrations are likely to exist.

5.4.8 Dust Resistivity

For satisfactory operation of ESP's, the dust resistivity should be between about 10^8 and 10^{11} ohm-cm. Below this range, the collected dust particles lose their charge too rapidly when they hit the collecting electrode causing weak adhesion forces and particle reentrainment. Low resistivity is more of a problem when collecting large particles where the inertial forces are much larger than the adhesion forces.

The more serious problem is caused by high resistivity. The buildup of highly resistive dust deposits on both the discharge and collecting electrodes will suppress the effective current and voltage, and drastically reduce the collection efficiency.

If the dust resistivity is greater than about 10^{11} ohm-cm, the voltage drop will cause a corona to form at the dust layer surface. This is termed a back corona, or reverse ionization, and may be seen as a faint glow at the dust surface. The end result is that sparking becomes excessive, the average voltage decreases, and ESP performance deteriorates.

5.4.8.1 Flue Gas Conditioning

The problem of high resistivity dust has been encountered with many ESP's operating at electric power generating plants which burn low sulfur coals. It has been found that the presence of an absorbed layer of sulfur trioxide provides a means for draining the charge from the collected dust, and thus reducing the effective resistivity of the dust layer. For this reason, the addition of SO_3 to the gas being cleaned has been used successfully in conditioning the flue gas to handle high resistivity dust (Patterson et al, 1979; Ferrigan et al., 1979). The SO_3 may be added in the stabilized anhydrous form, as vaporized H_2SO_4 , or as SO_3 from the catalytic oxidation of SO_2 . There are a number of other flue gas conditioning agents on the market (Gooch et al. 1979). Generally the effect of the conditioning agent will vary with the chemical composition of the ash or dust (Katz, 1979; Roehr, 1979).

Conditioning agents also are used to improve the adhesive and cohesive properties of the dust. In this way performance can be improved through reductions in the amount of reentrainment, especially during rapping. Ammonia has been used successfully as a conditioning agent for this purpose. It also has been suggested that ammonia reacts with SO_2 in the flue gas to form fine

ammonium sulfate particles which improve the space charge in the precipitator. In either case, the beneficial effects of ammonia injection, when they have been noted, have not appeared to be due to resistivity changes.

Flue gas conditioning to improve ESP performance is most important when modifying existing installations to accommodate changes in fuel type or in emissions regulations. New installations may be designed such that they need not rely on conditioning agents.

5.4.8.2 Hot-Side ESP's

Another way to overcome the high resistivity problem is to operate the precipitator at higher temperature. Fly ash resistivity decreases substantially as temperature is increased (see Figure 5.4.8-1).

In many electric power plants, ESP's are being used upstream from the air preheater at temperatures above 315°C (600°F). In these hot-side ESP's the dust resistivity is kept well below 10^{10} ohm-cm. This results in fewer fouling problems in the air preheater, less corrosion and hopper plugging, better electrical stability and higher corona current densities than are possible with low temperature precipitators treating high resistivity dust. However the higher temperature results in about 50% higher gas volumes to be treated. Also the lower gas density and higher gas viscosity cause lower operating voltages and lower migration velocities than at lower temperature. Structural problems involving materials and thermal expansion also can be severe.

Table 5.4.8-1 summarizes typical design parameters for hot-side ESP's.

5.5 ADVANCED DESIGNS

5.5.1 High Intensity Ionizers

Most emphasis on advanced designs is currently being directed towards further development of two-stage electrostatic precipitators using high intensity ionizers for particle charging. The purpose of the high intensity ionizer is to charge the particles to higher charge levels which results in a greater migration velocity in the precipitation section. The two-stage approach to electrostatic precipitation is illustrated in Figure 5.2-4. The particles are charged and collected in two separate electric fields.

The main advantage of two-stage precipitation is the ability to apply higher charging and precipitating voltages without sparking. The higher field strengths result in stronger electrostatic forces on the particles and therefore higher collection efficiency.

The success of this approach depends on the development of a high intensity ionizer for charging particles without collecting them. If particles collect in the ionizer they will cause back

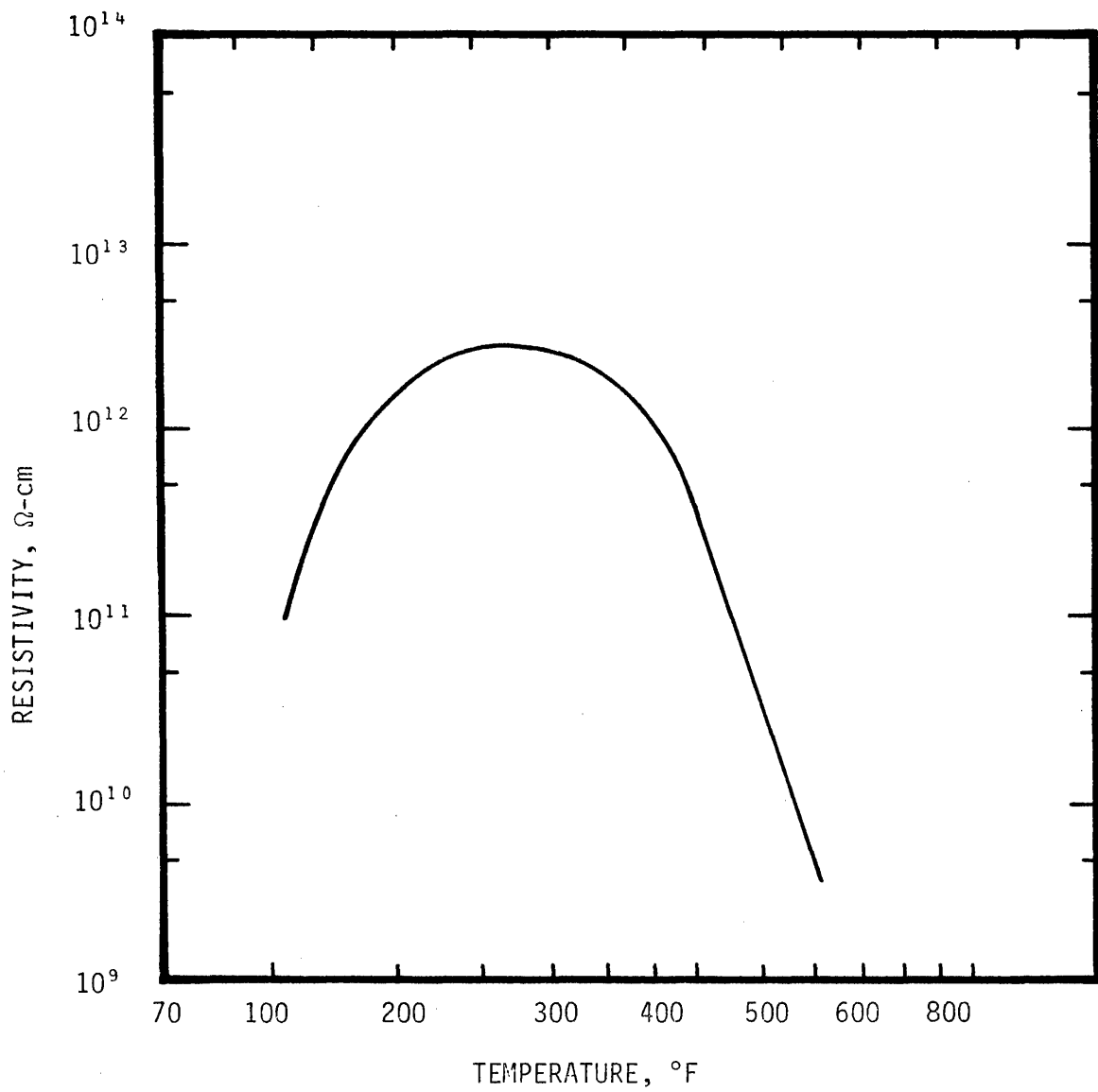


Figure 5.4.8-1. Typical temperature-resistivity relationship.

TABLE 5.4.8-1.

TYPICAL DESIGN PARAMETER RANGES FOR
A HOT-SIDE ESP ON A COAL FIRED UTILITY BOILER

Design Parameter

Gas temperature	340 - 400°C
Overall collection efficiency	99 - 99.7%
Collection area	30,000 - 60,000 m ²
Specific collection area (SCA)	0.7 - 1.0 m ² /Am ³ /min
Migration velocity	8 - 11 cm/s
Gas velocity	1.5 - 1.8 m/s
Rectifier sets:	
Number	12 - 64
Max. current rating	750 - 1,500 mA
Specific area	900 - 2,300 m ² /set
Series Fields	5 - 8
Fields/1,000 Am ³ /min	3 - 9
Current density	0.3 - 1.7 μA/m ²
Watts/Am ³ /min	7 - 18

corona and sparking, and reduce the benefit of the ionizer.

The EPA and EPRI are actively evaluating and demonstrating high intensity ionizers for utility applications where high resistivity fly ash problems are encountered. The following designs by Southern Research Institute, Union Carbides, and Masuda of Japan are all in various stages of development and evaluation.

5.5.1.1 EPA-SoRI Precharger

Southern Research Institute (SoRI) under EPA contracts has developed and evaluated a three-electrode particle precharger system for controlling the effects of back corona (Pontius et al., 1978, 1979a, 1979b). In this device two of the three electrodes are the conventional corona discharge and passive electrodes. The third is a screen electrode placed near the passive electrode as shown in Figure 5.5.1-1. Separate power supplies are provided for the corona discharge and screen electrodes. The passive electrode is set at ground potential.

The screen electrode is used as a sink for ions generated at the passive electrode as a result of back corona effects. If the screen electrode voltage is set equal to the original potential on the surface, the electric field will be practically undisturbed in comparison with the original field. Only the non-zero thickness of the wires in the screen will cause very localized modifications to the field. A corona current originating at the discharge electrode will be distributed such that a fraction of the total equal to the ratio of open area to total surface of the screen will reach the passive electrode. The remainder of the current will be intercepted by the screen.

Setting the potential on the screen electrode more negative will distort the field near the screen in such a way that negative ions from the discharge electrode will be repelled from the screen wires and forced toward the open area, through which they can proceed to the plate. If high resistivity particles are introduced into the system, deposition will occur on both the plate and the screen electrodes. Since negative ions from the discharge electrode are being repelled by the screen, it must have a lower current density than the plate, and hence corona from the screen electrode would probably not occur. If back corona occurs, the positive ions from the passive electrode will be attracted to the screen electrode, where many will be captured and removed from the system. If most of the positive ions resulting from back corona can be captured by the screen electrode, the ion field between the screen and the discharge electrode would be essentially unipolar.

The EPA-SoRI particle precharger has been evaluated in a pilot plant located in the EPA's Industrial Environmental Research Laboratory Research Triangle Park, North Carolina (Sparks et al., 1980; Pontius et al. 1979). The average grade penetration curve for the high resistivity fly ash ($\sim 10^{12}$ ohm-cm) for both precharger-off and precharger-on is shown in Figure 5.5.1-2.

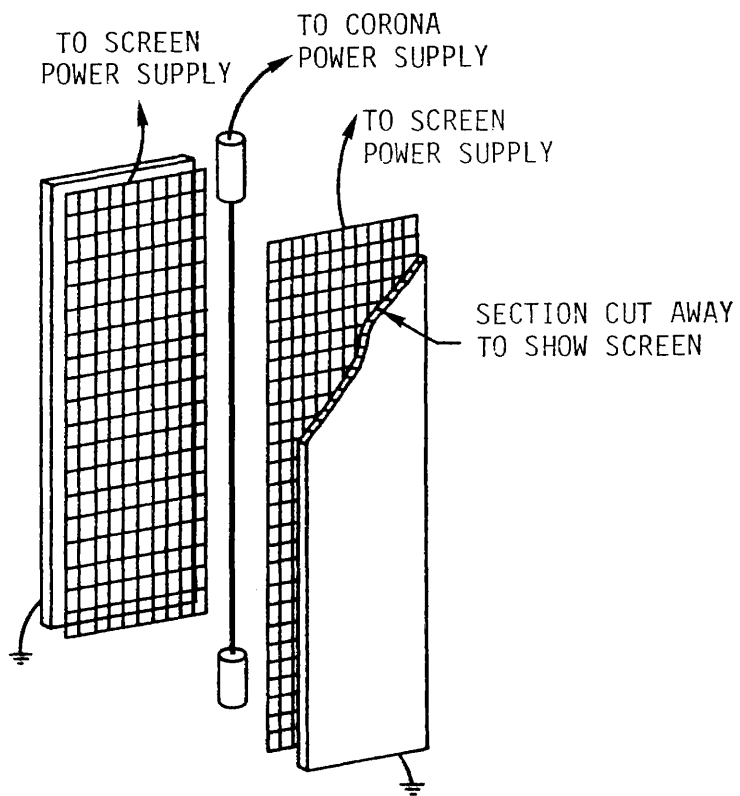


Figure 5.5.1-1. EPA-SORI three electrode precharger.

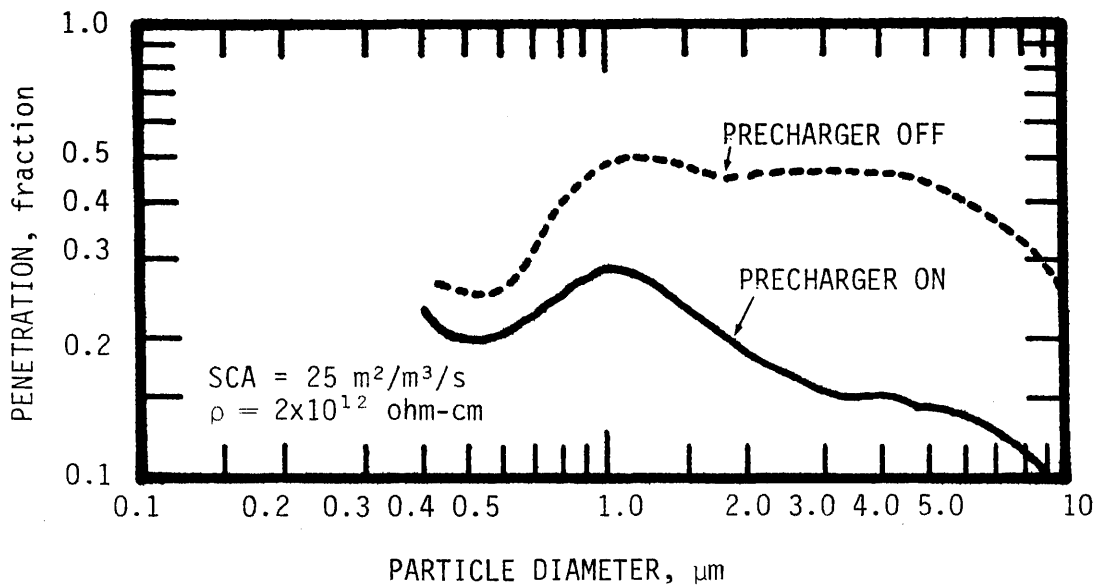


Figure 5.5.1-2. Graded penetration curves for high resistivity fly ash (Sparks et al., 1980).

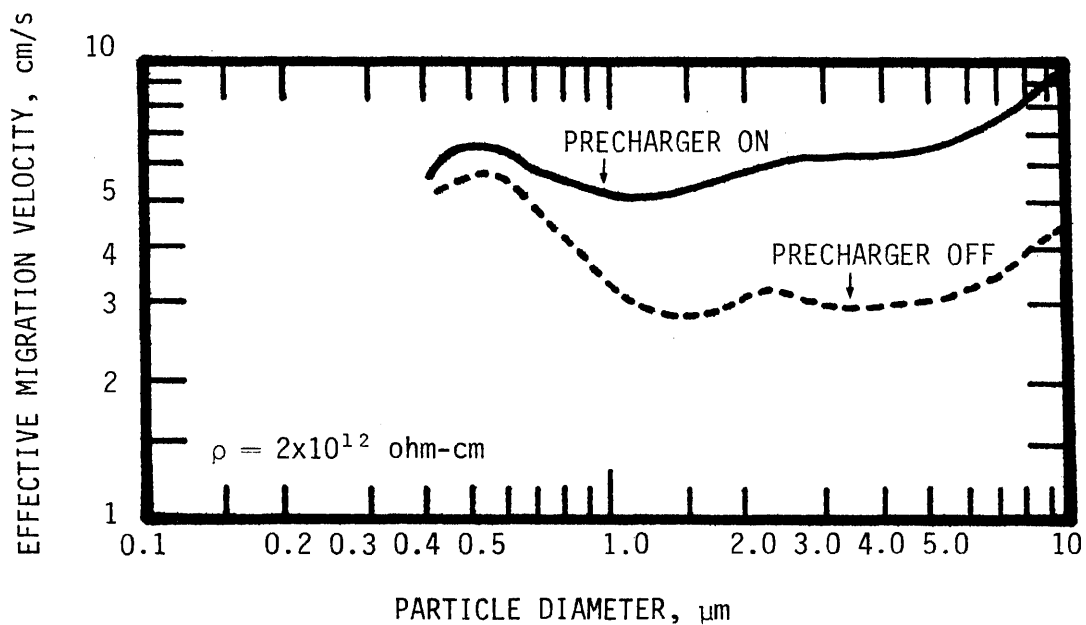


Figure 5.5.1-3. Effective migration velocity versus particle diameter for high resistivity fly ash (Sparks et al., 1980).

These grade penetration curves were used to back calculate the effective migration velocities, w_{pe} , shown in Figure 5.5.1-3.

The grade penetration curves indicate that rapping reentrainment may be a problem because the penetration of large particles is higher than expected. An optimized downstream collector should minimize the rapping reentrainment problem.

The graded penetration curve for the low resistivity case is shown in Figure 5.5.1-4. It appears that the precharger more than doubles the effective specific collection surface (SCA) of the ESP.

Initial capital cost estimates indicate that the precharger will cost about a third to half the cost of one conventional electrical section (Sparks et al. 1980). A conventional electrical section might increase the SCA of a small ESP, such as used for high sulfur coal, by as much as 33% and the SCA of a large ESP, such as used for low sulfur coal, by no more than 17%. Thus, the cost effectiveness of the precharger appears to be excellent.

The data were used to estimate the SCA needed to meet an emission standard of 13 ng/J (0.03 lb/10⁶ Btu) when collecting fly ash with electrical resistivity of about 10¹² ohm-cm. The estimated SCA is 70 m²/m³/s (355 ft²/10³ acfm) which compares with an estimated SCA of at least 180 m²/m³/s (930 ft²/10³ acfm) for a conventional ESP.

5.5.1.2 Boxer-Charger

Masuda and co-workers (1976, 1978, 1979a, 1979b, 1979c, 1980a, 1980b) have developed another novel type of charging device called the "Boxer-Charger" in which charging is accomplished by bombardment of unipolar ions in an AC field. The Boxer-Charger is designed for maximum particle charge levels without the problem of back corona. This device consists of the parallel planar electrode assemblies facing each other, between which the AC main voltage is applied to produce an AC charging field. In synchronization to this voltage, a high frequency exciting voltage is alternately applied to each one of the electrode assemblies to produce a plasma on its surface when it has negative polarity. The plasma emits negative ions to the charging space, so that dust particles coming into this space are bombarded by the negative ions from both sides alternately.

The charging current density of these negative ions is approximately one order of magnitude higher than that obtainable with conventional DC corona charging. As a result the charging speed is very high, allowing installation of a Boxer-Charger inside an inlet-duct of a collector where gas velocities are greater than 10 m/s. The charged dust particles undergo an oscillatory motion, so that most leave the charger without being collected on the electrode assemblies. The small amount of dust which does deposit the electrode assemblies does not cause back discharge, because the charge accumulation due to oncoming ions

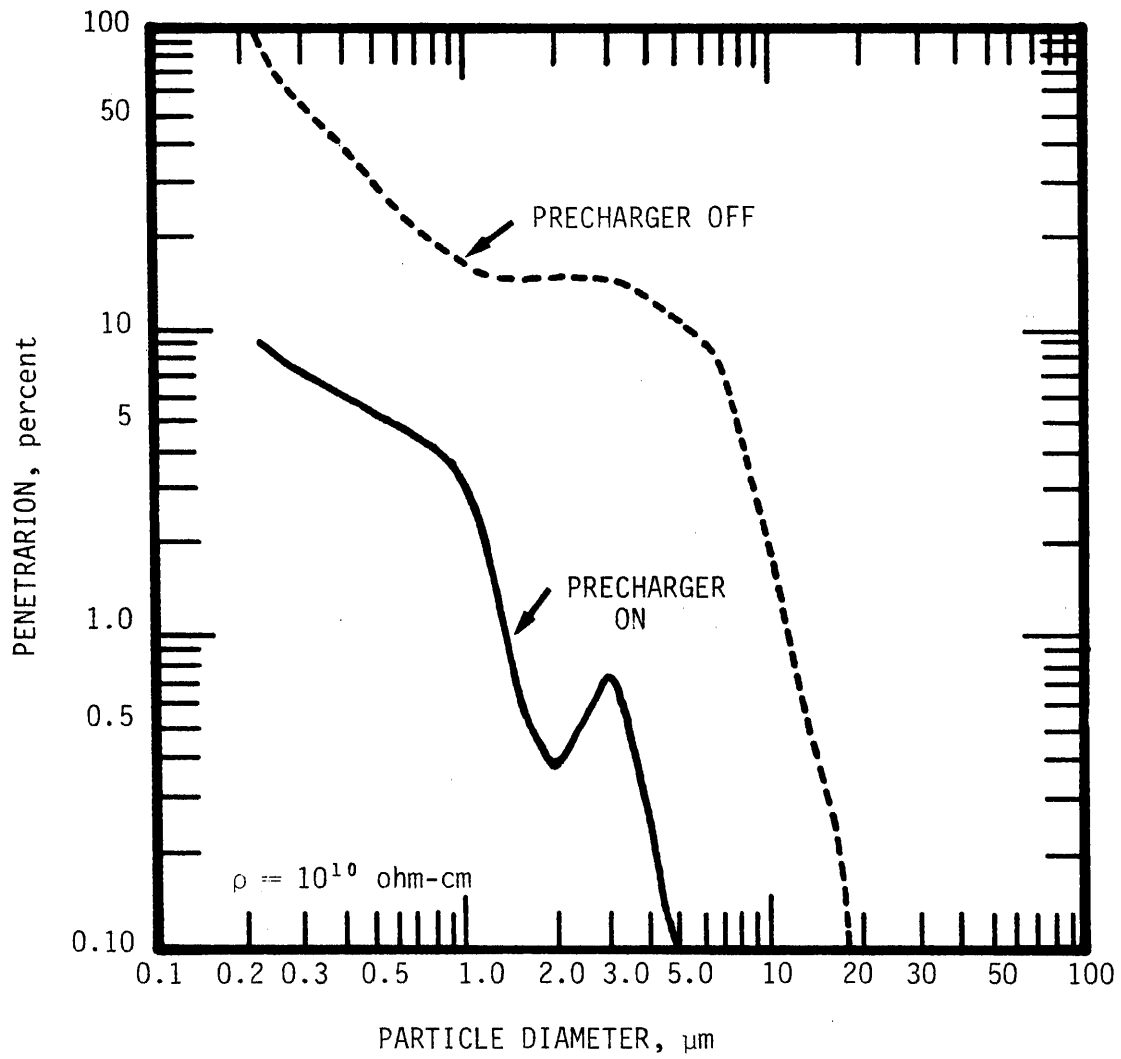


Figure 5.5.1-4. Graded penetration curves for low resistivity fly ash (Sparks et al., 1980).

is quickly neutralized by the plasma during the next excitation period. Back discharge does not occur in this device even at a very high dust resistivity (above 10^{15} ohm-cm).

Figure 5.5.1-5 illustrates the basic construction of the Boxer-Charger (Masuda, 1978). In Figure 5.5.1-5(a), three planar electrode assemblies are arranged parallel to each other in the gas flow direction. Each assembly consists of a number of parallel discharge electrodes, with every other unit connected to form two groups which are insulated from each other. Corona discharge occurs to form a planar plasma ion source along the electrode assembly when a DC or AC exciting voltage is applied between the two groups of the discharge electrodes. The main AC voltage of a sinusoidal or square wave form at a low frequency of 50-500 Hz is applied between the adjacent electrode assemblies (A) - (B) and (B) - (A') to produce the uniform AC charging fields. When an electrode assembly takes a predetermined polarity, negative in this case, it is supplied with the exciting voltage, which is a high frequency AC voltage at 1.5-20 kHz in this case, to produce the planar plasma ion source over this assembly. Thus, the electrode assemblies (A), (B) and (A') are alternately excited as shown in Figure 1(b) during the negative half period of the main voltage.

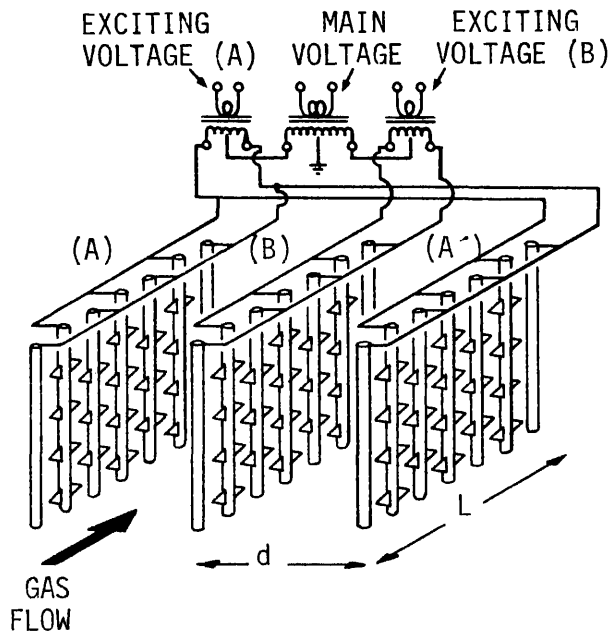
In the next positive half period, the excitation is interrupted so that no positive ions are supplied to the charging spaces. The excitation has to be stopped slightly ahead of the polarity change to allow the extinction of residual plasma capable of providing positive ions, so that the exciting period is made shorter than the half period of the main voltage.

The negative ions travel across the charging spaces in alternating directions, and bombard the dust particles coming into the charging spaces from both sides. The residual ions arrive at the opposite electrode assemblies to be absorbed there.

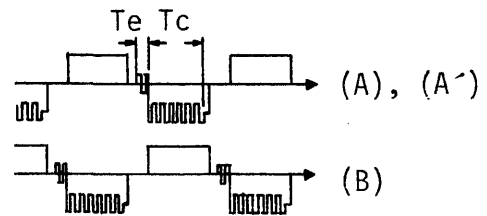
Figure 5.5.1-5(c) shows a double-helix electrode assembly of the Boxer-Charger "Mark III". This configuration has the advantages of:

1. Maintaining the wire-to-wire gap at a small and constant value without being affected by thermal deformation from the supporting system.
2. Avoiding the edge-effect which causes corona discharge in the unexcited period.
3. Ease in its support.

The small wire-to-wire gap does not allow a stable corona to appear uniformly along the wires because of excessive sparking. This difficulty is resolved by using a very short pulse voltage with 40 ns duration time which proceeds along the helix wires in a form of a traveling wave producing uniform streamer coronas.

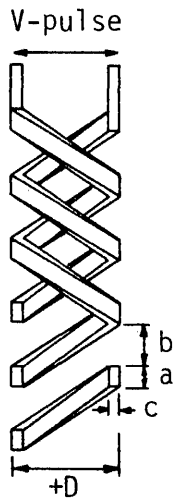


(a) Electrode assemblies.



(T_c : Charging period)
 (T_e : Elimination Period)

(b) Voltage applied to (A), (A') and (B).



(c) Double helix electrode

Figure 5.5.1-5. Construction of BOXER CHARGER.

The short duration pulse makes it possible to electrically isolate the two helix wires from each other by inductance-insulation. An inductance element, reflecting the wave, is used instead of an insulator. This simplifies the electrode construction and reduces its cost.

Masuda (1980) evaluated the double helix Boxer-Charger in a pilot plant ESP. Two Boxer-Chargers were used, one installed in the inlet-duct, and another located in the inter-field section between the first and second collection fields. The dust penetration was measured at the outlet of each field. The gas temperature was approximately 100°C and the dust resistivity was in the range of 10^{11} - 10^{12} ohm-cm, which would cause a severe back discharge in a conventional ESP.

Precharging the dust results in a substantial increase in the apparent migration velocity of the dust in the succeeding collection field to as high as 2.4 times of its original value. However, the apparent migration velocity drops to its original value from the next collection field on. This indicates the enhanced particle charge becomes diminished by positive ions from back discharge in the field section to an equilibrium value specific to the back discharge condition.

By superimposing a pulse voltage on the collection field, DC voltage, the apparent migration velocity becomes 1.6 times as high. The additional use of a Boxer-Charger in front of each collection field increases the apparent migration velocity to as high as 2.9 times the original value, corresponding to the migration velocity for the no back discharge condition. Masuda (1980) concluded that the advantage of particle precharging can be obtained only when the back discharge in the collection field is decreased.

5.5.1.3 Union Carbide High Intensity Ionizer (HI^T)

The HII system, as shown in Figure 5.5.1-6, consists of a purged bulkhead resting on support beams, with an array of installed HII throats and a high voltage discharge system (Chang and Rimensberger, 1980). Each throat consists of a bellmouth, diffuser, purge rings and an exit cone as shown in Figure 5.5.1-7. A supply of clean, heated gas is required to purge the rings in the HII throats, in order to effectively prevent back corona therein. The discharge electrode system consists of a mast and electrode assembly which is suspended from the ESP roof, supported by insulators and stabilized at the bottom. A velocity distribution device is located downstream of the bulkhead. A commercially available high voltage power supply and control system is used.

To install the HI^T system in an existing ESP presents two fundamental design challenges, namely, physically locating the HI^T and determining a source and system for the purge gas supply. To provide space for the HII system in an existing ESP, 1 meter

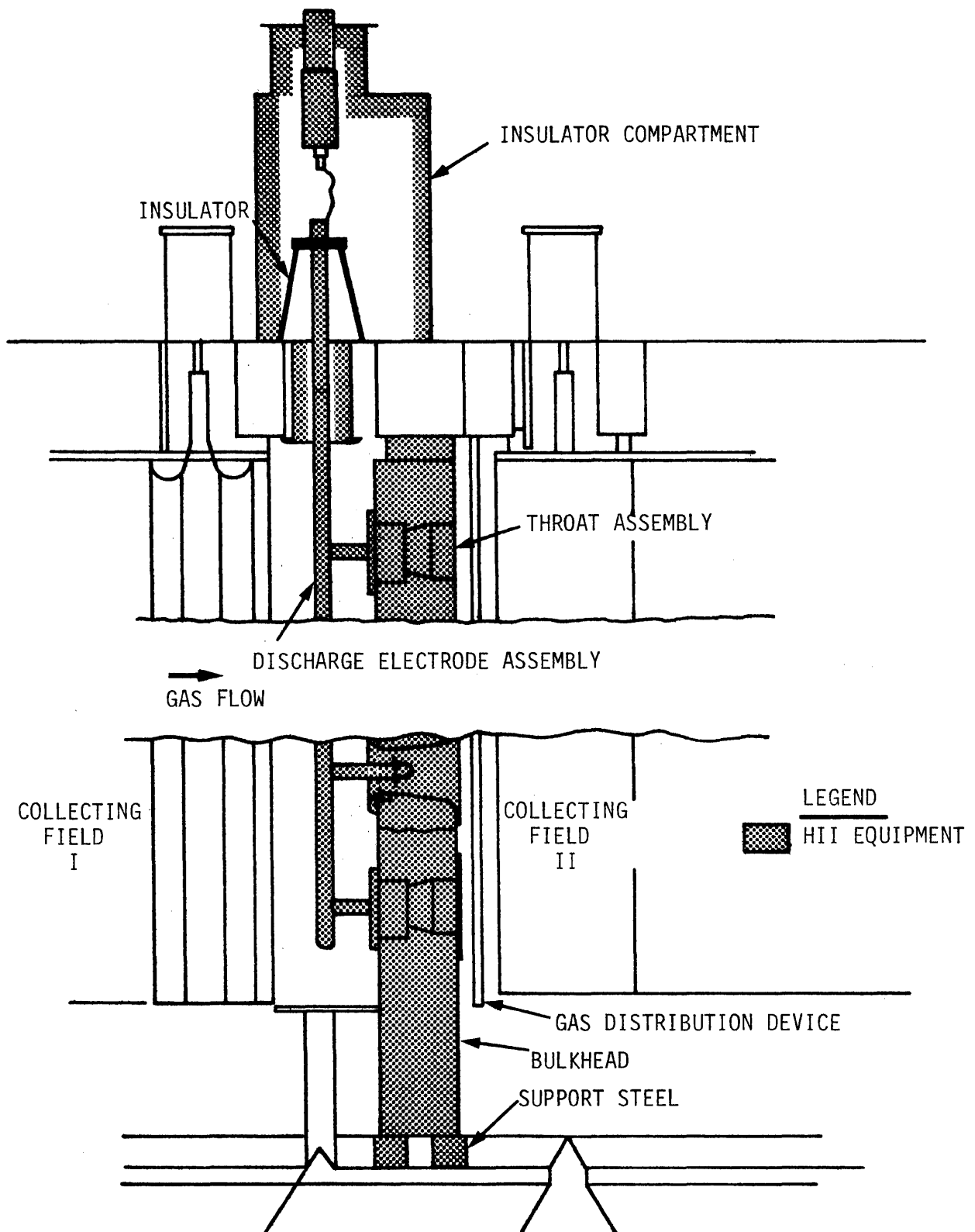


Figure 5.5.1-6. Union carbide high intensity ionizer system.

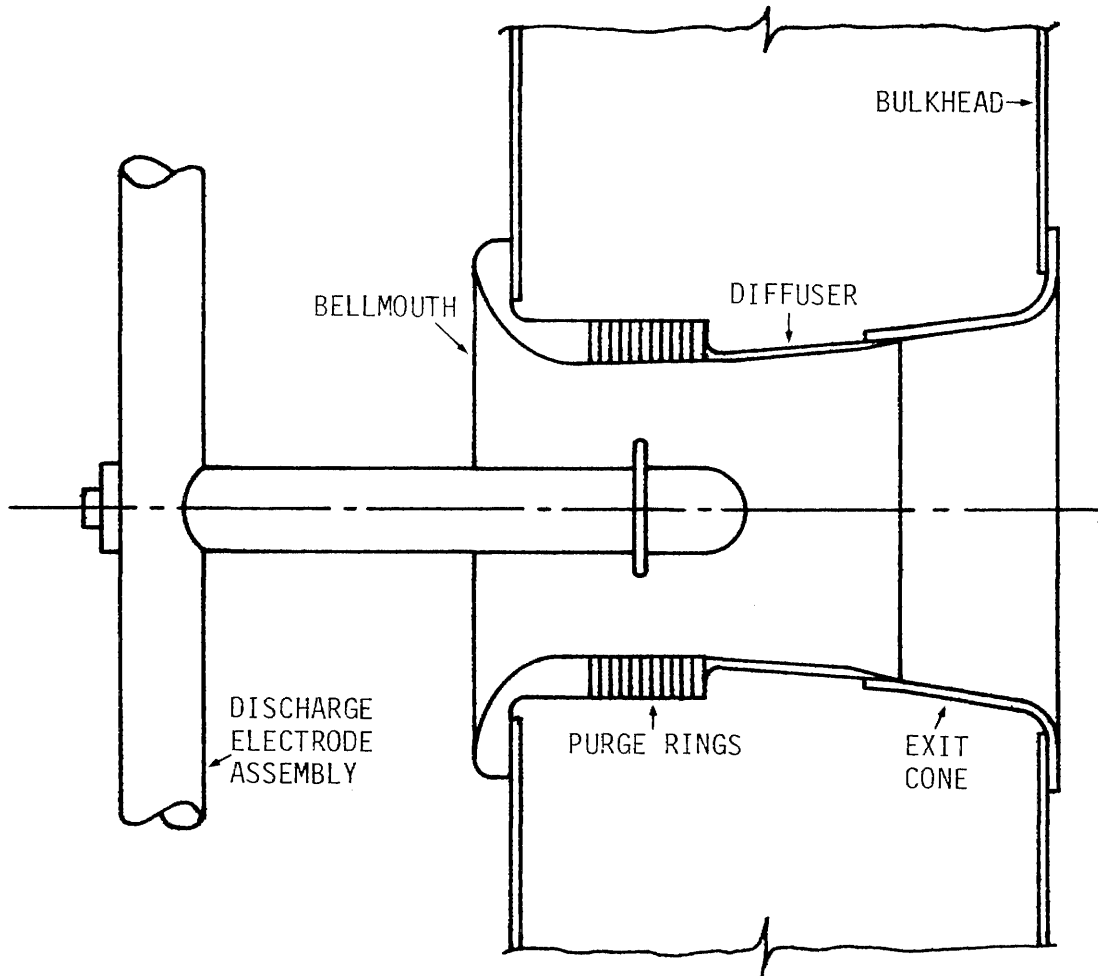


Figure 5.5.1-7. High intensity ionizer throat.

of collecting plate length from the second field has to be removed and the internal catwalk space between the fields has to be used as shown in Figure 5.5.1-8. In a side-loaded precipitator, temporary reinforcement of the side walls and roof is required before cutting an opening for the installation of the bulkhead. The bulkhead assembly can then be slid into the ESP on its support beams. The discharge electrode system and distribution device can also be installed from the same location. The high voltage power supply for the HII, e.g., transformer/rectifier, is located on the roof of the precipitator. In some cases, a relocation of the transformer/rectifier sets for the existing precipitator may be required to prevent interference. Insulator housings and the high voltage feed to the discharge electrode system are located on the precipitator roof.

Reliable operation of the HII system requires a continuous purging of the HIT anodes and a source of heat to temper the purge gas, as required. Several potential sources of heat are available in most applications: blow-off steam, air coming off the preheater, waste heat, e.g., boiler-house air, or clean flue gas.

5.5.2 Pulse Energization

Pulse energization or pulse charging uses high voltage pulses superimposed on the base voltage of either one-stage or two-stage ESP's. The base voltage is maintained just below the level where either sparking or back corona occur. This generates an electric field to maintain ion and particle migration toward the collection plate. The pulse is about two to three times the base voltage, but is of very short duration (50 to 200 μ s) so that sparking does not occur.

Pulse energization for improvement of the performance of precipitators was investigated about 30 years ago by White (1952). The principle has later been examined by a number of investigators in Japan, U.S.A., and Europe (Liithi, 1967; Masuda, 1976, 1979a; Penney and Gielfand, 1978; Feldman et al., 1978; Petersen et al., 1979; Lausen et al., 1979).

The advantages claimed for pulse energization in comparison with conventional DC-energization are:

1. Higher peak voltage without excessive sparking, and therefore improved particle charging in accordance with the classical theory for particle charging.
2. More effective extinguishing of sparks and better suppression of insipient back corona.
3. By variation of the pulse repetition frequency and pulse amplitude the discharge current can be controlled independently of precipitator voltage. This allows reduction of the discharge current to the back corona threshold limit for a high resistivity dust without reducing the ESP voltage.

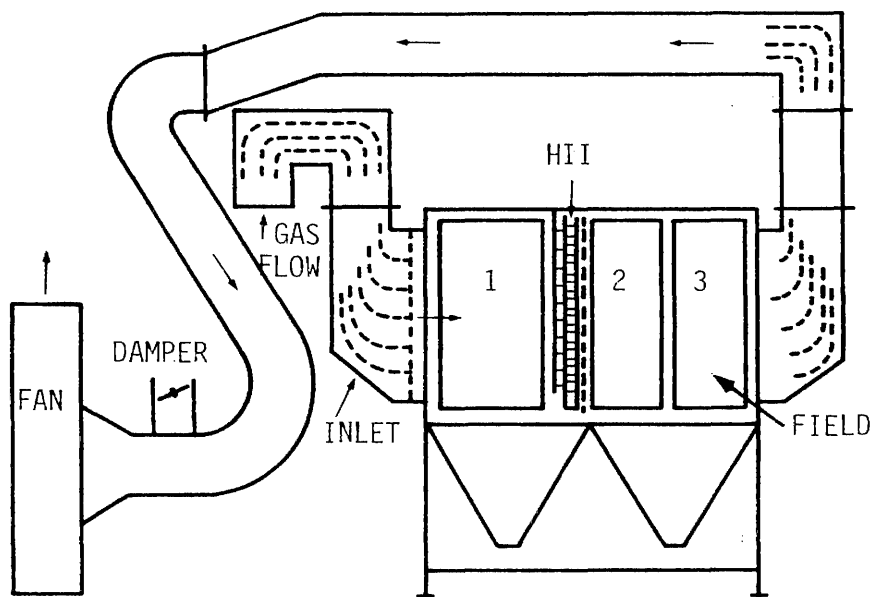


Figure 5.5.1-8. Installation of a HII in an existing ESP.

- 4 With short duration pulses the corona discharge takes place well above the corona onset level for constant DC voltage and is suppressed during the remaining part of the pulse by space charges. This results in a more uniformly distributed corona discharge along the discharge electrode.
5. Corona discharges from short duration pulses are less influenced by variations in gas and dust conditions. This improves the internal current distribution of a separately energized field.
6. Corona discharges are obtainable from surfaces with larger diameter curvatures. This permits the use of large diameter discharge wires, or rigid type discharge electrodes with comparatively short and blunt tips, reducing the risk of discharge electrode failures.
7. Permits a higher power input and thereby improves precipitator performance
- 8 Increases particle migration velocity particularly for high resistivity dusts, permitting reduction of the collection area for new installations or improvement of the efficiency of existing installations without increase of the collection area.

A mobile, double pipe test ESP in which the operation conditions of the two parallel pipes can be kept identical during slipstream testing has been used to study the differences between DC and pulse energization as well as the effect on precipitator performance of the different pulse energization parameters in the field (Petersen et al., 1980; Lausen et al. 1979).

An improvement factor, defined as the ratio between particle migration velocities for pulse and for DC energization, has been used to judge the result of the comparison tests. As seen from the following table, the improvement factor increases with high dust resistivity.

OPERATION CONDITION	IMPROVEMENT FACTOR
Without back ionization ~ 10^{11} ohm-cm	1.2
Moderate back ionization ~ 10^{12} ohm-cm	1.6
Severe back ionization ~ 10^{13} ohm-cm	>2

A commercial scale pulse energization system was recently demonstrated in Europe (Petersen et al., 1980). The precipitator was installed on a lime kiln emitting 50 g/Nm³ of dust with a resistivity from 10^{10} to 10^{12} ohm-cm at 350°C. the precipitator

operating parameters are listed in Table 5.5.2-1.

The sparking rate decreased from 60 sparks/min to 0.33 sparks/min when the pulse voltage was applied. The migration velocity increased by a factor of 1.3 to 1.4. No collection efficiency or particle size data were reported.

5.6 ENGINEERING MODELS

A very detailed computer model of electrostatic precipitation has been developed, expanded, and improved over a number of years (Gooch et al., 1975; Sparks, 1978, McDonald, 1978a,b; and Mosley et al., 1980). The model is complex and requires a large quantity of data to adequately define electrical, physical and thermal properties of the precipitator, gas, and particles. A simplified version of this model has been developed by Cowen et al. (1980). It is used as the basis for ESP performance predictions for this project. An explanation of the basic model follows.

5.6.1 Particle Charging

Particle charging generally takes place by two mechanisms: field charging and diffusion charging (see Section 5.3.2). For large particles, field charging is by far the dominant mechanism. Diffusion charging dominates for very small particles. Particles of major interest in air pollution (those with $0.1 \leq d_p \leq 2.0 \mu\text{m}$) are charged by both mechanisms. Pontius et al. (1977) have shown that the following approximation for the charge on a particle agrees with experimental data and detailed theory fairly well.

$$n_p = \frac{\pi d_p}{2} C_1 \left\{ \left[\frac{b_m d_p E_{Av} Nt}{2(b_m Nt + C_1)} \right] \left[1 + 2 \left(\frac{K-1}{K+2} \right) \right] + C_2 T \ln \left[\left(\frac{d_p v Nt}{2C_1 C_2 T} \right) + 1 \right] \right\} \quad (5.6.1-1)$$

where n_p = number of charges

$C_1 = 4 \epsilon_0 / e$

$C_2 = k/e$

ϵ_0 = permittivity of free space = 8.854×10^{-12} F/m

e = charge on electron = 1.6×10^{-19} C

k = Boltzmann's constant = 1.38×10^{-23} J/K

b_m = ion mobility, $\text{m}^2/\text{V-s}$

E_{Av} = average electric field V/m

T = absolute temperature, K

N = free ion density, $1/\text{m}^3$

TABLE 5.5.2-1. OPERATING PARAMETERS FOR ESP ON A LIME KILN WITH PULSE ENERGIZATION

Total collection area	=	1,400 m ²
Duct width	=	250 mm
Discharge electrode	=	2.7 mm dia; conventional helical type
Gas velocity	=	0.6 m/s
Residence time	=	6 s
Base operating voltage	=	30 kV
Operating voltage & Pulse voltage	=	60 kV

- t = residence time for charging, s
 K = particle dielectric constant, dimensionless
 v = mean thermal speed of ions, m/s
 d_p = physical particle diameter, m

The charge on a particle, q_p , in Coulombs is given by

$$q_p = n_p e \quad (5.6.1-2)$$

The average electric field used in the calculation is given by

$$E_{Av} = U/h_{wp} \quad (5.6.1-3)$$

where U = the applied voltage, V

h_{wp} = wire to plate spacing, m

The free ion density, N , is given by

$$N = \frac{j}{eb_m E_{Av}} \quad (5.6.1-4)$$

where j = current density, A/m²

5.6.2 Particle Collection

Particle collection in an ESP is given by the Deutsch-Andersen equation:

$$Pt_d = \exp [-w_p A_c / Q_G] \quad (5.6.2-1)$$

where w_p = electrical migration velocity of particles with diameter d_p , m/s

A_c = collection plate area, m²

Q_G = volumetric flow rate of gas, m³/s

Pt_d = penetration for particles with diameter " d_p ", fraction

The ratio " A_c/Q_G " is called the specific collection area (SCA).

The electrical migration velocity near the collection plate for small particles is given by Stokes' law as

$$w_p = q_p E_p C' / 3\pi\mu_G d_p \quad (5.6.2-2)$$

where q_p = the particle charge, C

E_p = the electric field at the plate, V/m

C' = the Cunningham correction factor = $1 + 2A \lambda / d_p$

$A = 1.26 + 0.40 \exp(-1.10 d_p / 2\lambda)$

λ = mean free path of gas, μm

μ_G = viscosity of gas, kg/m-s

McDonald (1978b) reported that for an ESP collecting fly ash:

$$E_p = E_{AV} / 1.75 \quad (5.6.2-3)$$

This estimate of " E_p " is used in the model.

McDonald (1978b) also reported that equation (5.6.2-2) underpredicts the migration velocity for a real ESP. Therefore, the migration velocity is corrected by an empirical factor to improve agreement between prediction and data. The corrected migration velocity is given by:

$$w_p = w_{pu} \times (1.7 - 0.45 \ln d_p) \quad (5.6.2-4)$$

where " w_{pu} " = uncorrected migration velocity, m/s. Equation (5.6.2-4) applies for $0.2 < d_p < 4.5 \mu\text{m}$. Outside this range equation (5.6.2-2) applies.

5.6.3 Non-Ideal Factors

The Deutsch-Andersen equation applies to an ideal situation. Non-ideal factors, such as non-uniform gas flow, sneakage, and reentrainment, exist in real ESP's which result in higher penetrations than those predicted by equation (5.6.2-1). Gooch et al. (1975) have shown that the effects of these non-ideal factors can be estimated from:

$$Pt'_d = \exp \left[\frac{-w_p A_c}{B_S F_G Q_G} \right] \quad (5.6.3-1)$$

where Pt'_d = corrected penetration for particle diameter " d_p ", fraction

B_S = the correction factor for sneakage and reentrainment not due to rapping
 F_G = correction factor for non-uniform gas flow

$$B_S = \frac{Pt_d}{N_S \ln[S_p + (1 - S_p)Pt_d^{1/N_S}]} \quad (5.6.3-2)$$

where N_S = number of baffled sections

S_p = the fraction of particles that are reentrained and that by-pass the electrified region per section

$$F_G = 1 + 0.766[1 - Pt_d] \sigma_G^{1.786} + 0.075 \sigma_G \ln[1/Pt_d] \quad (5.6.3-3)$$

where σ_G = the normalized standard deviation of the gas flow ($\sigma_G=0.25$ is generally considered good)

5.6.4 Correction for Rapping Reentrainment

The corrections described in Section 5.6.3 do not take into account reentrainment due to rapping. McDonald (1978a) described an empirical correction for rapping reentrainment:

$$Y_1 = (0.155) X^{0.905} \quad (5.6.4-1)$$

$$Y_2 = (0.618) X^{0.894} \quad (5.6.4-2)$$

where Y_1 = rapping emissions for cold side ESP, mg/DSCM

Y_2 = rapping emissions for hot side ESP, mg/DSCM

X = estimated mass collected by last electrical section, mg/DSCM

5.7 METHODS OF TECHNICAL EVALUATION
 5.7.1 Devices for Further Evaluation

The electrostatic precipitator, pulse energization ESP, and ESP with SoRI precharger were chosen for efficiency and cost calculations. The calculation methods are explained in the following sections.

5.7.2 Methods for Predicting Collection Efficiency
 5.7.2.1 Electrostatic Precipitator

ESP efficiency is predicted from equation (5.6.2-1) and is corrected for sneakage, reentrainment, and rapping reentrainment. A computer program is written based on the method of Cowen et al. (1980). The program assumes that the ESP has six fields and a current density equal to the smaller value calculated from the following two equations:

$$J = 4.12 \times 10^{-3} E_{AV}^5 \quad (5.7.2-1)$$

$$J_M = 6.7 \times 10^4 / \rho_D^{0.987} \quad (5.7.2-2)$$

where J = current density, A/m²
 J_M = maximum allowable current density, A/m²
 E_{AV} = average applied field strength, V/m
 ρ_D = particle resistivity, Ohm-m

Equation 5.7.2-1 is the V-I curve for the ESP and was derived from the gas resistivity reported by Potter (1978) for power plant flue gas. Equation 5.7.2-2 is derived based on Hall's (1971) experimental data which show the effect of resistivity on allowable current density in a precipitator. When $J_M > J$, the applied voltage is reduced to the value so that $J = J_M$.

The ion speed and ion mobility are calculated from the following two equations:

$$v = 25.72 T_G^{0.5} \quad (5.7.2-3)$$

$$b = 1.1 \times 10^{-6} T_G \quad (5.7.2-4)$$

where v = ion speed, m/s
 b = ion mobility, m²/V-A
 T_G = gas temperature, K

The program needs input on SCA, plate-to-plate spacing, applied voltage, gas velocity, and particle size distribution and concentration. The computer then calculates the residence time according to

$$t = \frac{(SCA)}{H/2} \quad (5.7.2-5)$$

where t = residence time, s
 SCA = specific collection area, $m^3/s/m^2$
 H = plate-to-plate spacing, m

and divides the time into six increments. The division of the ESP into time increments is to account for the time dependent nature of the particle charging and particle collection processes. For each time increment, the particle charge, particle migration velocity, and particle penetration through the increment are calculated for several particle diameters. The penetration of a given particle diameter through the ESP is given by:

$$Pt_d = \prod_{i=1}^{n_t} Pt_{di} \quad (5.7.2-6)$$

where Pt_{di} = penetration of particles of diameter d_p through the i^{th} increment
 n_t = number of time increments

The calculated " Pt_d " is then corrected for sneakage, non-uniform gas flow, and reentrainment not due to rapping. First, an effective migration velocity for each diameter for the entire ESP is back calculated from:

$$w_{pe} = \frac{-\ln Pt_d}{A_c/Q_G} \quad (5.7.2-7)$$

The penetration corrected for non-ideal factors $Pt'd_p$ is then calculated from:

$$Pt'd_p = \exp \left(- \frac{w_{pe} A_c/Q_G}{B_S F_G} \right) \quad (5.7.2-8)$$

The non-ideal correction factors " B_S " and " F_G " are calculated from equations 5.6.3-2 and 5.6.3-3 with " S_p " and " σ_G " assumed to be 0.1 and 0.25; respectively.

For ESP on coal-fired power plants, the penetration is corrected for rapping reentrainment according to equation 5.6.5-1 or 5.6.5-2.

In order to obtain the grade penetration curve for the ESP the rapping emissions must be given a size distribution. McDonald (1978a) suggested to use a log-normal size distribution with a mass median diameter of 6.0 μm and a geometric standard deviation of 2.5. This estimate was based on studies of ESP controlled utility boilers.

The rapping reentrainment is added to the "no-rap" outlet emissions to obtain the total outlet mass emissions and particle size distribution.

Although rapping is an important part of the electrostatic precipitation process, the present version of the model does not take into account the temporal and dynamic nature of the rapping process. The time-dependent aspects of the rapping process are of significance because different electrical sections are rapped at different time intervals and the thickness of the collected particulate layer changes with time. The dynamic aspects of the rapping process are of significance because (1) a suitable mechanical force must be applied to a collection electrode in order to remove the collected particulate layer, (2) the force which is necessary to remove the collected particulate layer from the collection electrode depends on such variables as the electrical forces in the layer, the cohesiveness and adhesiveness, etc., and (3) the reentrained particles are recharged and re-collected as the gas flow carries them downstream. Although the empirical procedure employed in the present version of the model represents a useful interim technique for estimating the effects due to rapping reentrainment in precipitators, it is important that models be developed in the future to describe the temporal and dynamic aspects of the rapping process.

5.7.2.2 ESP With Precharging

The basis of the computer model for an ESP with a precharger is the same as a conventional ESP, with a few modifications. This program requires that two applied voltages be given, the precharger voltage and the collector voltage. The initial particle charge is calculated based on the precharger applied voltage. This charge level may increase due to diffusional charging as the particle travels through the ESP. Other parameters and calculation methods remain the same as for a conventional ESP.

5.7.2.3 ESP with Pulse Charging

A theoretical model for estimating efficiency of an ESP with pulse charging is not available. The computer program for con-

ventional ESP's was modified with an empirical relationship reported by Feldman and Milde (1979). The relationship uses a modified migration velocity defined by:

$$1 - \eta = \exp[-(w_k A_C/Q_G)^m] \quad (5.7.2-9)$$

where w_k = modified migration velocity, m/s

m = exponent depending on inlet particle size distribution

Feldman and Milde did not indicate the method of determining the value of "m." However, they used a value of $m = 0.5$ for estimating the efficiency of a pulverized coal boiler. This value was used in the calculations for coal-fired boilers. Values for other sources have not yet been determined.

The computer program calculates the migration velocity without pulsing from the penetration calculated for each particle diameter using the model for a conventional ESP. As was discussed in Section 5.6, this penetration has been corrected for reentrainment, non-uniform gas flow, and sneakage.

$$w_k = \frac{[-\ln Pt_d]^{1/m}}{SCA} \quad (5.7.2-10)$$

where w_k = the modified migration velocity for particles with diameter " d_p " for conventional charging, m/s

$$SCA = A_C/Q_G, \text{ m}^2/\text{m}^3/\text{s}$$

The penetration for an ESP with pulse charging is calculated as follows:

$$w_{kp} = h_p w_k \quad (5.7.2-11)$$

$$Pt'_d = \exp[-(w_{kp} SCA)^m] \quad (5.7.2-12)$$

where Pt'_d = penetration for an ESP with pulse charging, fraction

w_{kp} = modified migration velocity for particles with diameter d_p , using pulsed charging, m/s

h_p = empirical enhancement factor, dimensionless

The enhancement factor, h_p , is equal to the ratio of modified migration velocity with pulsing over that without pulsing. Feldman and Milde (1979) reported that the enhancement factor was 1.33 for a dust resistivity of 2.5×10^{11} ohm-cm and 2.53 for resistivity of 5×10^{12} ohm-cm. In this study, the enhancement factor was determined by interpolation with these two points.

5.7.3 Cost Data
 5.7.3.1 Conventional ESP

The cost of the basic electrostatic precipitator is a function of the plate area. Neveril et al. (1979) gave the following equations for purchase prices of dry type electrostatic precipitators.

uninsulated ESP:

$$p_p = 127,500 + 46.84A \quad (5.7.3-1)$$

insulated ESP:

$$p_p = 198,000 + 70.19A \quad (5.7.3-2)$$

where p_p = purchase price, \$
 A = plate area, m^2

The price is in December, 1981 U.S. dollars and it includes the cost for mechanical rappers or vibrators. It does not include special instruments, such as automatic voltage control.

5.7.3.2 Pulse Charging ESP and ESP with SoRI Precharger

Costs for pulse charging ESP and ESP with SoRI precharger are estimated from the cost data presented by Feldman and Wilde (1978) and Sparks et al. (1980) and the following extrapolation formula of Viner and Ensor (1981):

$$p_p = \left(\frac{SCA}{SCA'} \right)^{0.94} (Q_G/Q'_G)^{0.97} \quad (5.7.3-3)$$

where SCA' = specific collection area of the ESP whose price is known, $m^2/m^3/s$
 Q'_G = gas volumetric flow rate of the ESP whose price is known, Am^3/min

SECTION 5

REFERENCES

- Chang, C. M. and A. D. Rimensberger, 1980. High Intensity Ionizer Technology Applied to Retrofit Electrostatic Precipitators. In: Second Symposium on the Transfer and Utilization of Particulate Control Technology, Vol. II, EPA-600/9-80-039b, U. S. Environmental Protection Agency, Research Triangle Park, North Carolina. pp. 314-333.
- Cowen, S. J., D. S. Ensor, and L. E. Sparks, 1980. TI-59 Programmable Calculator Programs for In Stack Opacity, Venturi Scrubbers, and Electrostatic Precipitators. EPA 600/8-80-024. U. S. Environmental Protection Agency, Research Triangle Park, North Carolina. 152 pp.
- Engelbrecht, H. L., 1979. Air Flow Model Studies for Electrostatic Precipitation. In: Symposium on the Transfer and Utilization of Particulate Control Technology: Volume I. Electrostatic Precipitators. EPA-600/7-79-044a, Environmental Protection Agency, Research Triangle Park, North Carolina. pp. 57-78.
- Feldman, P. L. and H. I. Milde, 1978. Pulsed Energization for Enhanced Electrostatic Precipitation in High-Resistivity Applications. In: Symposium on the Transfer and Utilization of Particulate Control Technology, Vol. I. EPA 600/7-79-044a, U. S. Environmental Protection Agency, Research Triangle Park, North Carolina. pp. 253-279.
- Ferrigan, J. J. III, and J. Roehr, 1980. SO₂ Conditioning for Improved Electrostatic Precipitation Performance Operating on Low Sulfur Coal. In: Second Symposium on the Transfer and Utilization of Particulate Control Technology, Vol. I. EPA 600/9-80-039a, U. S. Environmental Protection Agency, Research Triangle Park, North Carolina. 170-183 pp.
- Gooch, J. P., J. R. McDonald, and S. Oglesby, Jr., 1975. A Mathematical Model of Electrostatic Precipitation, EPA 650/2-75-037, U. S. Environmental Protection Agency, Research Triangle Park, North Carolina. 162 pp.
- Gooch, J. P., R. E. Bickelhaupt, and L. E. Sparks, 1980. Fly Ash Conditioning by Co-Precipitation with Sodium Carbonate. In: Second Symposium on the Transfer and Utilization of Particulate Control Technology, Vol. I. EPA 600/9-80-039a, U. S. Environmental Protection Agency, Research Triangle Park, North Carolina. pp. 132-153.

- Katz, Jacob, 1979. The Art of Electrostatic Precipitation. Precipitator Technology, Inc. Munhall, Pennsylvania. 346 pp.
- Kubo, V. Semi Wet Type ESP for Reducing Rapping Loss. In: Proceedings of the U. S.-Japan Seminar on Measurement and Control of Particulates Generated from Human Activities. November 11-13, 1980, Kyoto, Japan. pp. 175-192.
- Lausen, P., H. Henriksen, and H. Hoegh Petersen, 1979. Energy Conserving Pulse Energization of Precipitators. IEEE-IAS Annual Meeting, Cleveland, Ohio, October 1979. Conference Records, pp. 163-171.
- Luthi, J. E., 1967. Grundlagen zur Electrostatischen Abscheidung von hochohmigen Staeben. Diss. No. 3924, ETHZ, Zurich.
- Masuda, S., I. Doi, M. Agyama and A. Shibiya, 1976. Bias Controlled Pulse Charging System for Electrostatic Precipitator. Strub-Reinhalt, Luft. 36, November 1, pp. 19-26.
- Masuda, S., M. Washizu, A. Mizuno and K. Akutsu, 1978. Boxer-Charger - A Novel Charging Device for High Resistivity Powders. Record of the IEEE/IAS 1978 Annual Meeting, Toronto, Canada. pp. 16-22.
- Masuda, S., 1979a. Novel Electrode Construction for Pulse Charging. In: Symposium on the Transfer and Utilization of Particulate Control Technology, Vol. I. EPA 600/7-79-044a, U. S. Environmental Protection Agency, Research Triangle Park, North Carolina. pp. 241-252.
- Masuda, S., and M. Washizu, 1979b. Ionic Charging of a Very High Resistivity Spherical Particle. Journal of Electrostatics. 6:57-67.
- Masuda, S., A. Mizuno and H. Nakatani, 1979c. Application of Boxer-Charger in Electrostatic Precipitators. Record of the IEEE/IAS Annual Meeting, October 1979, Cleveland, Ohio.
- Masuda, S., and H. Nakatani, 1980a. Boxer-Charger - A Novel Charging Device for High Resistivity Dusts. In: Second Symposium on the Transfer and Utilization of Particulate Control Technology, Vol. II. EPA 600/9-80-033b, U. S. Environmental Protection Agency, Research Triangle Park, North Carolina. pp. 334-351.

- Masuda, S., 1980b. Present Status of Wide-Spacing Type Precipitator in Japan. In: Second Symposium on the Transfer and Utilization of Particulate Control Technology, Vol. II. EPA 600/9-80-033b, U. S. Environmental Protection Agency, Research Triangle Park, North Carolina. pp. 483-501.
- McDonald, Jack R., 1978a. A Mathematical Model of Electrostatic Precipitation (Revision 1): Vol. I. EPA 600/7-78-111a. U. S. Environmental Protection Agency, Research Triangle Park, North Carolina. 645 pp.
- McDonald, Jack R., 1978b. A Mathematical Model of Electrostatic Precipitations (Revision 1): Vol. II. EPA 600/7-78-111b, U. S. Environmental Protection Agency, Research Triangle Park, North Carolina. 645 pp.
- McDonald, J. R. and A. H. Dean, 1980. A Manual for the Use of Electrostatic Precipitators to Collect Fly Ash Particles. EPA 600/8-80-025, U. S. Environmental Protection Agency, Research Triangle Park, North Carolina. 782 pp.
- McDonald, J. and L. Sparks, 1977. A Precipitator Performance Model: Application to the Nonferrous Metals Industry. Proceedings: Particulate Collection Problems Using ESP's in the Metallurgical Industry. EPA-600/2-77-208, U. S. Environmental Protection Agency, Raleigh Durham, North Carolina. 72 pp.
- Mosley, R. B., M. H. Anderson, and J. R. McDonald, 1980. A Mathematical Model of Electrostatic Precipitation (Revision 2). EPA 600/7-80-034, U. S. Environmental Protection Agency, Research Triangle Park, North Carolina. 401 pp.
- Oglesby, S., Jr., and G. B. Nichols, 1970. A Manual of Electrostatic Precipitation Technology, Part I and II. National Air Pollution Control Administration, Cincinnati, Ohio. 322 pp.
- Patterson, R. G., P. Riersgard, R. Parker, and S. Calvert, 1979. Effects of Conditioning Agents on Emissions from Coal-Fired Boilers: Test Report No. 1. EPA-600/7-79-104a, U. S. Environmental Protection Agency, Research Triangle Park, North Carolina. 61 pp.
- Penney, G. W. and P. C. Gielfand, 1978. The Trielectric Electrostatic Precipitator for Collecting High Resistivity Dust. Journal of the Air Pollution Control Association. Vol. 28, No. 1, pp. 53-55.

- Peterson, H. Hoegh and P. Lausen, 1980. Precipitator Energization Utilizing an Energy Conserving Pulse Generator. In: Second Symposium on the Transfer and Utilization of Particulate Control Technology. Vol. I. U. S. Environmental Protection Agency, Research Triangle Park, North Carolina. pp. 352-368.
- Pontius, D. H., L. G. Felix, J. R. McDonald, and W. B. Smith, 1977. Fine Particle Charging Development. EPA 600/2-77-173, U. S. Environmental Protection Agency, Washington, D.C. 222 pp.
- Pontius, D. H. and L. E. Sparks, 1978. A Novel Device for Charging High Resistivity Dust. Journal of the Air Pollution Control Association. 28:698.
- Pontius, D. H., P. V. Bush, and W. B. Smith, 1979a. Electrostatic Precipitators for Collection of High Resistivity Assoc. EPA 600/7-79-189. U. S. Environmental Protection Agency, Research Triangle Park, North Carolina. 187 pp.
- Pontius, D. H., P. V. Bush, and L. E. Sparks, 1979b. A New Precharger for Two Stage Electrostatic Precipitation of High Resistivity Dust. In: Symposium on the Transfer and Utilization of Particulate Control Technology: Volume I. EPA-600/7-79-044a, U. S. Environmental Protection Agency, Research Triangle Park, North Carolina. pp. 275-286.
- Roehr, Jack D, 1980. Composition of Particulates, Some Effects on Precipitation Operation. In: Second Symposium on the Transfer and Utilization of Particulate Control Technology, Vol. II. EPA 600/9-80-039b. U. S. Environmental Protection Agency, Research Triangle Park, North Carolina, p. 208-218.
- Smith, W., K. Cushing, and J. McCain, 1977. Procedures Manual for Electrostatic Precipitator Evaluation. EPA-600/7-77-059, Environmental Protection Agency, Research Triangle Park, North Carolina. p. 18.
- Sparks, L. E., 1978. SR-52 Programmable Calculator Programs for Venturi Scrubbers and Electrostatic Precipitators. EPA 600/7-78-026. U. S. Environmental Protection Agency, Washington D.C. 70 pp.
- Sparks, L. E., G. H. Ramsey, B. E. Daniel and J. H. Abbott, 1980. Pilot Plant Tests of an ESP Preceded by the EPA-SORI Precharger. In: Second Symposium on the Transfer and Utilization of Particulate Control Technology, Vol. II. EPA 600/9-80-039b. U. S. Environmental Protection Agency, Research Triangle Park, North Carolina. 535 pp.

- Surati, H., M. R. Beltran, and I. Raigoradsky, 1980. Tubular Electrostatic Precipitators of Two Stage Design. In: Second Symposium on the Transfer and Utilization of Particulate Control Technology, Vol. II. EPA 600/9-80-039b, U. S. Environmental Protection Agency, Research Triangle Park, North Carolina. pp. 469-482.
- Szabo, M. and R. Gerstle, 1977. Electrostatic Precipitator Malfunctions in the Electric Utility Industry, Section 2. EPA-600/2-77-77-006, U. S. Environmental Protection Agency, Rsearch Triangle Park, North Carolina. pp. 16.
- White, H. J., 1952. A Pulse Method for Supplying High-Voltage Power for Electrostatic Precipitation. Transactions of the AIEE, Nov. 1952.
- White, H. J., 1963. Industrial Electrostatic Precipitation. Addison Wesley Publishing Co., Inc., Reading Massachusetts. 376 pp.
- White, H. J., 1977. Electrostatic Precipitation of Flyash. Journal of the Air Pollution Control Association. 17:15-21, 114-120, 206-217, 308-318.

SECTION 6

FILTERS

6.1 INTRODUCTION

As an industrial air pollution control device gas, filters may be broadly classified into one of two kinds--fabric, or cloth filters and in-depth, or bed filters. The former is represented by various fabric bag arrangements while the latter is most frequently encountered as a fibrous array, a paperlike mat, and occasionally, as a deep packed bed. Fabric filters are generally utilized with gas or air streams having a dust loading of order of 1 g/m^3 . Fibrous packings or paper filters, are applied when the particule concentration is several orders of magnitude less, and find their most extensive use in air conditioning, heating and ventilating systems. Therefore, fibrous filters will not be considered in this report.

There are three major performance criteria for a filter: pressure loss; collection efficiency; and lifetime, which is related to endurance and dust holding capacity. Pressure loss is usually expressed in terms of centimeters of water (water column) and is directly proportional to the required fan or blower horsepower, or energy. The pressure loss is a major index of the operating cost of a filtration system.

Fabric filters remove particles from the gas stream by inertial impaction, diffusion, direct interception, and sieving. The first three processes prevail only briefly, during the first few minutes of filtration with new or just-cleaned fabrics; the sieving action of the dust cake on the filter surface predominates thereafter. Pinholes can form in the dust cake which decreases the particle collection efficiency.

The lifetime of a filter is very important from the economic standpoint because the cost of the filtering medium is a major portion of the initial expense as well as of long-term operating costs. It is difficult, however, to estimate filter life from desired operating conditions for any application unless a background of experience is first established.

6.2 GENERAL DESIGN FEATURES

Fabric filters can be designed to operate either with the gas flowing out of the bag (dust deposited on the inside), or with the gas flowing into the bag (dust deposited on the outside). Eventually the dust will build up on the fabric surface to form a fine porous cake. The cake must be removed periodically in order to keep the gas pressure drop across the filter within acceptable limits (typically 10 to 50 cm W.C.).

A wide range of dust concentrations (mass loadings) and size distributions can be handled by fabric filters. Usually they are

used for controlling large concentrations of fine dust or fume. They are not suitable for controlling gases which contain large quantities of sticky or liquid particles. The presence of moisture can cause excessive pressure drop, chemical or biological attack, and mechanical failure of the fabric. When dust hardens after being wetted, subsequent cleaning can cause fiber breakage.

Commercially available fabrics are limited to temperatures below 290°C (550°F) although higher temperature fabrics are likely to be available in the future. The temperature limit varies with the fabric and is determined by the temperature at which accelerated fabric deterioration or abrasion occurs.

6.2.1 Types of Fabric

Selection of the filter fabric is one of the most important decisions in baghouse design. The properties of many common natural and synthetic fibers are listed in Table 6.2.1-1. Most of these materials are available as both woven and felted fabrics.

The most important properties to be considered are the maximum operating temperature, chemical resistance, and abrasion resistance. In general, lower operating temperatures (but above the dew point) will result in longer bag life and therefore lower operating costs. However fabric costs vary over an order of magnitude from glass (inexpensive) to Teflon (expensive) and therefore must be considered in defining an acceptable bag life.

Of the many synthetic fiber fabrics on the market there are none which show good properties in all applications. Once the temperature and chemical composition of the gas are known, it is possible to identify a number of fabrics which are suitable. Then, the choice among suitable fabrics must involve cost, abrasion resistance, the desired cleaning method, and general or specific experience.

6.2.2 Bag Geometry

The most common baghouse filter element is a circular cylindrical tube 12 to 15 cm (5 to 6 in.) in diameter. Glass fiber bags of 30 cm (12 in.) diameter are sometimes used in high temperature applications. Smaller bags provide a larger surface to volume ratio and therefore have the advantage of providing more filter surface for a given bag length. Bag lengths are typically 1.5 to 3 m (5 to 10 ft), but can be 9 m (30 ft) or longer.

6.2.3 Cleaning Methods

The major distinction between bag house designs is the method used to remove the dust cake from the bags. Various bag cleaning methods are compared in Table 6.2.3-1. The basic designs can be broken down into seven general methods: mechanical shaking, reverse air flow, reverse air jet, high energy pulse,

TABLE 6.2.1-1. CHARACTERISTICS OF FABRIC FILTER MATERIALS^{f, g}

Fiber Name	Trade Name	PHYSICAL CHARACTERISTICS				RESISTANCE TO ATTACK BY			Fabric Type	Surface Treatment Required?	Comment
		Flex Resistance	Specific Gravity	Moisture Content %	Maximum Temp. °F	Acid	Base	Organic Solvent			
Acrylic		Fair	-	-	275	Good	Good	-	Woven, Felt	No	
Acrylonitrile	Orlon	Fair	1.2	1	250	Good	Fair	Good ^a	-	-	
Asbestos		Poor	3.0	1	500	Fair ^b	Fair	Good	-	-	
Cotton		Good	1.6	7	180	Poor	Fair	Good	Woven	-	Low Cost
Glass	Fiberglass Huyglas	Good	2.5	0	550	Good ^c	Good	Good	Woven	Yes	Poor Resistance To Abrasion
		Excellent	-	-	550	Good	Good	Good	Felt	Yes	
Graphitized Fiber		Poor	2.0	10	500	Fair	Good	Good	-	-	Expensive
Nylon (Polyamide)		Good	1.1	5	220	Fair	Good	Good ^d	Woven	-	Easy to Clean
	(Aramid) Nomex	Excellent	1.4	5	450	Fair	Good	Good	Woven, Felt	Yes	Poor Resistance To Moisture
(Aramid) Kevlar		Fair	-	-	450	Poor	Good	-	Woven	No	
Paper		Poor	1.5	10	180	Poor	Fair	Good	-	-	Low Cost
Polybenamidazole	PBI	Excellent	-	-	500	Excellent	Excellent	-	Woven, Felt	No	Pilot Plant
Polyester	Dacron	Good	1.4	0.4	280	Good	Fair	Good ^e	-	-	
Polyethylene		Good	1.0	0	250	Fair	Fair	Fair	-	-	
Polyimide	PRD-14	Good	-	-	500	Excellent	Excellent	-	-	No	Experimental
Polyoxadiazol	Oxylon	Fair	-	-	500	Good	Fair	-	-	No	Experimental
Polyphenylene Sulfide	Ryton	Good	-	-	350	Excellent	Excellent	-	Woven, Felt	No	
Tetraflouro - Ethylene	Teflon	Fair	2.3	0	500	Excellent	Excellent	Good	Woven, Felt	No	Expensive
Vinylidene Chloride	Vinyl	Fair	1.7	10	210	Good	Fair	Good	-	-	
Wool		Good	1.3	15	210	Fair	Poor	Good	-	-	
	Stilan	Excellent	-	-	500	Excellent	Excellent	-	-	No	Experimental

^aExcept heated acetone

^bExcept SO₂

^cWith proper surface treatment

^dExcept phenol and formic acid

^eExcept phenol

^fInoya etc. (1977)

^gPower (1980)

TABLE 6.2.3-1. COMPARISON OF BAG CLEANING METHODS

Cleaning method	Uniformity of cleaning	Bag attrition	Equipment ruggedness	Type fabric	Filter velocity	Apparatus cost	Power cost	Dust loading	Submiron efficiency
Shaking	A	A	A	Woven	A	A	L	A	G
Reverse flow, no flexing	G	L	G	Woven	A	A	M-L	A	G
Reverse flow, with collapse	A	H	G	Woven	A	A	M-L	A	G
Pulse-compartment	G	L	G	Felt, woven	H	H	M	H	H
Pulse-bags	A	A	G	Felt, woven	H	H	H	VH	H
Reverse-jet	VG	A-H	L	Felt, woven	VH	H	H	H	VH
Vibration, rapping	G	A	L	Woven	A	A	M-L	A	G
Sonic assist	A	L	L	Woven	A	A	M	-	G
Manual flexing	G	H	-	Felt, woven	A	L	-	L	G

Note: A=average; G=good; H=high; L=low; M=medium; VG=very good; VH=very high.

phenum pulse, vibration or rapping and sonic assist.

All cleaning methods have the same purpose; that is, to remove the dust cake from the filter surface quickly and uniformly without removing too much residual dust, without damaging the fabric, and without excessively redispersing the collected dust particles.

6.2.3.1 Mechanical Shaking

Bags are shaken from above with a combination of horizontal and vertical motion as shown in Figure 6.2.3-1. The dust cake collected on the inside of the bag breaks off and falls into the hopper.

Filtration must be stopped while shaking or the dust will work through the filter and decrease the efficiency. The filtration cycle should be much longer than the cleaning cycle to allow time for the formation of good cake and, more important, to prevent too many units from being off line for cleaning at one time. For this reason, shaker-type baghouses are not used where very heavy dust loadings are encountered.

Low initial capital investment makes this cleaning method preferable for very large installations. However, bag life can be shorter than with other cleaning methods.

6.2.3.2 Reverse Flow

Two basic designs are used in reverse gas flow cleaning: simple collapsing and reserve flow without flexing. Figures 6.2.3-2 and 6.2.3-3 show both types. In simple collapsing, the reverse flow of gas causes the bag to collapse almost completely. The dust cake will break off in large pieces. Reverse flow without flexing is achieved by supporting the bag with metal rings or mesh sewn into the fabric. This is the gentlest method of cleaning and is effective only if the dust can be released from the filter easily.

Either type of reverse flow cleaning requires the filter to be off-line during cleaning. One disadvantage of these cleaning methods is that the gas used for cleaning must be refiltered through the on-line units. This increases the effective flow through the baghouse system.

Reverse air flow cannot be used to clean panel type filters or felted filters. Wear caused by flexing and abrasion of the fabric on the support rings during the cleaning cycle results in serious problems.

6.2.3.3 Reverse-Air Jet

Reverse-air jet filters are designed as shown in Figure 6.2.3-4. Filtration occurs continuously and the dust is removed by a reverse jet of pressurized air (15 to 70 cm W.C. pressure) blown through a ring which travels up and down the outside of the

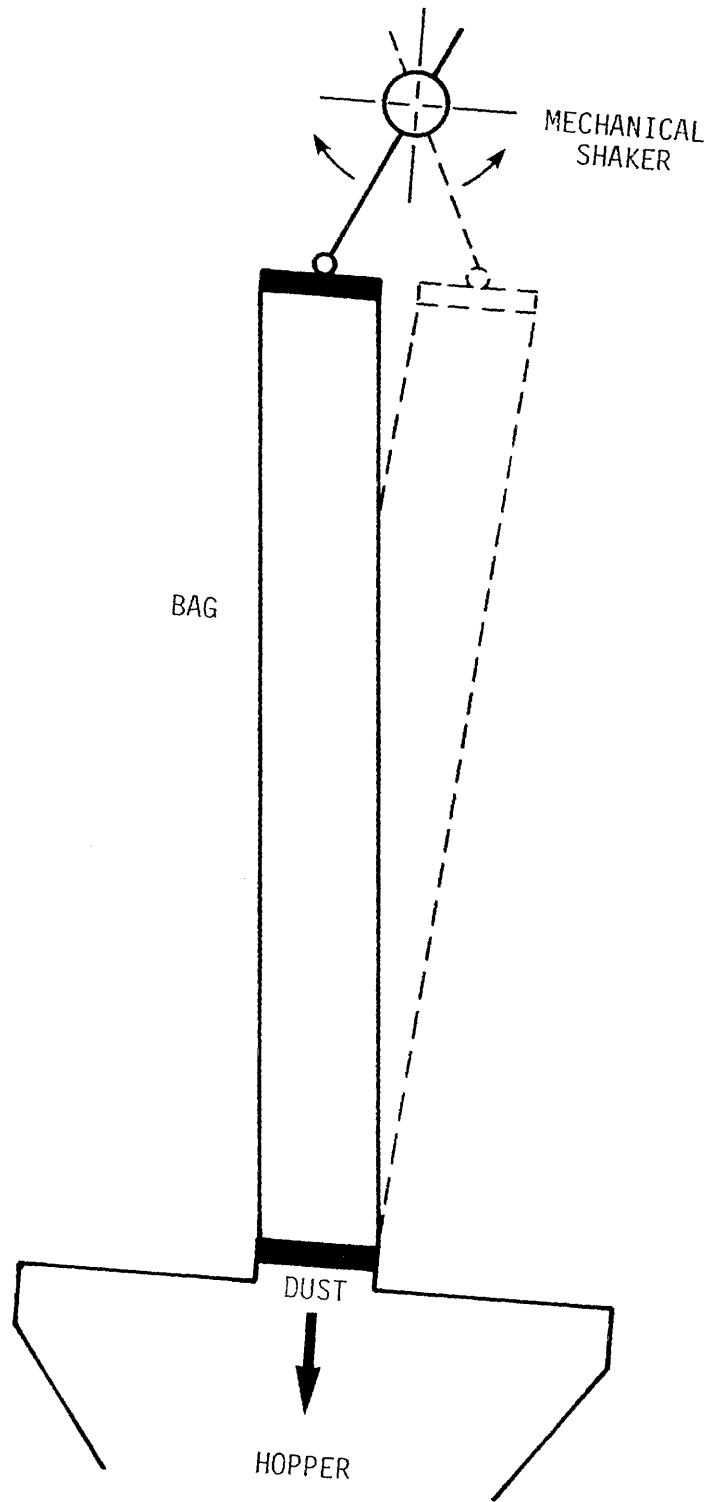


Figure 6.2.3-1. Shaker cleaning method.

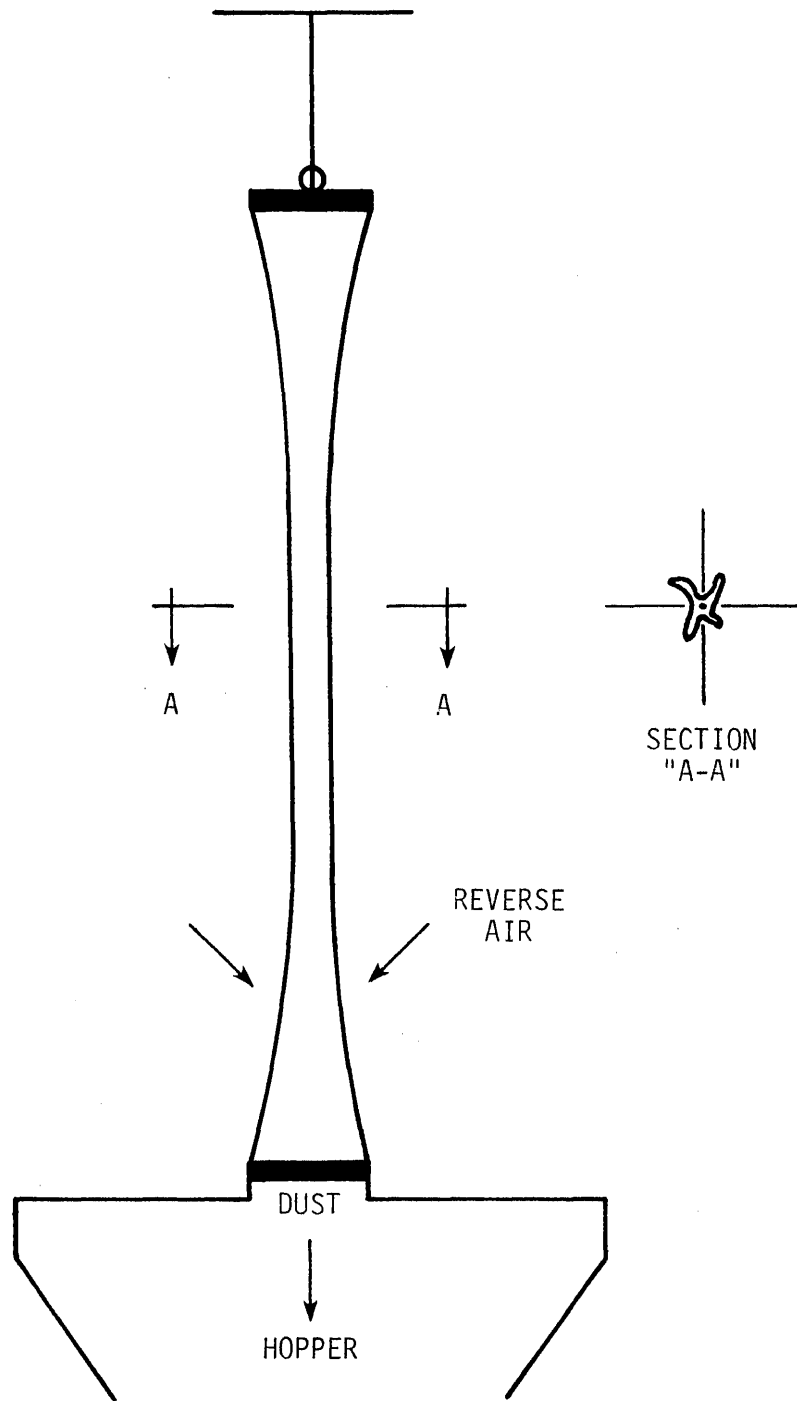


Figure 6.2.3-2. Reverse flow simple collapse cleaning method.

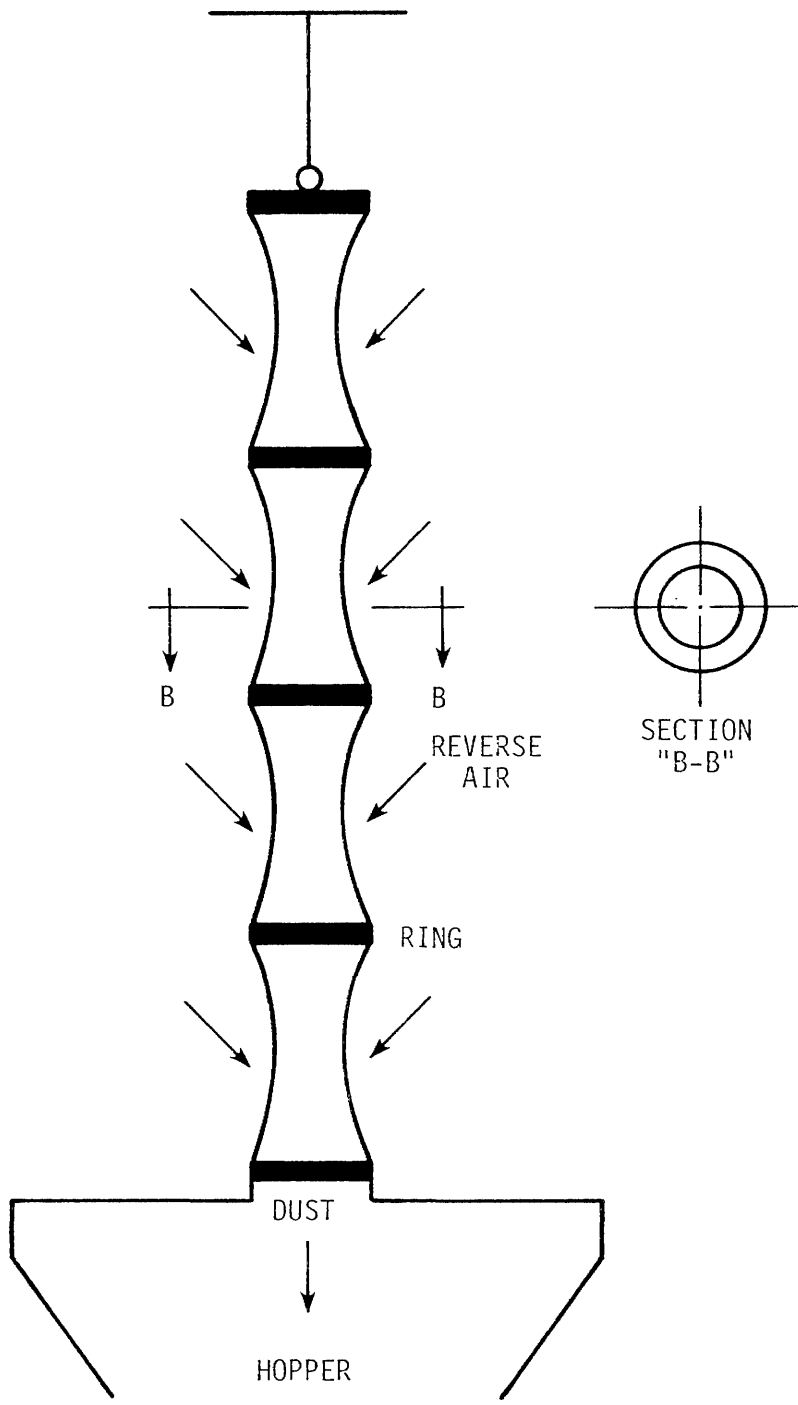


Figure 6.2.3-3. Reverse flow without flexing cleaning method.

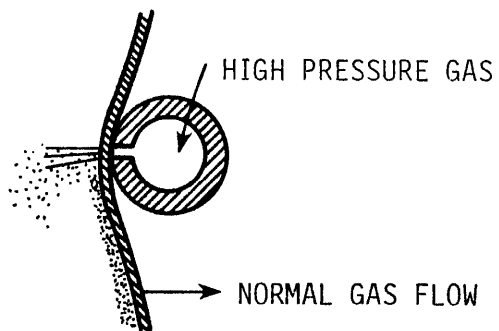
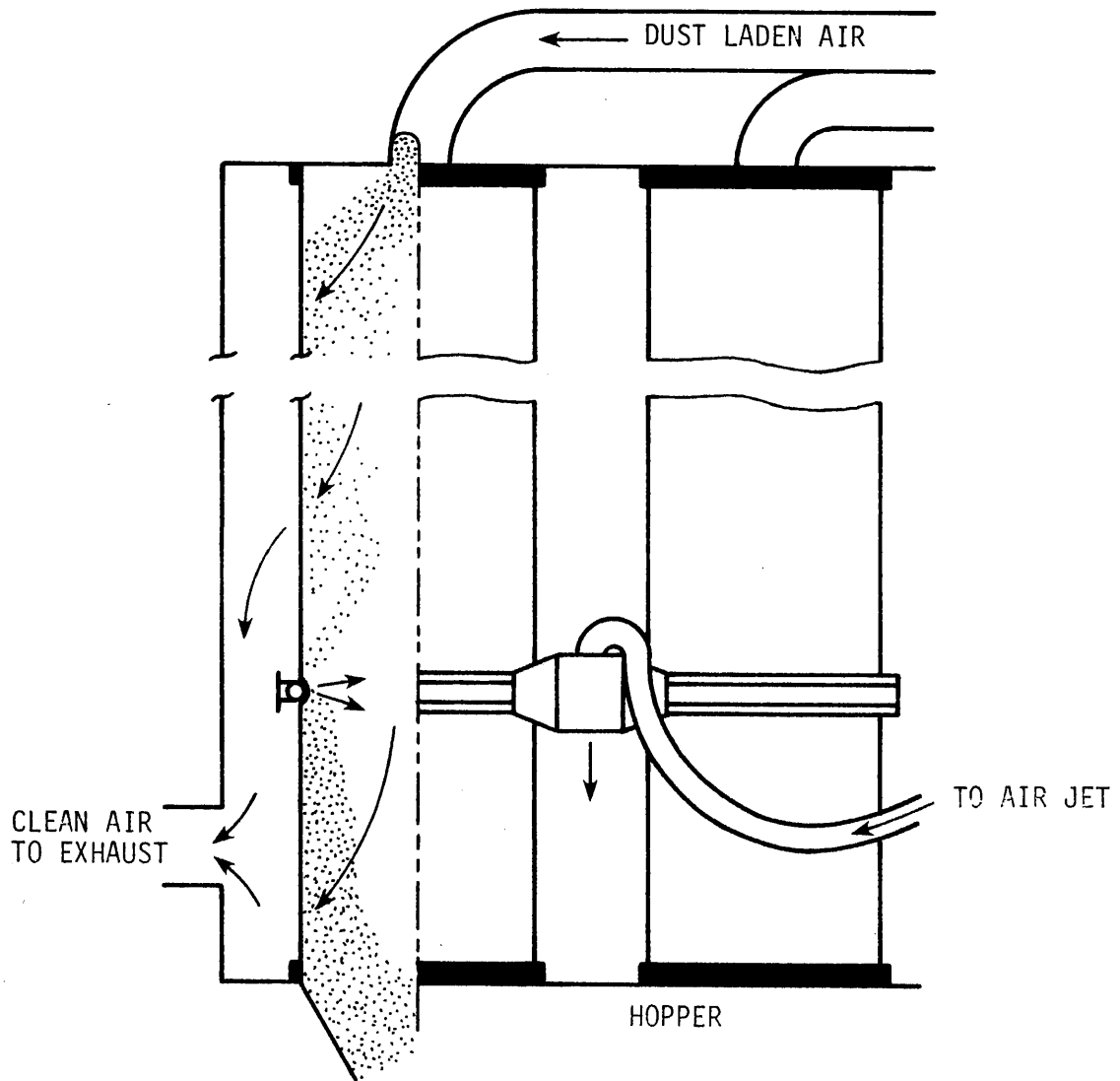


Figure 6.2.3-4. Reverse-air jet filter cleaning method.

bag. This is very effective in removing the dust, even to the extent of removing much of the residual dust inside the fabric. Consequently, it is used most commonly with felted fabrics which can achieve very high collection efficiencies without relying on the presence of residual dust.

Although very high air-to-cloth ratios are permissible (on the order of 1.5 to 9 m³/min/m²), the collector has not been used extensively on large air pollution control applications. The expense and complication of the media-cleaning machinery (motors, drives, and switches for both ring and fan) have limited the unit to rather small air-flows. It has found most favor in the process industries where it is used as a pneumatic conveying receiver.

6.2.3.4 High Energy Pulse

The high energy pulse filter is illustrated in Figure 6.2.3-5. Cleaning is achieved by a pulse of reverse compressed air while the adjacent bags are filtering. The fabric receives a minimum of flexural wear and the filter installation is smaller because cleaning is carried out while the filter is on-line. The cleaning pulse requires a negligible amount of time (0.1 sec).

Felt bags are used in high energy pulse systems, since woven cloths tend to be overcleaned by pulsing. Because felts can handle higher filtration velocities than woven cloth, pulse filter installations can be smaller than shaker or reverse flow installations. Also, pulse cleaning can handle very heavy dust loadings because frequent cleaning can be achieved without severely restricting the gas flow.

Pulse filters are generally more expensive to operate, largely because of the power requirements of the compressor. Felted fabrics are relatively expensive but generally have a longer life than woven cloth. The absence of moving parts and the ease of replacing the bags, means less time is needed for maintenance in high energy pulse systems.

6.2.3.5 Plenum Pulse

This method attempts to overcome some of the difficulties associated with other methods of cleaning. In this kind of equipment a sharp pulse of compressed air is released in the plenum chamber giving rise to some combination of shock, fabric deformation and flow reversal. The result is the removal of the dust deposit without more than a brief interruption of the filtering flow. The fabric receives a minimum of flexural wear, and the filter installation is smaller because the fabric is in use practically all the time.

The main distinction of pulsed equipment is the brief cleaning time, typically around one-tenth of a second. The very low ratio of cleaning time to filtering time makes pulsed equipment useful at high dust loadings.

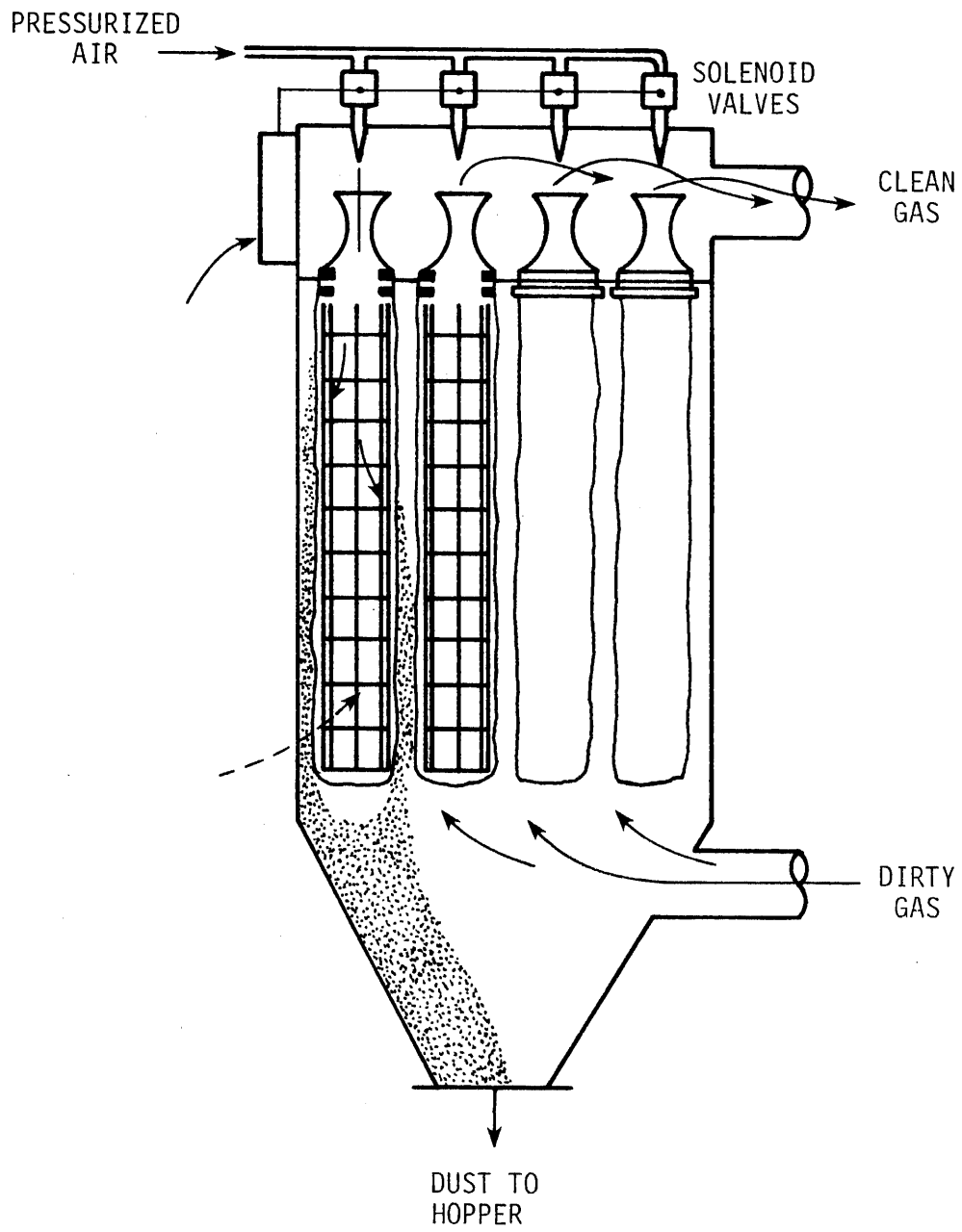


Figure 6.2.3-5. High energy pulse cleaning method.

6.2.3.6 Vibration or Rapping

This method of cleaning is particularly successful with deposits that adhere relatively loosely to the bags. The vibration or rapping causes stresses at the fabric-cake interface which, in turn, release the dust cake from the fabric.

6.2.3.7 Sonic Assist

Agitation frequencies still higher than those used in vibration or rapping have been attempted with ultrasonic and sonic cleaning methods. Although these frequencies are known to slightly improve the preagglomeration of a few fine dusts, they have not, on the whole, been very effective in fabric cleaning.

6.3 BAGHOUSE FILTER FUNDAMENTAL

With fabric bags, filtration is principally accomplished by the particle layer that accumulates on the fabric surface. Therefore, it is difficult to predict filter pressure loss and collection efficiency without making preliminary tests. The bag filter has not been successfully analyzed theoretically, because of the filtering action of the dust layer.

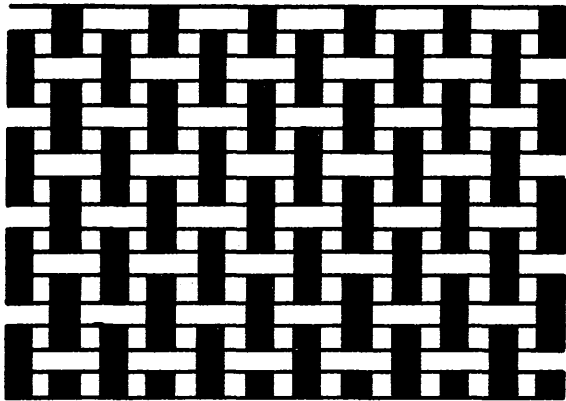
6.3.1 Weave Characteristics

Table 6.2.1-1 presents the basic properties of fibers that are widely used at the present time and Figure 6.3.1-1 shows weave types--twill and sateen being favored. The performance of any fabric is greatly influenced by thread density, fiber composition, and nap, i.e., the hairy or down texture of the cloth surface.

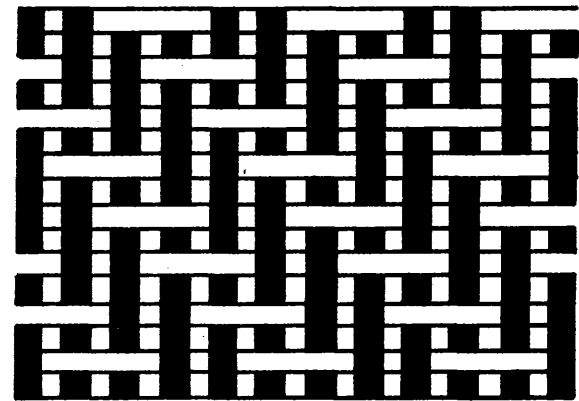
The electrostatic properties of both the dust and the collecting fabric influence filtering and cleaning performance (Silverman et al., 1955; Whitby et al., 1961; Frederick, 1961; Butterworth, 1964; Lundgren et al., 1965). Fibers and fabrics conform to a triboelectric series as indicated in Table 6.3.1-1 and dusts may be classified in a similar series. The charge intensity developed on either the fabric or the dust, or both, depends upon the processing conditions, as well as on the nature of the materials themselves. The charge dissipation rate is an especially important property in the dust cleaning process. A fabric bag into which is woven stainless-steel fibers or wire is most effective when dislodging dust that is particularly adhesive because of retained electrostatic charges and for protection from fire arising from electrostatic discharges. As yet, not enough is known about how best to utilize these factors in the design and operation of particular systems.

While in the past, most filter media were woven fabrics, recent years have seen the introduction of nonwoven materials such as fleeces and felts (Rudiger, 1971). The term "fabric

PLAIN



TWILL 2/2



SATEEN

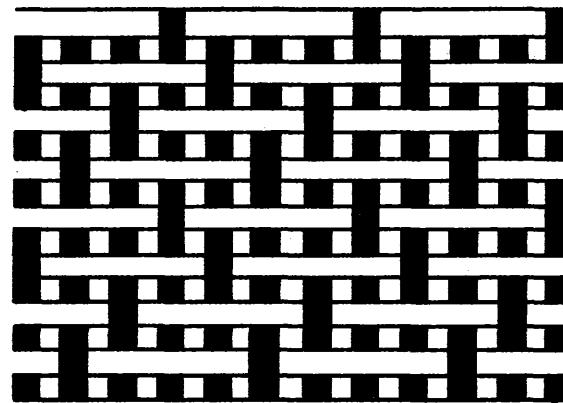


Figure 6.3.1-1. Filter cloth weaves.

TABLE 6.3.1-1.. ELECTROSTATIC CHARGING ORDER OF FILTER FIBERS^a.

<u>Material</u>	<u>Relative Charge generation</u>
Wool	+20
Silicon-treated glass (filament and spun)	+15
Woven wool felt	+11
Nylon (spun)	+7 to +10
Cotton (sateen)	+6
Orlon (filament)	+4
Dacron (filament)	0
Dynel (spun)	-4
Orlon (spun)	-5 to -14
Dacron (spun)	-10
Steel	-10
Polypropylene (filament)	-13
Acetate	-14
Saran	-17
Polythylene (filament and spun)	-20

a.. Frederick (1961)

filters" is not applied to this type of medium; instead the more general term "filter cloth" is used.

6.3.2 Pressure Loss

In general, gas flow through fabric filters is laminar (Davies, 1952; Cunningham et al., 1954; Iinoya et al., 1956). The pressure loss, being the sum of the loss due to the filter itself and the deposited particle layer, may be written as:

$$\Delta P = \Delta P_O + \Delta P_p = (k_1 + k_2 W) u_S \mu_G \quad (6.3.2-1)$$

where ΔP = pressure loss, N/m²

ΔP_O = pressure loss due to filter only, N/m²

ΔP_p = pressure loss due to deposited particle layer, N/m²

k_1 = pressure loss coefficient for clean filter, 1/m

k_2 = average specific resistance of collected particle layer, m/kg

W = collected dust loading in the filter, kg/m²

u_S = filtering gas velocity (superficial), m/s

μ_G = gas viscosity, kg/m-s

The pressure loss coefficient for a clean filter depends upon the fabric; it usually is negligibly small in practical applications. However, its value should be larger than a certain minimum for initial collection performance. For clean fabric, the filtering air velocity at which the pressure loss, ΔP_O , equals 1.3 cm W.C. is called the permeability.

The average specific resistance of a collected particle bed depends upon the particle size, the volumetric voids in the bed, and the density of the particles. Values as indicated by Figure 6.3.2-1 (Kimura et al., 1965) are typical. The terms of Equation (6.3.2-1) might have values as follows:

$$k_1 = 7 \times 10^7 \text{ m}^{-1}$$

$$k_2 = 3.0 \times 10^{10} \text{ m/kg}$$

$$W = 0.12 \text{ kg/m}^2$$

$$u_S = 0.017 \text{ m/s}$$

$$\mu_G = 1.81 \times 10^{-4} \text{ kg/m-s (at 760 mm Hg and 20°C)}$$

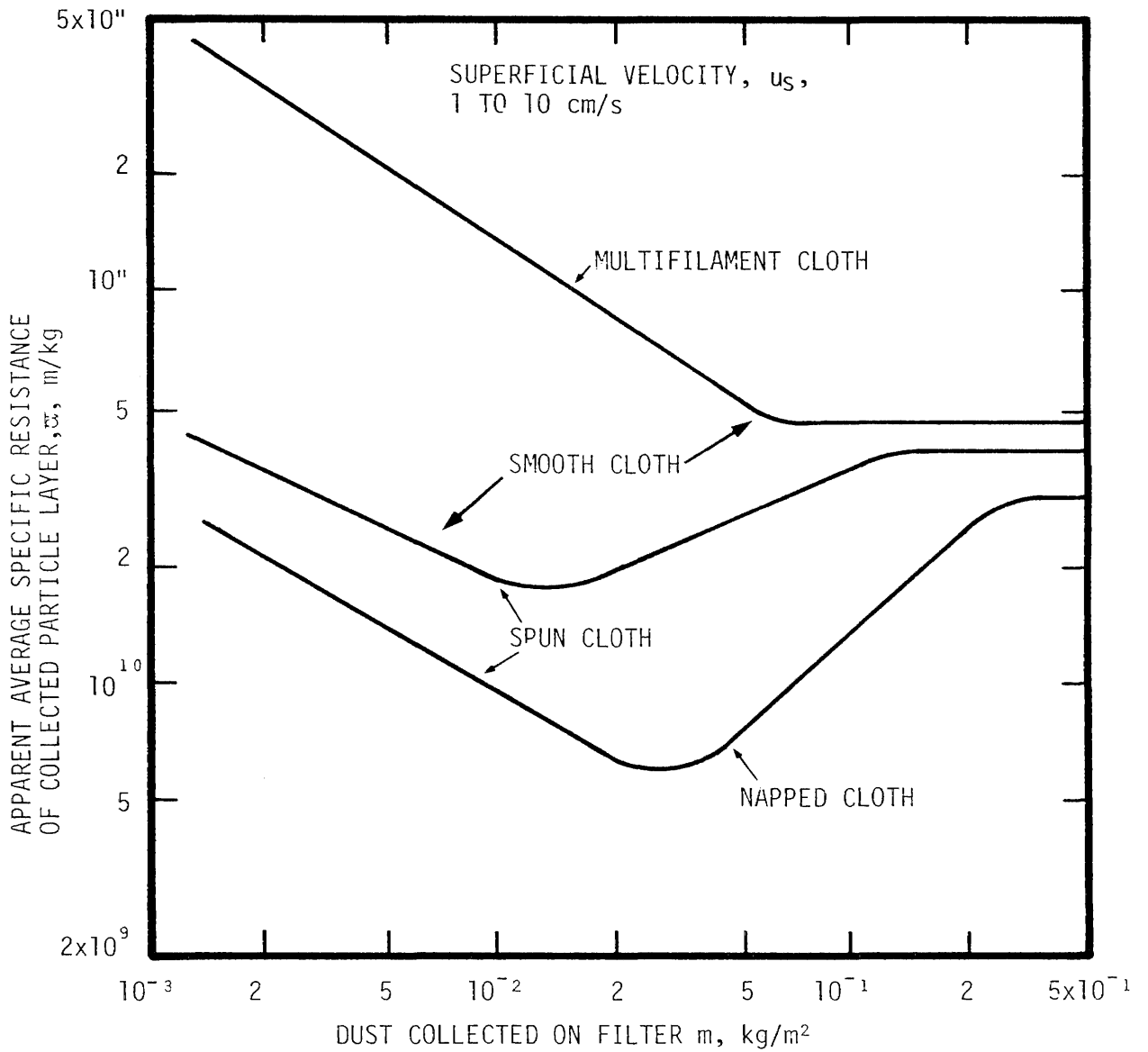


Figure 6.3.2-1. Effect of fabric on average specific resistance of dust layer, Kimura et al, (1965).

Substituted into the equation, these result in a pressure loss of 11.5 cm W.C. (or 4.4. in. W.C.).

The change in pressure loss due to collected particles during filtration may be obtained from the Kozeny-Carman relationship (Kimura et al., 1965) written

$$\frac{d(\Delta P_p)}{dW} = \frac{180\mu_G u_s (1-\epsilon_a)}{g_c \rho_p d_{ps}^2 \epsilon_a^3} \quad (6.3.2-2)$$

where ϵ_a = apparent volumetric void fraction of particle layer, dimensionless

ρ_p = density of particle, kg/m³

d_{ps} = specific area diameter of particle, m

The apparent volumetric void is obtained from Figure 6.3.2-2. For example, using the values of " u_s " and " μ_G " as above, $\rho_p = 3,000$ kg/m³, $d_{ps} = 0.40 \times 10^{-5}$ m, and $\epsilon_a = 0.96$, equation (6.3.2-2) gives a value for " $d(\Delta P_p)/dW$ " of 53.2 cm W.C./kg of dust/m² of cloth area. However, the permeability of the dust cake on the cloth varies with the operating conditions of the bag filter in a way that significantly affects the pressure drop (Borgwardt et al. 1968).

Typical gas flow behavior to be expected within a multicompartment baghouse is presented in Figures 6.3.2-3 and 6.3.2-4. (Walsh, et al., 1960; Robinson, et al., 1967; Solvach, 1969) The effect of the number of compartments on the cleaning cycle is shown in Figure 6.3.2-5, which indicates that many compartments prolong the cleaning period (Tanaka et al., 1973).

A nonwoven cloth is often the more favorable filter medium because the pressure loss after cleaning is lower and remains essentially constant if a strong cleaning method, for example, a pulsating reverse air jet, is employed (Dennis, 1952).

The following values are common for conventional bag filters under normal operations:

$$\Delta P = 10-20 \text{ cm W.C.}$$

$$W = 0.05-0.03 \text{ kg/m}^2$$

$$k_2 = 10^{10}-10^{11} \text{ m/kg}$$

$$u_s = 0.8-5 \text{ cm/s}$$

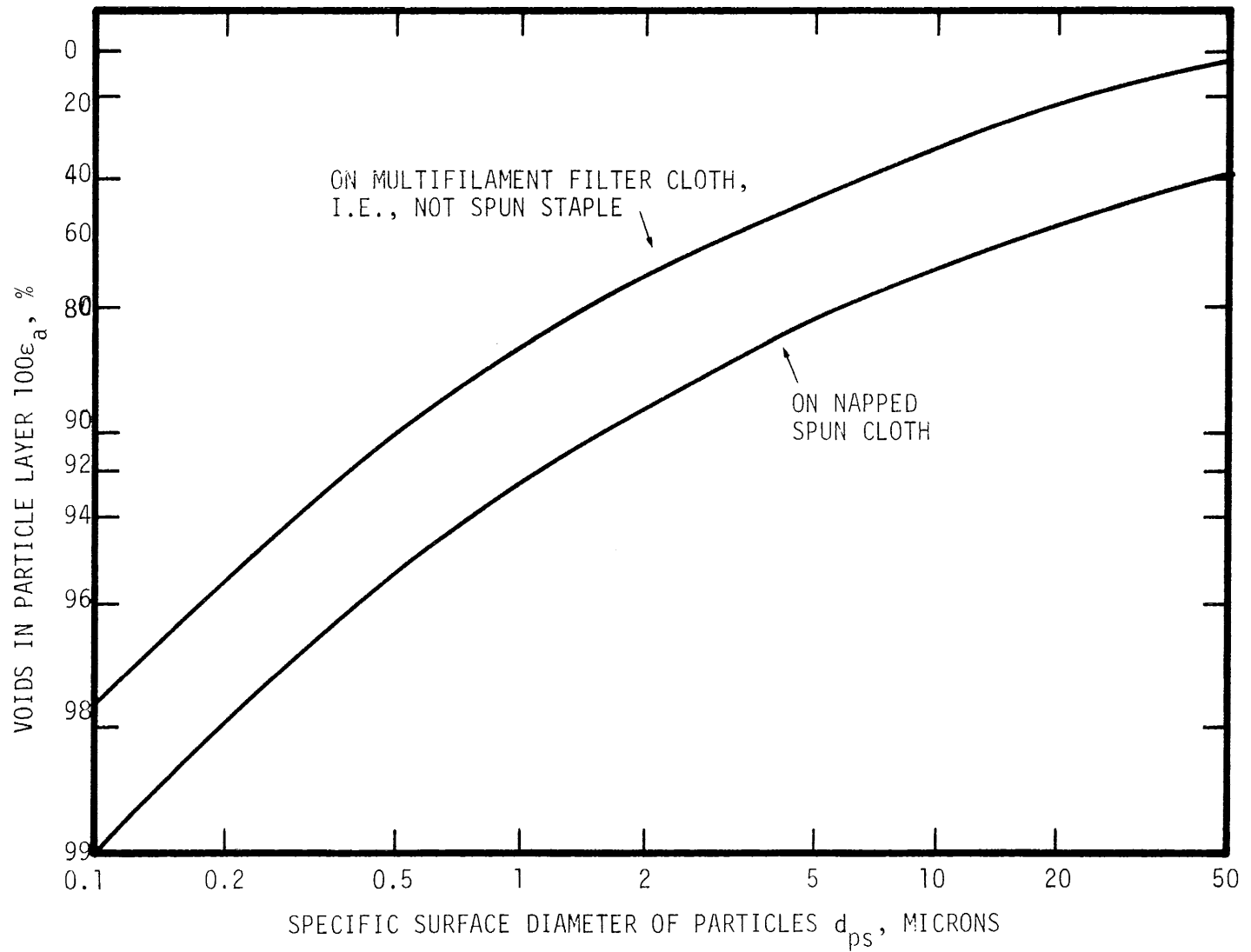


Figure 6.3.2-2. Relation between specific surface diameter of particles to be collected and voids of collected particle layer, Kimura et al. (1965).

6T-9

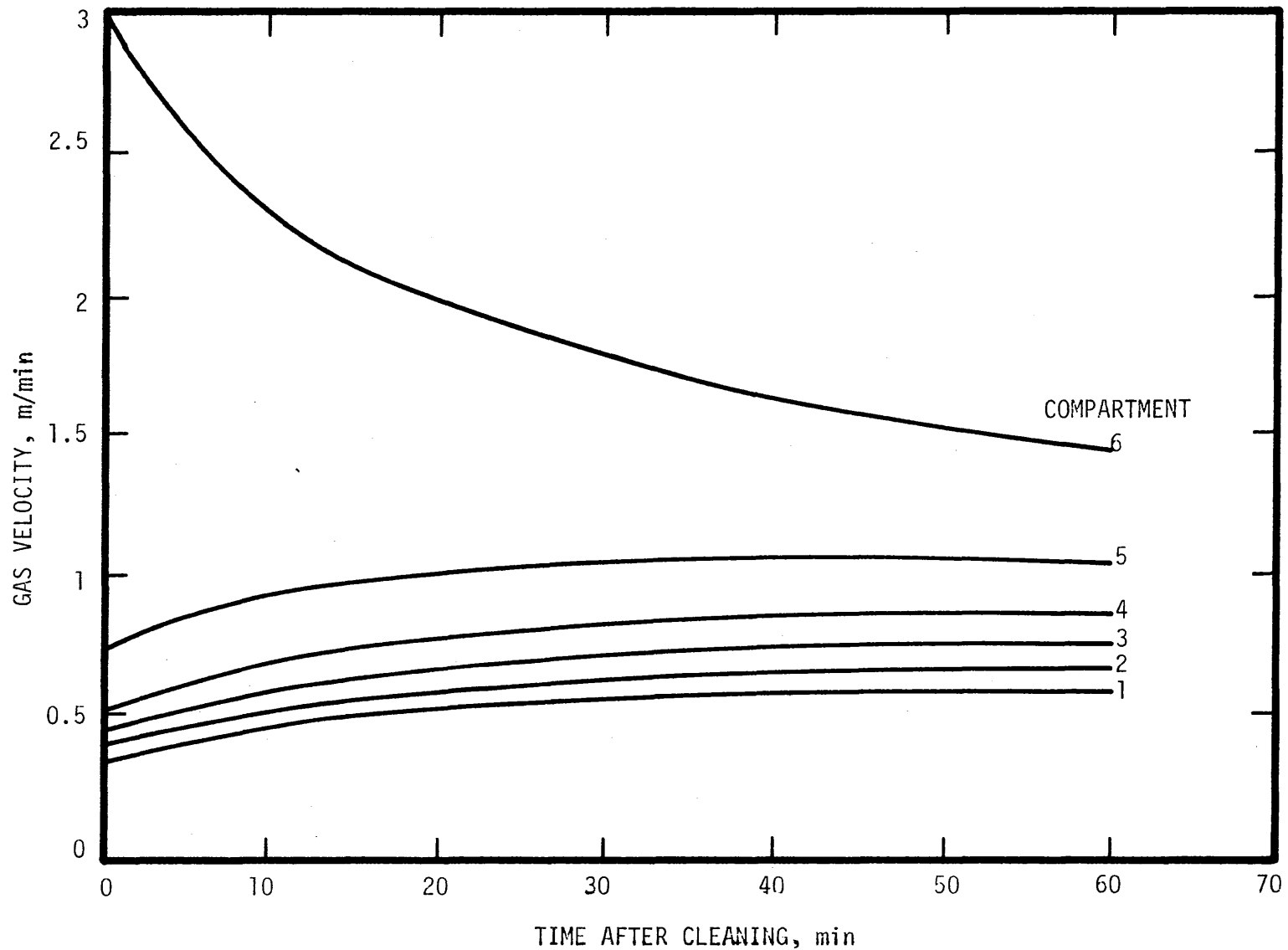


Figure 6.3.2-3. Velocity pattern in six-compartment bag house as a function of time. Average velocity, 1 m/min; initial compartment pressure loss, 1.7 cm W.C./m/min; final compartment pressure loss, 17 cm W.C./m/min.

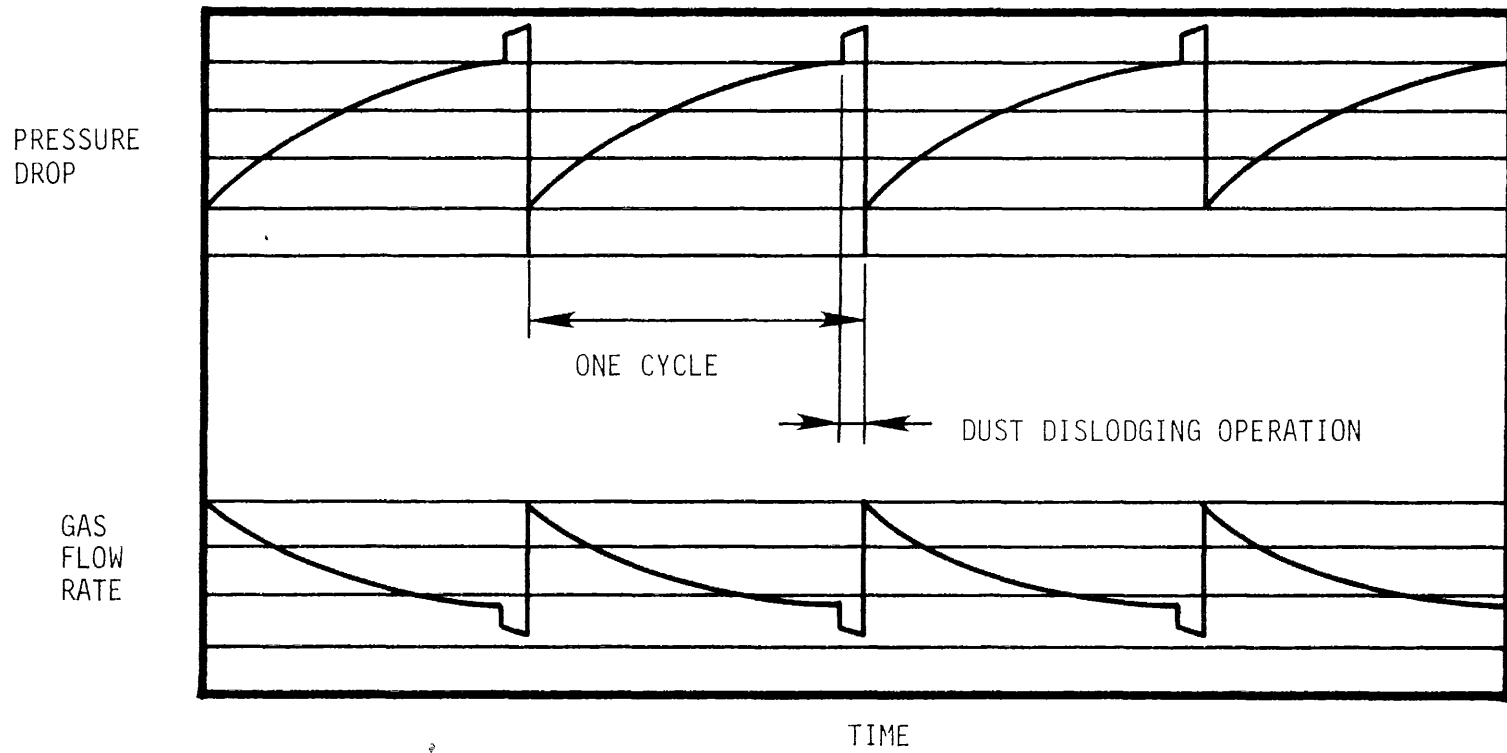


Figure 6.3.2-4. Flow and pressure loss variations as a function of time in a multicompartment baghouse. Average velocity, 1 m/min; initial compartment pressure loss, 1.7 cm W.C./m/min; final compartment pressure loss, 17 cm W.C./m/min.

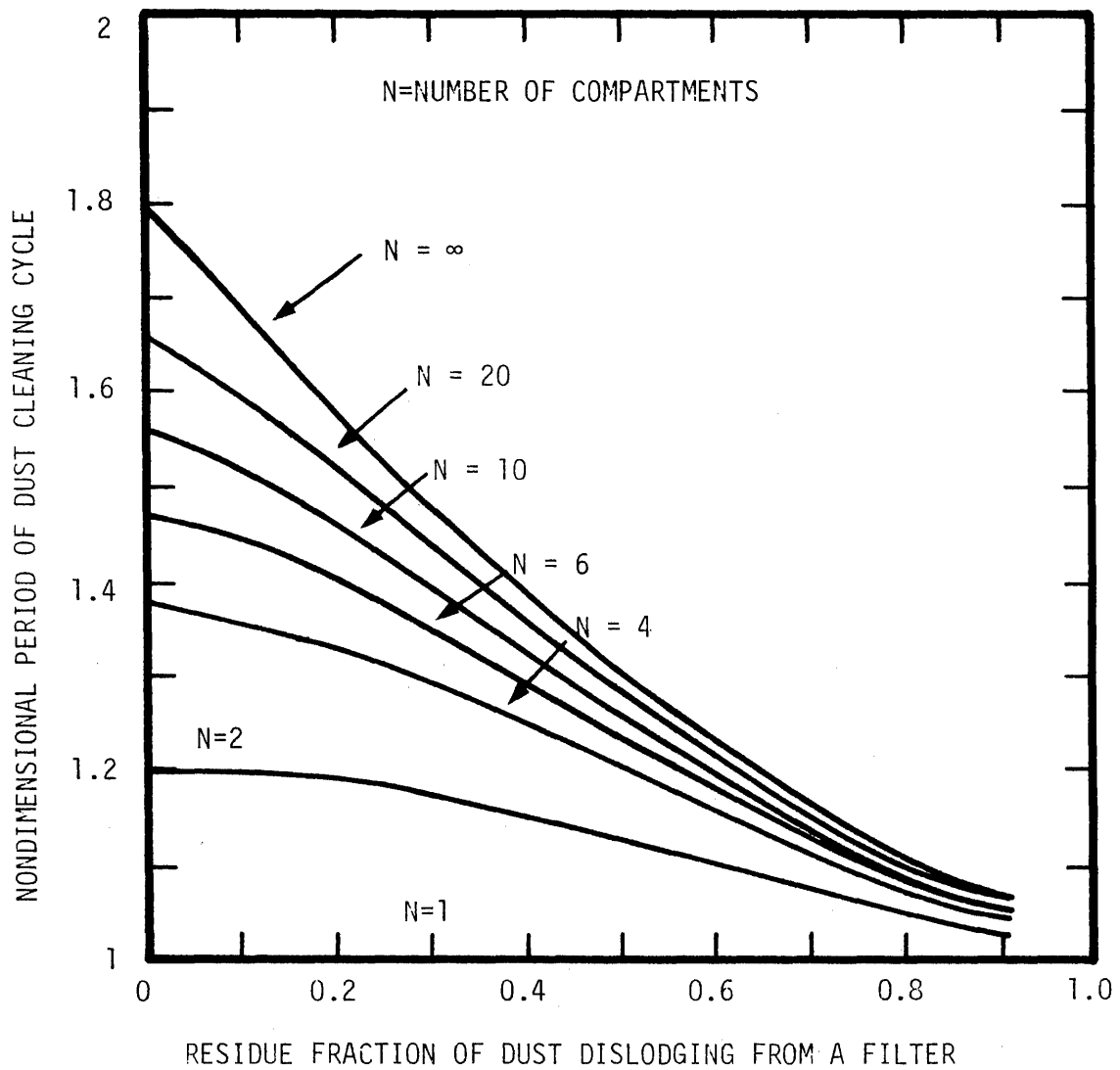


Figure 6.3.2-5. Effect of the number of compartments on cleaning cycle periods (Tanaka et al. 1973).

6.3.3 Collection Efficiency

Particle separation by fabric is more than simple entrapment of the particles by single fibers, since the open spaces through such media are usually many times the size of the individual particles which are collected. Actually, separation with filters is poor until enough particles have been captured to form an arching bed across the openings (Loeffler, 1970). Once the particle bed has been formed, separation efficiency will rise to values near 99% as indicated in Figure 6.3.3-1. Failure to achieve high collection efficiency is almost always due to excessive cleaning, torn bags, bypass leakage, or an excessive gas flow rate which produces pinholes within the deposited particle bed. Instantaneous efficiency values usually are higher than cumulative collection efficiencies for an operating cycle, because the collection efficiency generally increases with the dust deposit (Kimura and Shirato, 1970; Kimura and Iinoya, 1970).

Twill or broken twill fabrics usually give less residual pressure loss and better collection efficiency than other weaves (Nakai and Iinuy, 1972).

6.4 FACTORS INFLUENCING PERFORMANCE

Parameters important to fabric filtration system design include air-to-cloth ratio, filter cake, pressure drop, cleaning mode and frequency of cleaning, composition and weave of fabric, degree of sectionalization, type of housing, and gas cooling. Baghouses are relatively insensitive to process variables such as gas composition (providing that the correct bag fabric is chosen), particle size, electrical resistivity, etc.; thus, there tends to be very little substantial design difference from one application, or indeed from one manufacturer to the other, when comparing baghouses with the same cleaning mechanism. Differences that do exist are generally related to maintenance (e.g., number of bag rows accessible from a given interior walkway; method of bag cuff attachment to cell plate; etc.).

6.4.1 Air-to-Cloth Ratio

The air-to-cloth (A/C) ratio, a major factor in the design and operation of a fabric filter, is the ratio of the quantity of gas entering the filter in m^3/min (ft^3/min) to the surface area of the fabric in m^2 (ft^2). The ratio is therefore expressed as m^3/min per m^2 (ft^3/min per ft^2), or sometimes also as filtering velocity m/min (ft/min). In general, a lower ratio is used for filtering gases containing small particles or particles that may otherwise be difficult to capture.

The air-to-cloth ratio usually is chosen to keep the overall baghouse pressure drop within acceptable limits and has generally been based on industry practice or the recommendation of the filter manufacturer. Typical air-to-cloth ratios are shown in

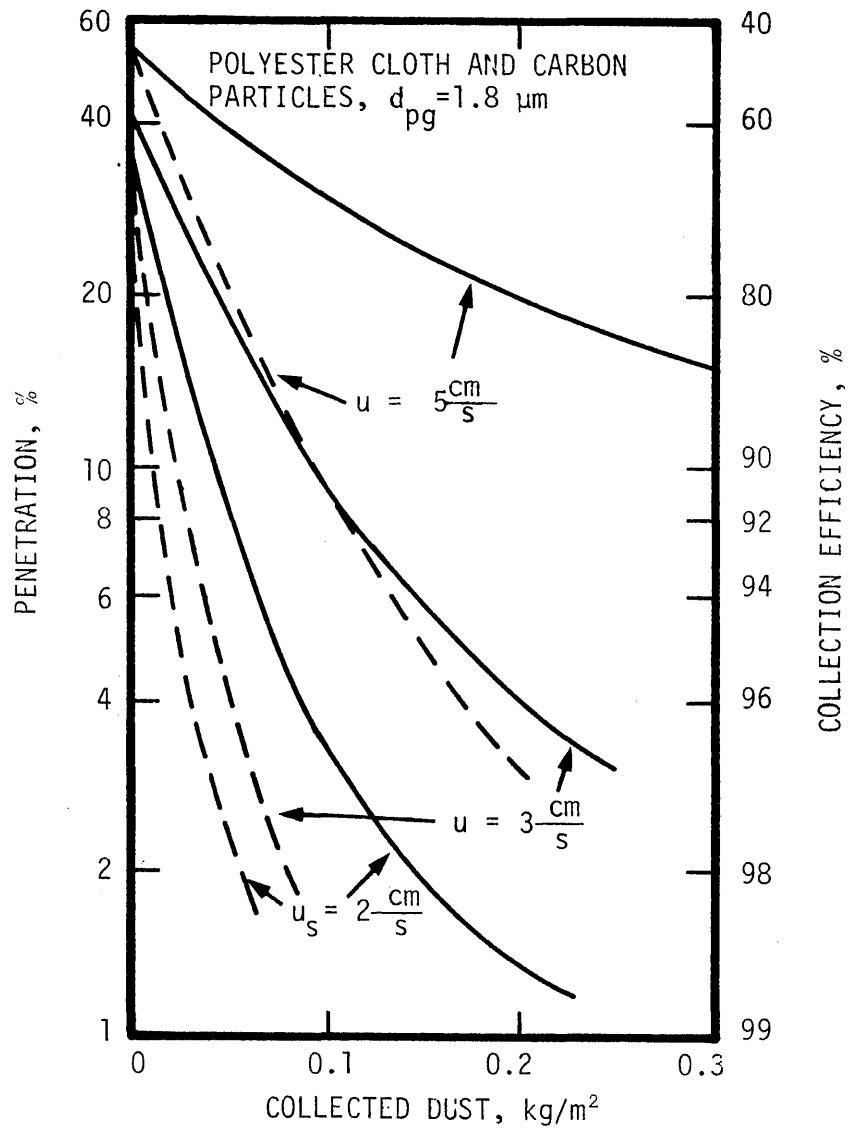


Figure 6.3.3-1. Collection efficiency of fabric filters. The solid lines show cumulative collection efficiencies and the broken lines show instantaneous ones.

Table 6.4.1-1 for a number of industrial sources.

Operation of fabric filters at high air-to-cloth ratios reduces space requirements and equipment capital costs. However, increased velocity also increases pressure loss and cleaning frequency which will eventually override the advantage of reduced equipment and space costs (Billings et al., 1970). Less well understood is the relationship between face velocity and outlet concentration.

Because flow through pinholes at a fixed filter resistance varies directly with pinhole area, it is essential that pore bridging be completed as soon as possible. With typical inlet loadings of 2.3 to 7.0 g/m³, nearly complete bridging takes place with a few minutes leaving only the larger pores to be closed. The extent to which the remaining pores become blocked is velocity dependent. At higher velocities, an equilibrium may develop between the dust deposition and reentrainment rates such that certain larger pores are never blocked. The effect of velocity, u_s , and fabric loading, W , on outlet concentration, C_o , is indicated in Figure 6.4.1-1.

Outlet concentrations decrease rapidly during the early loading phase followed by an asymptotic decline to a lower limit that ranges from 5×10^{-4} g/m³ at a face velocity of 0.39 m/min to 2×10^{-1} g/m³ at 3.35 m/min. Thus, there is a 400 fold increase in minimum outlet concentration as a result of the velocity increase. These measurements indicate that emission levels may determine the maximum air-to-cloth ratios.

6.4.2 Filter Cake

The predominant particle capture mechanism at high loadings, >0.5 g/m³, is sieving by the dust layer that builds up on the fabric surface (Billings et al., 1970; Dennis et al., 1977). Only during the first few minutes of filtration with new or just cleaned fabrics, do the classical collection mechanisms prevail; i.e., inertial impaction, diffusion and interception with or without augmentation by secondary processes. An ideal filter should function as a supporting substrate for the dust layer which, without discontinuities in the form of cracks or pinholes, constitutes a nearly impenetrable layer for particles of the same size making up the dust cake. Unfortunately, normal variations in fabric structure such as nonuniform pore size or an absence of free fibers within the pores may lead to significant dust penetration. Only when the fabric pores (interyarn openings) are spanned by an intercepting fiber array is it possible to obtain complete pore bridging and hence a solid dust cake as shown in Figure 6.4.2-1.

A typical grade penetration curve for a coal-fired power plant is shown in Figure 6.4.2-2. This figure shows that the apparent collection efficiency decreases in the particle size

TABLE 6.4.1-1. TYPICAL AIR-TO-CLOTH RATIOS^a

Dust	Usual air-cloth ratio (m ³ /min/m ²)		
	Shaker collector	Pulse jet	Reverse-air collapse
Alumina	0.82-0.91	2.4-3.0	-
Asbestos	0.91-1.1	3.0-3.7	-
Bauxite	0.76-0.98	2.4-3.0	-
Carbon black	0.46-0.61	1.5-1.8	0.33-0.46
Coal	0.76-0.91	2.4-3.0	-
Cocoa, chocolate	0.85-0.98	3.7-4.6	-
Clay	0.76-0.98	2.7-3.0	0.46-0.61
Cement	0.61-0.91	2.4-3.0	0.37-0.46
Cosmetics	0.46-0.61	3.0-3.7	-
Enamel frit	0.76-0.91	2.7-3.0	0.46-0.61
Feeds, grain	1.1 -1.5	4.3-4.6	-
Feldspar	0.67-0.85	2.7-3.0	-
Fertilizer	0.91-1.1	2.4-2.7	0.56-0.61
Flour	0.91-1.1	3.7-4.6	-
Graphite	0.61-0.76	1.5-1.8	0.46-0.61
Gypsum	0.61-0.76	3.0-3.7	0.55-0.61
Iron ore	0.91-1.1	3.4-3.7	-
Iron oxide	0.76-0.91	2.1-2.4	0.46-0.61
Iron sulfate	0.61-0.76	1.8-2.4	0.46-0.61
Lead ozide	0.61-0.76	1.8-2.4	0.46-0.55
Leather dust	1.1 -1.5	3.7-4.6	-
Lime	0.76-0.91	3.0-3.7	0.49-0.61
Limestone	0.82-1.0	2.4-3.0	-
Mica	0.82-1.0	2.7-3.4	0.55-0.61
Paint pigments	0.76-0.91	2.1-2.4	0.61-0.67

(cont.)

TABLE 6.4.1-1. TYPICAL AIR-TO-CLOTH RATIOS^a (CONT.)

Dust	Usual air-cloth ratio (m ³ /min/m ²)		
	Shaker collector	Pulse jet	Reverse-air collapse
Paper	1.1 -1.2	3.0-3.7	-
Plastics	0.76-0.91	2.1-2.7	-
Quartz	0.85-0.98	2.7-3.4	-
Rock dust	0.91-1.1	2.7-3.0	-
Sand	0.76-0.91	3.0-3.7	-
Sawdust (wood)	1.1 -1.2	3.7-4.6	-
Silica	0.70-0.85	2.1-2.7	0.37-0.46
Slate	1.1 -1.2	3.7-4.3	-
Soap, detergents	0.61-0.76	1.5-1.8	0.37-0.46
Spices	0.82-1.0	3.0-3.7	-
Starch	0.91-1.1	2.4-2.7	-
Sugar	0.61-0.76	2.1-3.0	-
Talc	0.76-0.91	3.0-3.7	-
Tobacco	1.1 -1.2	4.0-4.6	-
Zinc oxide	0.61-0.76	1.5-1.3	0.46-0.55

^aAmerican Air Filter Co., 1973

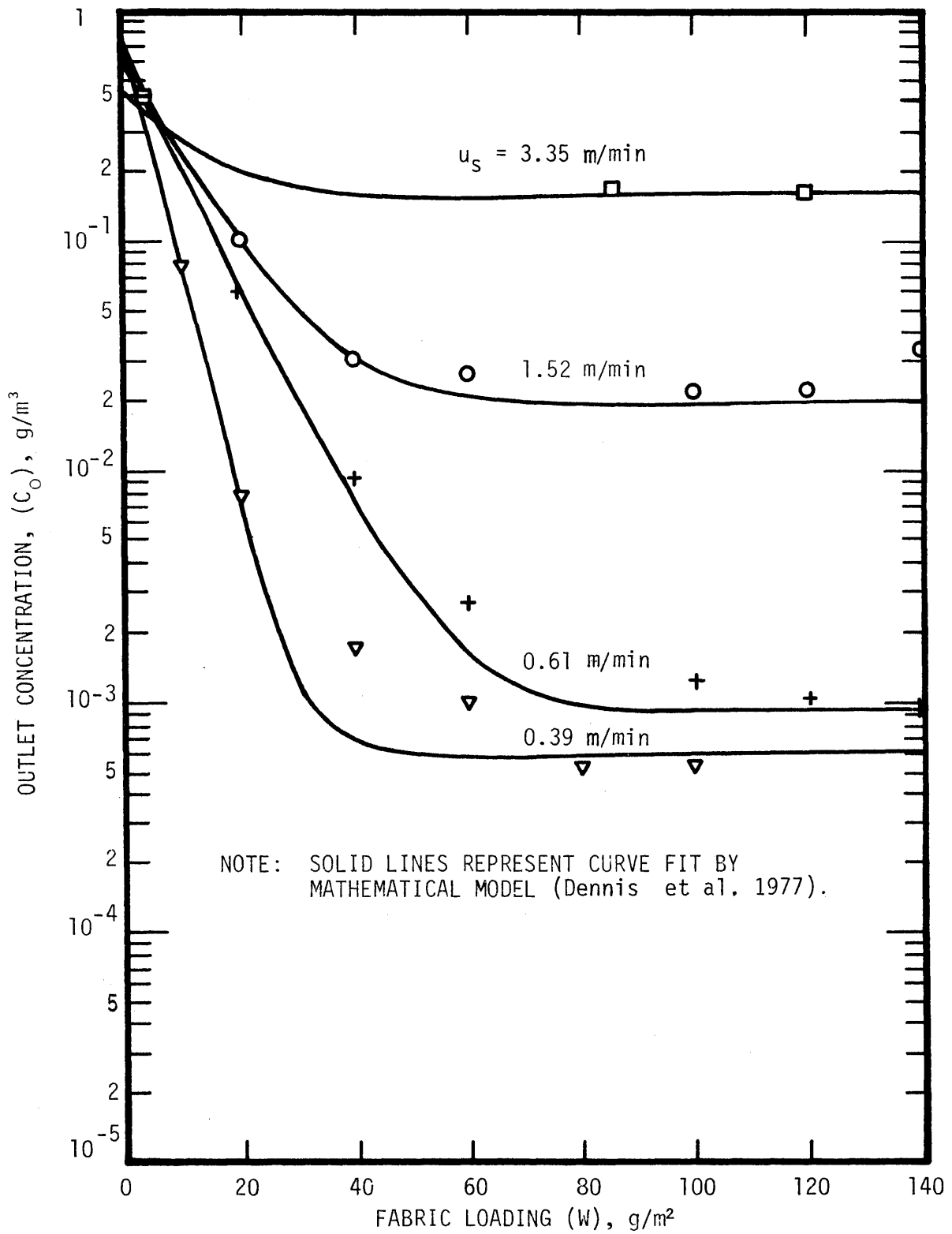
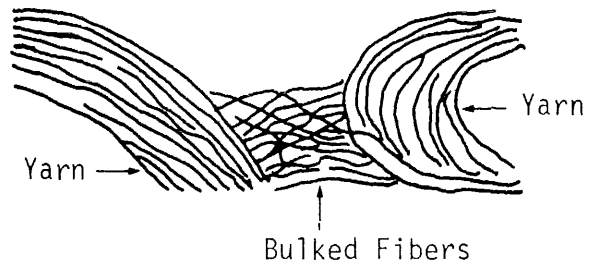
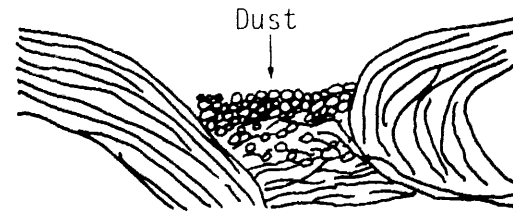


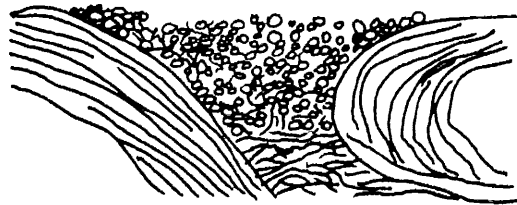
Figure 6.4.1-1. Effect of fabric loading and face velocity on outlet concentrations. Bench tests with coal fly ash and woven glass fabrics.



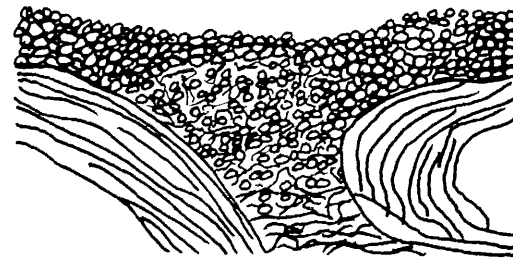
UNUSED FABRIC



EARLY DUST BRIDGING OF FIBER SUBSTRATE



SUB SURFACE DUST CAKE DEVELOPMENT



SURFACE DUST CAKE DEVELOPMENT

Figure 6.4.2-1. Schematic of dust accumulation on woven glass fabrics.

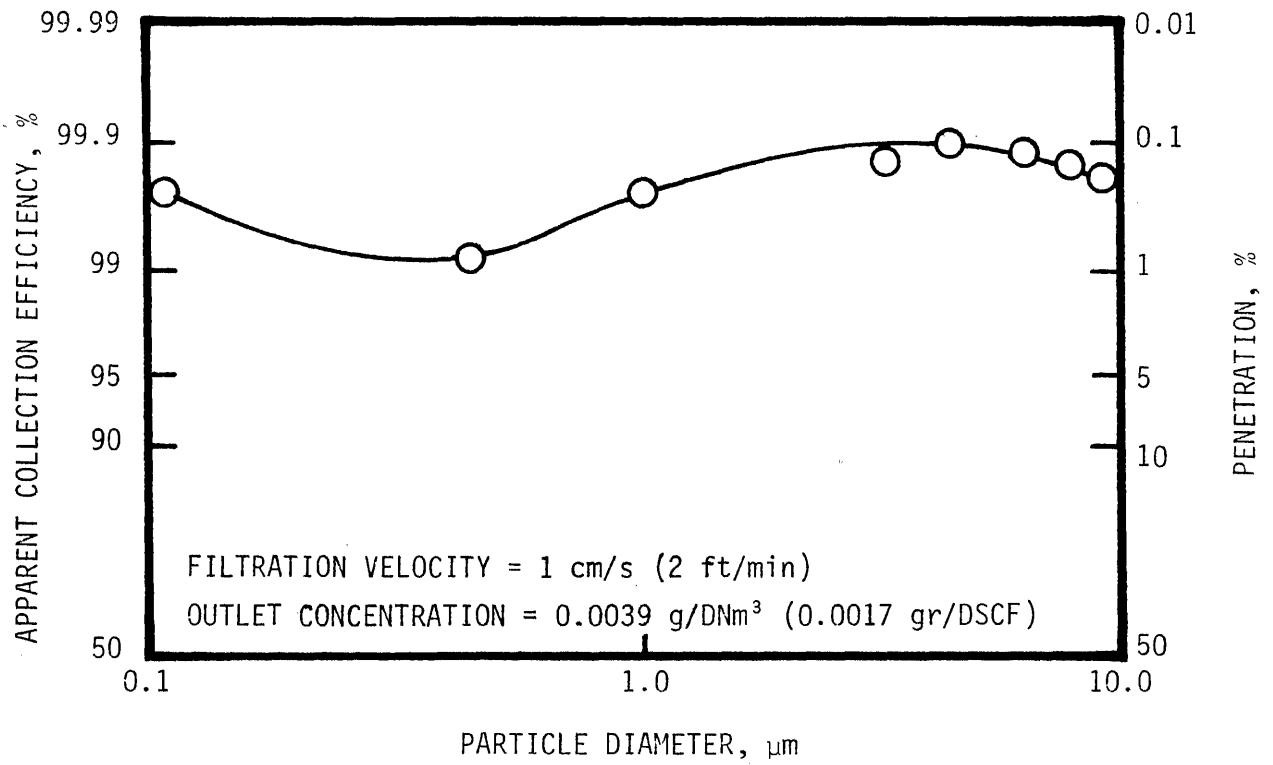


Figure 6.4.2-2. Baghouse performance at Sunbury Steam Electric Station.

range of 0.2 to 0.6 μm . Leith et al. (1976) showed that high velocity filtration can lead to decreased collection efficiency for particles. The three mechanisms for particle penetration are as follows:

1. **Straight Through Penetration:** Immediately after cleaning, many particles collect upon the exposed fibers. Soon, however, a continuous dust deposit forms on the fabric surface and particles collect upon previously deposited dust. Particles not collected by the filter, but which pass through without stopping, penetrate the filter by the "straight through" mechanism.
2. **Seepage:** Once a particle lands on or in the fabric, it need not necessarily remain at its point of initial impact. As the dust deposit builds up, pressure drop can increase to several times its initial value. Meanwhile, the fabric substrate may stretch, allowing some previously collected particles to work through. Filter behavior of this sort is "seepage".
3. **Pinhole Plug:** Small diameter pinholes occur at the surface of dust deposit on woven fabrics. Similar holes on a needle-punched felt may correspond to the places where needles penetrated the cloth during its manufacture. A plug of deposited particles may dislodge from the dust deposit and pass through the fabric all at once as the supporting fibers move and stretch beneath it, leaving behind such a pinhole. Particles which pass through the filter in this way do so by a "pinhole plug" mechanism.

Therefore, particles can pass through the filter by the "straight through" mechanism, without being stopped, whereas previously collected particles can make their way through by the "seepage" and "pinhole plug" mechanism. The fraction of the total fabric filter penetration due to "pinhole plugs" can be as high as 70%. This can account for the presence of large particles on the outlet side of baghouses in amounts not expected by considering classical filtration theory.

6.4.3 Pressure Drop

Pressure drop in a fabric filter is caused by the combined resistances of the fabric and the accumulated dust layer and typically ranges from 10 to 50 cm W.C. The resistance of the fabric alone is affected by the type of cloth and the weave; it varies directly with air flow. The permeability of various fabrics to clean air is usually specified by the manufacturer as the air flow rate (m^2/min) through 1 m^2 of fabric when the pressure differential is 1.3 cm W.C. in accordance with the American Society of Testing and Materials (ASTM). At normal filtering velocities, the resistance of the clean fabric is usually less than 10% of the total resistance (Gorman et al., 1975).

The pressure drop through the accumulated dust layer is

directly proportional to the thickness of the layer (see Section 6.2.4.2). Resistance also increases with decreasing particles size according to Gorman et al. (1975). Even though several studies have been devoted to filtration theory, it is difficult to relate collection efficiency and pressure drop on an industrial scale.

6.4.4 Cleaning of Fabric Filters

Fabric filtration is effective only when the filter can be cleaned periodically and economically without impairing collection efficiency or disturbing the system gas flow. Overcleaning to reduce the flow resistance will frequently result in a lower overall efficiency. It also can shorten the useful life of the fabric and thereby increase rather than decrease the total operating costs. Depending on the dust loading and allowable pressure drop, cleaning cycle frequencies can range from once every 30 seconds to once every few hours.

Although fabric filters have been used for many years, the cleaning process has only recently been examined quantitatively as shown in Table 6.2.3-1. These methods were discussed in Section 6.2.3. Highlights of recent studies on filter cleaning by (a) mechanical shaking, (b) reverse flow, or (c) combinations of (a) and (b) are discussed below (Dennis, et al., 1978).

In a simple shaking system, the oscillation of the shaker arm alternately accelerates and decelerates the dust laden bag surfaces. The resulting tensile and/or shearing forces exerted at the fabric/dust layer interface, if greater than local adhesive forces, will remove slabs or flakes of dust from the fabric.

The separating force (assuming that tensile and shear forces are roughly equivalent) can be estimated from the dust loading, W , and the average acceleration as imparted to the dust laden fabric (Dennis et al., 1977). The acceleration is computed from shaker arm amplitude (half-stroke) and shaking frequency. Field and laboratory tests have indicated that average acceleration must be at least 3 g's to impart the shaking motion over the entire bag (Dennis et al., 1975). Low frequencies, <4 cps, and small amplitudes, <1 cm, generate acceleration forces appreciably less than that attainable in a gravity field.

Bag collapse accompanied by a clean, reverse air flow (usually less than the face velocity) is a preferred method of cleaning glass fabrics because it avoids the stresses caused by mechanical shaking. Here the cleaning principle is the same as that for shaking except that the dislodging force is now defined by the product of "W" times "g" rather than "W" times "a". The flexing rate and the bag curvature after collapse, which may also play important roles in dust dislodgement, require further study.

Although dust removal forces may be approximated for shaking or reverse flow systems, determination of the actual amount and location of the separated dust requires information on dust/fabric adhesion. Rough estimates of adhesion have been proposed for

selected fly ashes and twill weave glass and sateen weave cotton fabrics, (Billings et al., 1970; Dennis et al., 1977). These measurements provide insights as to (a) how dust separates from a fabric, and (b) how adhesive forces are probably distributed.

First, because fly ash usually forms low porosity ($\epsilon < 0.7$) deposits, the cohesive forces within the dust cake, because of multiple particle contacts, far exceed the adhesive forces between widely spaced yarns and the interface particles. Therefore, dust separates at the dust/fabric interface where the bonds are weakest. The cleaned region beneath the dislodged dust always displays the same residual dust holding, W_R , and the same cleaned cloth drag. Residual dust on glass fabrics averages about 50 g/m^2 , whereas cotton sateen retains more, 75 g/m^2 , because of increased fiber cover. In both cases, the residual dust is found mainly within the bulked, loosened fibers and rarely on the smooth surfaces of multifilament yarns.

An empirical approach has been proposed which allows the cleaned bag area, A_C , to be estimated from the fabric dust loading before cleaning, W , or the separation force, F_S , when the dust loading is acted upon by gravity or shaking acceleration (Dennis et al., 1977). Since the adhesive force, F_A , is just exceeded by the separating force at the instant of dust dislodgement, Figure 6.4.4-1 also furnishes a rough measure of adhesive force.

Despite the data scatter, the description of dust separating forces in terms of the products, "W" times "g" or "W" times "a" appears as a rational means for estimating the amount of cleaning accomplished by reverse flow and mechanical shaking. The principal limitation to this approach is that each dust/fabric combination possesses its unique adhesion properties as suggested by glass and cotton fabric data, Figure 6.4.4-1. Thus, until an improved theory is developed, it will be necessary to determine " A_C " by special laboratory studies or by detailed analyses of field measurements.

6.4.5 Frequency of Cleaning

The cleaning cycle should be as short as possible so that no sizable portion of the total fabric will be out of service at any given time. With shake cleaning equipment, for example, a common cleaning-to-deposition time ratio is 0.1 or less (McKenna et al., 1975). With a ratio of 0.1, 10% of the compartments in the baghouse are out of service at all times during operation. Therefore, the frequency of cleaning should be designed to minimize this ratio. As mentioned previously, with pulsing equipment, the cleaning time is very brief, thus a very low ratio of cleaning time to filtering time.

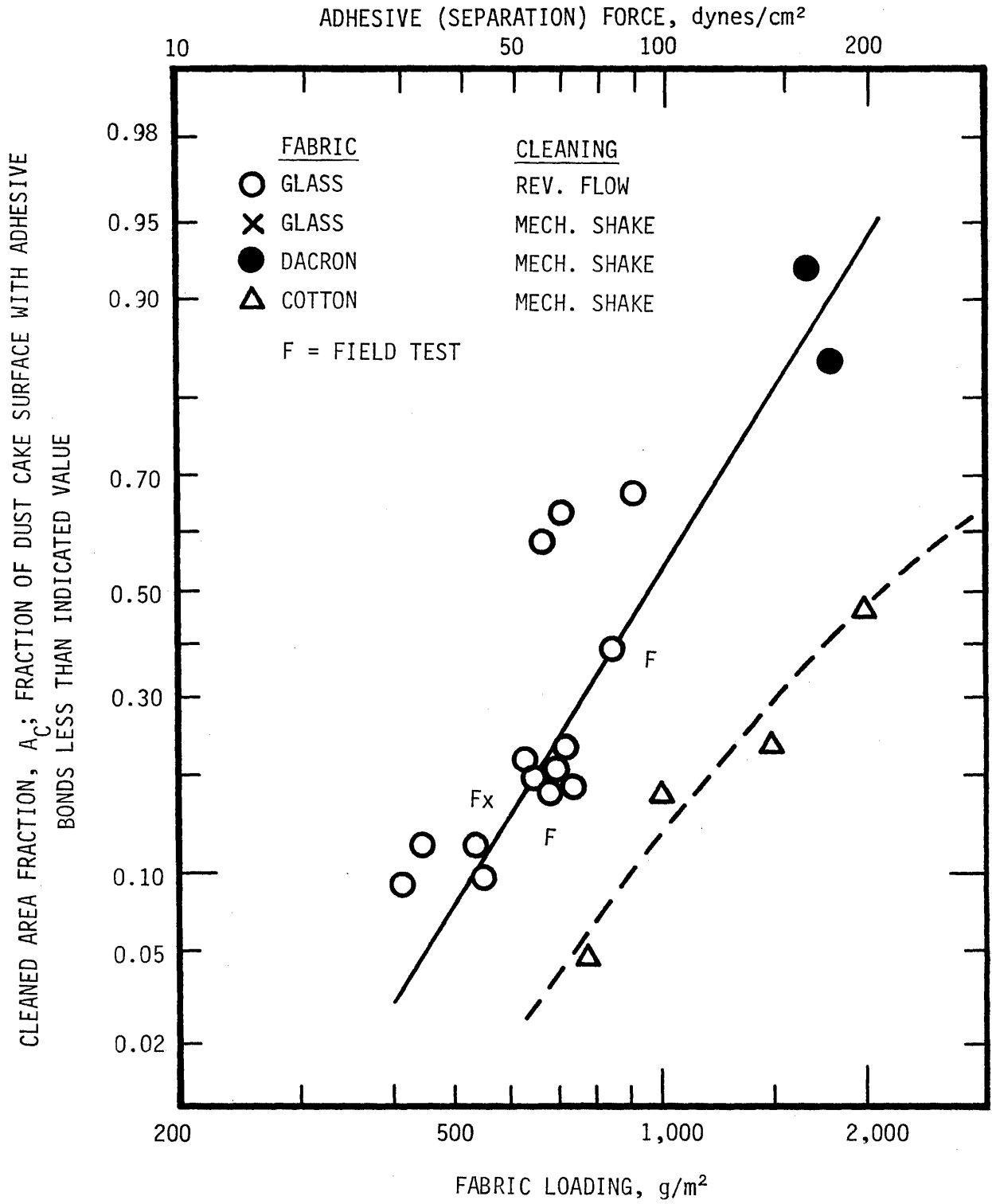


Figure 6.4.4-1. Fabric cleaning and distribution of adhesive (separation) forces versus fabric loading and adhesive (separating) force-Coal fly ash, Dennis et al. (1975).

6.4.6 Selection of Fabric

Selection of fabric is generally based on the operating temperature and on the resistance of the fabric to abrasion and corrosiveness of the gases (see Section 6.2.1). Table 6.2.1-1 shows typical characteristics of various fabrics, which include cotton, wool, fiberglass, and other man-made fibers. Many fabric weaves are available; or the fabric may be felted, a process whereby the identity of the separate yarns tends to be replaced by a more uniform mat. Felted fabrics are almost always cleaned by reverse jet or pulse-jet methods. Fabric characteristics may also be altered by further treatment for specific purposes, such as to decrease adhesion or improve wearability. Silicones are often used on fiberglass to reduce abrasion.

6.4.7 Degree of Sectionalization

Design of fabric filter sectionalization (the number of separate filter compartments) requires knowledge of the variation in gas flow with respect to process or plant ventilation, the sizes of commercially available units, and the expected frequency of maintenance (McKenna et al., 1975). Individual compartments in small collectors may contain as little as 10 m² of fabric surface, although some large units with a capacity of 1,400 m³/min may have only one compartment. The largest collector to date is under construction in the electric utility industry and has a capacity of 1.3 x 10⁵ Am³/min. With the exception of reverse jet and pulse jet units, it should be noted that at least one compartment in any collector will be out of service during the cleaning cycle.

6.4.8 Filter Housing

Configuration of the filter housing depends on the required fabric surface area and on the temperature, moisture content, and corrosiveness of the gases. When the baghouse is designed so that the dirty gas enters the inside of the bags under positive pressure, housing may be needed only for weather protection or for emission measurements.

The floor area required for baghouses depends on the filtering surface area, size of the bags, and spacing between bags. For example, 160 m² of filtering area can be provided in about 7.4 m² of floor area by using bags 15 cm in diameter, 3 m long, and allowing 10 cm between bags. If 30 cm diameter bags are used, they must be about 4.3 m long to provide the same filtering area in the same floor space, though 30 cm diameter bags can easily be obtained in lengths of 6 m or more when there is adequate head room. The length/diameter ratio affects the stability of vertical bags, so care must be taken to ensure that bags do not rub together during operation or cleaning. The length/diameter ratio ranges from 5 to 40 (Gorman et al., 1975),

but more commonly varies between 10 and 25.

Design consideration must be given to allow adequate space for the collecting hopper below the filter bags. Hoppers are commonly designed with 45° or 60° sloping sides to provide adequate sliding, and with some dusts a 70° slope is required. Dust collected in the hopper can be removed by screw conveyors, rotary valves, trip gates, air slides, and other methods.

The most common construction material for the housing is steel; other materials, such as concrete and aluminum, are also used. Corrugated asbestos cement paneling is often used for the exterior roofing and siding of the housing in combination with interior walls and partitions of steel (Billings et al., 1970).

6.4.9 Gas Conditioning or Cooling

The gases to be cleaned are frequently too hot to go to the baghouse immediately, so they are cooled before entering the filtration system. Use of a fabric filter on a sintering process generally does not require gas cooling. In the ferroalloy branch, however, electric arc furnace fumes are usually cooled by radiation or forced convection; whereas electric arc furnace fumes in the steel industry are cooled only if there is direct evacuation of the gases.

Three methods which can be used for cooling the hot gases are radiation and convection cooling, addition of outside air, and spray cooling with water.

Radiation and convection cooling do not dilute the gas and do not raise the dew point, but require large and costly equipment. To cool 9,300 m³/min of air from 315° to 150°C requires a surface area of 9,300 m² if the heat transfer rate for the cooler were 173 watts/m²-°C. Addition of outside air is simple, but it increases the gas volume to be handled, thus requiring more filter area and energy consumption. Spraying can provide the greatest amount of cooling at the lowest total cost but its main disadvantage is that it increases the gas dewpoint. This can result in wetted bags and/or increased bag wear due to higher gas corrosiveness (Billings, et al., 1970). Table 6.4.9-1 cites the advantages and disadvantages of different methods of temperature conditioning.

6.5 ADVANCED DESIGNS

6.5.1 Granular Bed Filters

A granular bed filter is defined as any filtration system comprised of a stationary or slowly moving bed of separate, relatively close packed granules or particles which act as the filter medium. In order to prevent plugging of the interstices between granules and excessive pressure drop across the bed because of the collected particulate matter, the device must have some means of periodic or continuous cleaning of the dirty bed. This description automatically excludes continuously fluidized or

TABLE 6.4.9-1. METHODS OF TEMPERATURE CONDITIONINGa

Radiation-Convection Cooling (long, uninsulated inlet ducts)

Advantages: Lowest flow volume of the three methods. Smoothing or damping of flow, temperature, pressure or other surges, or peaks in the process effluent stream. Saving of heat (building space heating).

Disadvantages: Cost of extensive ducting. Space requirements of ducting. Possibility of duct plugging by sedimentation.

Evaporation (by water injection well ahead of the filter)

Advantages: Low insntallation cost, even with automatic controls. Capability of close and rapid control of temperature. Capability of partial dust removal and/or gas control by scrubbing.

Disadvantages: Danger of incomplete evaporation and consequent wetting of the filter or chemical attack of the fabric or filter. Increased danger of exceeding the dewpoint and increased possibility of chemical attack. Increased steam plume visibility, a hazard near highways. Possible increase in volume filtered.

TABLE 6.4.9-1. (cont.)

Dilution (by adding ambient air to the process effluent stream)

Advantages: Lowest installation cost, especially at very high initial temperatures.

Disadvantages: Substantial increase in total filtering volume. Automatic control of both temperature and filtering velocity is not possible. Uncontrollable intake of ambient moisture, dust, etc., without prior conditioning of the dilution air.

a. Billings et al., 1970

dispersed beds, where the bed material is left in motion by the gas being cleaned.

Granular bed filters may be classified with respect to the bed cleaning method as continuously moving, intermittently moving and fixed bed filters (Yung et al., 1979).

Continuously moving bed filters are usually arranged in a cross-flow configuration. The bed consists of a vertical wall of granules held in place by louvered walls. The gas passes horizontally across the bed while the granules and collected dust continuously move downward and are removed from the bottom. The dirty granules are usually mechanically cleaned and recirculated.

The intermittently moving bed is essentially the same as the continuously moving bed. The bed actually behaves as a fixed bed during most of the filtration period. Intermittently, the dirty granules are removed and replaced with a clean bed while the dirty bed is cleaned prior to recirculation.

As opposed to the continuously and intermittently moving beds, fixed bed filters do not require recirculation of the bed material. When the bed becomes dirty it is cleaned, in place, mechanically or, pneumatically and the bed material is ready for reuse.

The principal parameters governing the performance of granular bed filters are the granule diameter, bed depth and superficial velocity. These parameters can have a wide range of values which, in turn, have a strong effect on pressure drop and particle removal efficiency.

The particle collection mechanisms in operation in the above mentioned granular bed filter configurations are essentially the same. They include:

1. Inertial impaction
2. Interception
3. Diffusional collection
4. Gravity settling
5. Sieving.

To further enhance particle collection, electrostatic augmentation has been used. The methods used have included pre-charging of the particulate matter and/or charging of the bed material. This was found to improve particle collection.

6.5.2 Spray Drying

Spray drying of SO₂ sorbents can be used in combination with baghouses or ESP's to achieve control of SO₂ emissions as well as particle emissions. Baghouses are the most common collection device used so spray drying is included in this section. The efficiency of the baghouse or ESP for fine particle collection is the same as for installations where spray drying is not used. Refer to Section 5 for description of ESP's. Spray dryers can

achieve collection efficiencies as high as 90% for low concentrations of SO₂ (Blythe et al., 1980).

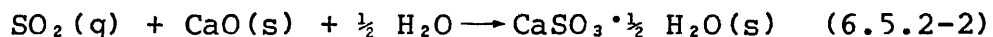
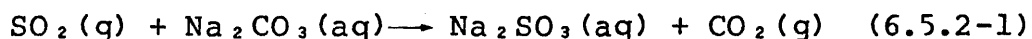
According to Smith et al. (1981), one utility boiler is operating using a spray dryer and 4 utility boiler installations are under construction. Industrial boilers are reported to be operating with spray dryers.

6.5.2.1 General Design Features

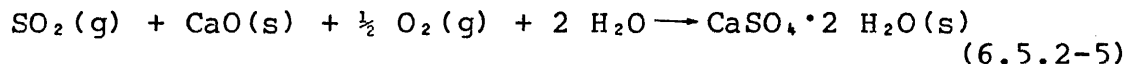
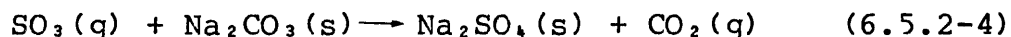
In spray drying, an alkaline slurry such as sodium carbonate or lime is sprayed into the flue gas as shown in Figure 6.5.2-1. The flue gas enters the spray dryer at a temperature of 120-150°C (250-300°F). As the drops travel through the spray dryer, the gaseous SO₂ is sorbed into the liquid where it reacts with the sorbent material. Simultaneously, the moisture is evaporated, so that the reagent leaves the spray dryer as a powder. The spent reagent is collected, along with the flyash, in a baghouse or an ESP.

Dickerman and Johnson (1979) gave the following reactions for sodium carbonate and lime reagents:

Primary reactions



Secondary reactions



A sodium carbonate solution will achieve a higher level of SO₂ removal than a lime slurry for the same gas temperature, SO₂ concentration and sorbent stoichiometry. However, lime is less expensive and the reaction products are less water soluble. Pilot scale tests have demonstrated 85% removal of SO₂ using lime sorbent, with a sorbent utilization near 100% (Blythe et al., 1980).

Liquid to gas ratios are generally 2.7 x 10⁻⁵ to 4 x 10⁻⁵ m³/m³ (0.2-0.3 gal/MCF). The sorbent stoichiometry is varied by

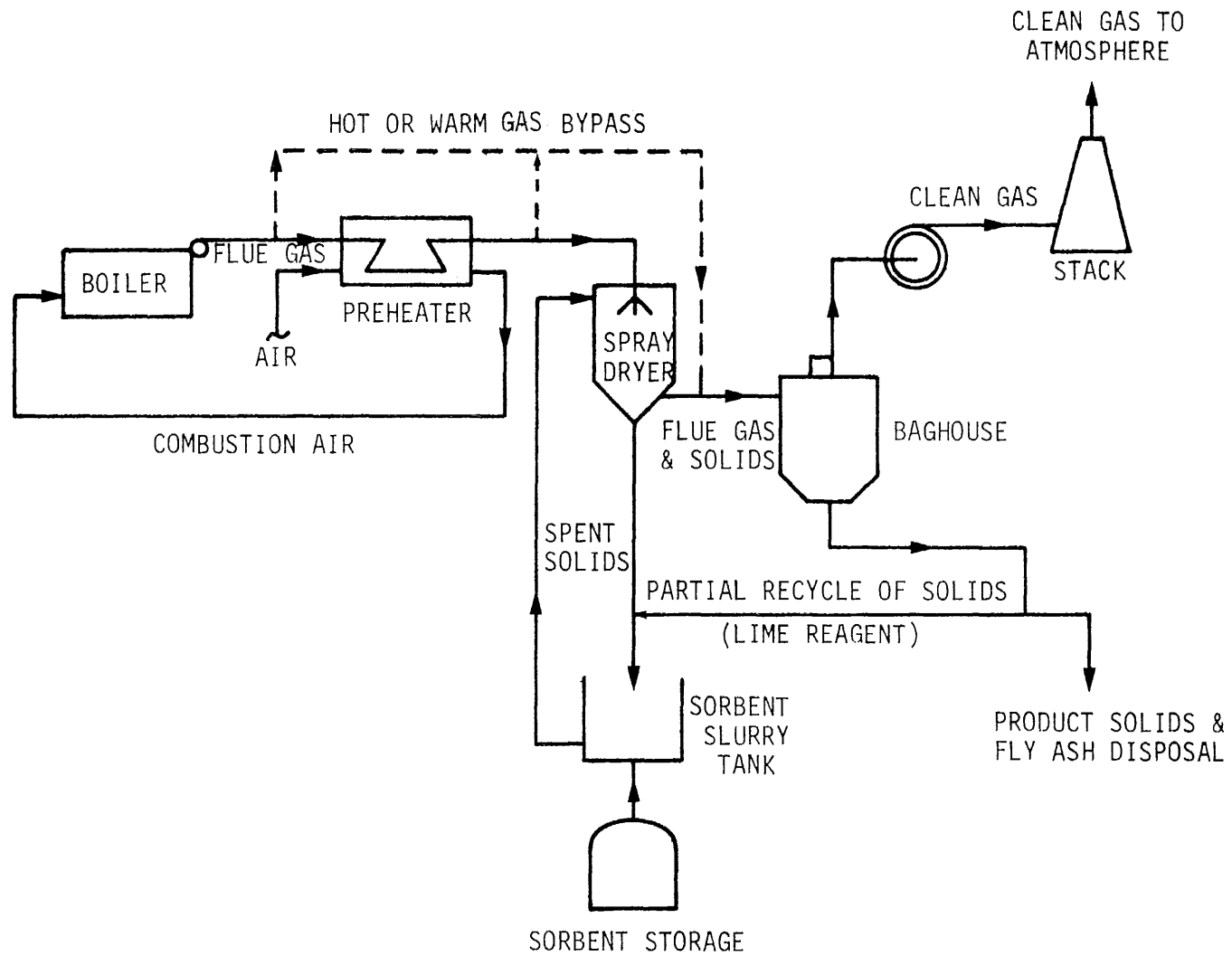


Figure 6.5.2-1. Typical spray dryer/particulate collection flow diagram (Blythe et al., 1980).

changing the concentration of the reactants in the slurry with the amount of water held constant. Increasing the sorbent stoichiometry will increase SO₂ removal. However, utilization of the sorbent decreases such that sorbent and disposal costs increase faster than the increase in SO₂ removal. Also, there is a limit to the amount of sorbent which can be kept in solution or suspension in a given amount of water.

As the moisture evaporates from the atomized slurry, it cools the gas adiabatically. The closer to the adiabatic saturation temperature the spray dryer is operated, the higher the SO₂ removal and sorbent utilization will be. As the saturation temperature is approached, the evaporation rate decreases. Therefore, the life of the drop increases and the dried product will have a higher residual moisture content. According to Blythe et al. (1980), the mechanisms for SO₂ removal are not well understood. It is not known whether the increase in SO₂ removal is due to the increased droplet residence time or the increased residual moisture in the reagent or both.

Practically, the gas temperature must be kept 17-28°C (30-50°F) above the saturation temperature to avoid condensation in the baghouse or ESP and to avoid plume opacity due to condensation (Dickerman and Johnson, 1979). For a baghouse the temperature must be at least 15°C (25°F) above the saturation. According to Blythe et al. (1980), an ESP may be operated within 15°C (25°F) of the saturation temperature, because it is less sensitive to condensation than a baghouse.

If the gas is reheated before it enters the collection device, the spray dryer can be operated closer to the saturation temperature. Reheating can be achieved by bypassing a certain amount of gas around the spray dryer and adding it to the gas stream at the spray dryer exit (see Figure 6.5.2-1). If gas from the preheater outlet (warm gas) is used there will be no energy cost. However, the SO₂ level in the untreated gas will eventually cancel the increase in SO₂ removal. Using hot gas from upstream of the preheater will reduce the amount of gas needed for reheat but will decrease the heat load to the air preheater, resulting in an energy cost (Blythe et al. 1980).

The sorbent which is collected in the spray dryer and/or a portion of the particle collection device catch can be reused. This recycling increases the utilization of the sorbent. When the collection device catch is recycled, any alkalinity in the flyash can be utilized (Blythe et al., 1980).

Baghouses have an advantage in SO₂ collection because further SO₂ removal can occur as the gas passes through the filter cake, which contains unreacted reagent. However, the total SO₂ removal occurring in the baghouse is unknown. Results of one pilot test indicated that up to 20 percent of the system's total SO₂ removal occurred in the baghouse with sodium as the sorbent and up to 10 percent with lime sorbent. There have been tests showing virtually no SO₂ removal in the baghouse, however (Dickerman and Johnson, 1979).

6.5.2.2 Advantages and Problems

SO₂ control systems which use lime/limestone wet scrubbing, or other wet scrubbing techniques, have been in use for a number of years. Dry scrubbing techniques are believed to have several cost advantages over wet methods. However, spray drying installations are only beginning to be operated commercially, so cost estimates are based on pilot tests.

Wet scrubbing methods require more equipment than dry scrubbing, much of this is slurry handling equipment. Conventional fly ash handling equipment can be used to transport the waste product from spray drying (Janssen and Erikson, 1979).

Dry scrubbing requires less water and therefore less energy for pumping. Many dry scrubbing configurations require no energy for reheat, which is commonly required in wet methods according to Blythe et al. (1980). For two spray dryer controlled utility boilers now under construction, Janssen and Ericksen (1979) estimated that energy requirements for spray drying will be 25 to 50% of that required for a wet system and water requirements will be approximately 50% that of a wet scrubber. Maintenance is also expected to be less, due to the elimination of large slurry and sludge handling equipment.

Spray dryers are expected to be much more flexible than wet scrubbers in adjusting to boiler load variations. Wet scrubber modules usually must be left in service even at low loads to recirculate the slurry and avoid scaling (Blythe et al. 1980). In spray drying systems, modules or individual atomizers can be quickly removed from service when the load decreases.

To achieve the same efficiency, spray dryers require a higher stoichiometric ratio of sorbent to SO₂ than do limestone wet scrubbing systems. Also, the reagents used in spray drying are significantly more expensive than limestone.

Techniques have not been fully developed for disposal of waste from dry scrubbing (Blythe et al. 1980). However the process is expected to be simpler than for wet scrubber waste which often requires settling ponds. The main concern is the solubility of the reagent material. According to Janssen and Erikson (1979), the solubility of a sodium based product is 50 to 60%, while the solubility of a calcium based product is 3-7%. Furlong et al. (1980) reported that sanitary landfill methods, chemical fixation, or sintering of the waste are all feasible methods of disposal. Janssen and Erikson (1979) reported that landfill methods will be used to dispose of waste from two spray dryer installations now under construction. Tests are needed to determine exact procedures.

Spray drying has been applied only to installations burning low sulfur coals. Most tests have been run for SO₂ concentrators under 2,000 ppm (Blythe et al. 1980). Further study is necessary to determine if spray drying can be applied to the combustion of high sulfur fuels.

6.5.3 Electrostatic Augmentation

The major approach to advanced baghouse design is to use electrostatic augmentation. It has been shown through theoretical studies and laboratory experiments that the addition of electric fields can improve the particle collection efficiency of fabric filters. Experiments also revealed that electrified filters have a lower pressure drop than the non-electrified filter when the particles are charged. Higher collection efficiency coupled with lower pressure drop could result in a lower energy consumption in operating the electrified filters.

The charged dust particles preferentially deposit in clusters rather than as uniform deposits on the filter surface. The uneven deposit results in regions of relatively low pressure drop (high porosity) and relatively high pressure drop.

The electrostatic forces also augment the primary deposition mechanisms of interception, Brownian diffusion and inertial impaction. However, the porous, low pressure drop regions in the surface cake are somewhat less effective at removing particles by these primary mechanisms as compared to conventional filter cake.

The net effect of electrostatic augmentation on overall collection efficiency will depend on the electrode spacing and geometry, field strength, particle size, resistivity, and other properties. Insufficient data are presently available to demonstrate that electrostatic augmentation improves fractional collection efficiency for all particle sizes. Experiments are being conducted under an EPA contract to obtain more data for charged and uncharged particles in the range of 0.1 to 10 microns.

6.6 METHODS OF TECHNICAL EVALUATION

6.6.1 Devices for Further Evaluation

The baghouse and the granular bed filter will be evaluated in the second phase of this project. The evaluation will include an estimation of the cost required to achieve several levels of particle control efficiency for specific services. Electrostatically augmented fabric filters will also be evaluated for certain sources.

The format which will be used to present efficiency and cost data is explained in Section 3. The purpose of this section is to explain how efficiency and cost estimations will be made.

6.6.2 Methods of Predicting Collection Efficiency

6.6.2.1 Baghouses

Because of the complexity of the particle removal process and the difficulty of characterizing the effects of the various influencing factors, there is no single model available which can adequately predict baghouse performance. A search of available literature revealed that the most important parameter affecting collection efficiency was the air-to-cloth ratio or filtering

velocity. Published data from field tests at a number of industrial particulate emission sources was collated and average curves for penetration versus particle size for various air-to-cloth ratios were generated as shown in Figure 6.6.2-1. These curves were used in performance calculations.

6.2.2.2 Electrostatically Augmented Baghouse

Performance calculations were based on the field test results reported by Felix and McCain (1979) on an Apitron electrostatically augmented baghouse. Figure 6.6.2-2 shows the principle of operation of the Apitron dust collector. It is a wire-pipe electrostatic precipitator connected in series with the filter bag. The SCA of the ESP section is about 8 to 9 m²/Am³/s. The gas flow enters near the bottom and passes upward through the wire-pipe precipitator in which the particle is charged and much is precipitated. The flow continues upward and passes through the filter bag where the final filtration takes place.

Figure 6.6.2-3 shows the grade penetrations when the ESP was operated at full power and at 25% power. These curves were used in performance calculations for electrostatically augmented baghouses.

6.6.3 Cost Data

6.6.3.1 Baghouse

The cost reference for baghouses is based on the net cloth area. Net cloth area is defined as the total filter area available for on-stream filtration exclusive of the filter area in compartments which are isolated for cleaning (in the case of intermittent filters, the net cloth area is actually the gross cloth area). The net cloth area is determined by the air-to-cloth ratio recommended for a particular application, which is principally based on the type of fabric, type of dust, carrier gas composition, and the dust concentration. The cost options of the fabric filter are therefore based on the following parameters as determined by the type of application.

1. Type of fabric and air-to-cloth ratio.
2. Intermittent or continuous duty.
3. Pressure or suction type construction.
4. Standard or custom design.
5. Type of cleaning mechanism.
6. Materials of construction.

Prices for mechanical shaker, pulse-jet, reverse-air, and custom fabric filters have been established by Neveril et al (1979). Table 6.6.3-1 shows the cost equations. All costs have been updated to December, 1981 U.S. dollars with the Chemical Engineering plant cost index. Baghouse prices are flange-to-flange, including the basic baghouse compartments without bags,

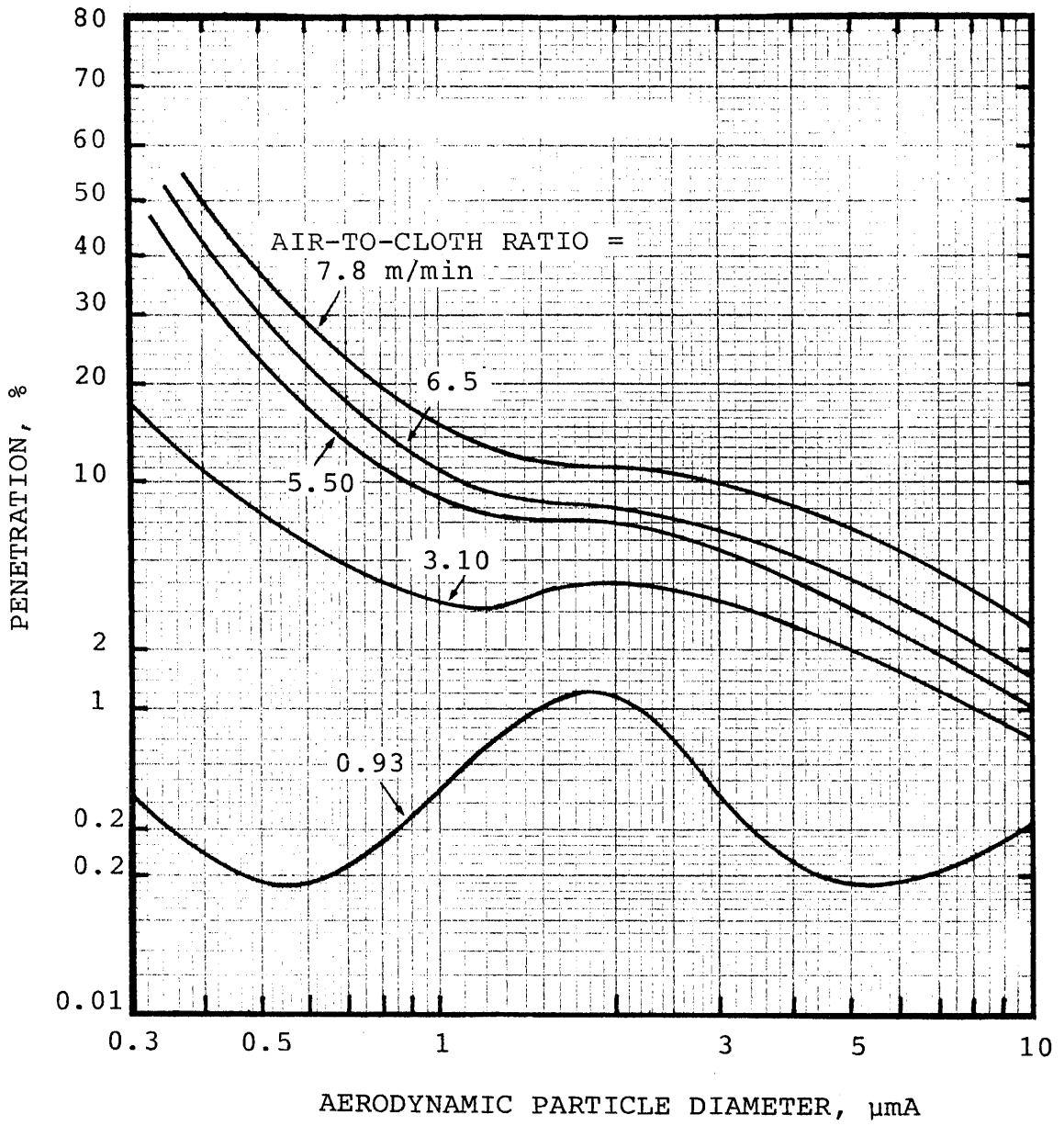


Figure 6.6.2-1. Baghouse grade penetration as a function of air/cloth ratio (FPEIS data for coal fired boilers)

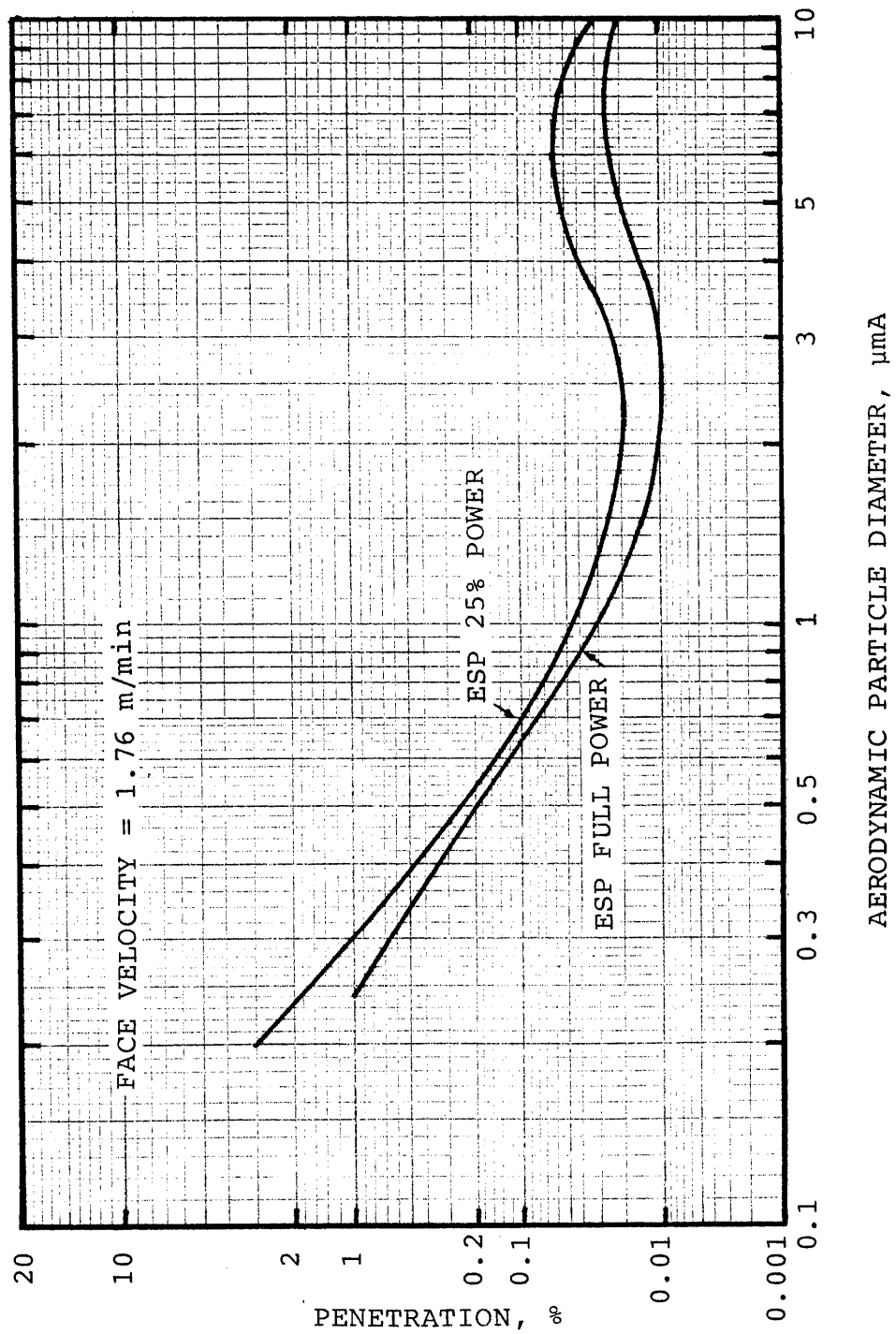


Figure 6.6.2-3. Grade penetration of the Apitron electrostatically augmented filter (Felix and McCain, 1979).

3.3m (10 ft) support clearance, and inlet and exhaust manifolds.

The prices for bags are determined from Tables 6.6.2-2 and 6.6.2-3. From Table 6.6.2-2 obtain factor to calculate gross cloth area, and from Table 6.6.2-3 obtain the price per square meter for the appropriate cloth and baghouse type.

6.6.3.2 Heat Exchanger

In this study, "U" tube heat exchangers are used to cool the gas to a temperature compatible with the filter bag materials. The fabricated cost of heat exchanger can be estimated from

Table 6.6.2-1. Bag house prices (December 1981, U.S. Dollars).

Bag House Type	Intermittent, Forced-draft, Mechanical Shaker	Continuous, Forced-draft, Mechanical Shaker	Pulse air (Forced or induced draft)	Forced-draft reverse air	Custom Design (Forced or induced draft)
Basic bag house	4,943 + 29.21A	24,574 + 55.55A	7,921 + 120.63A	37,879 + 47.61A	17,258 + 49.21A
Stainless steel add on	4,042 + 17.79A	10,827 + 30.15A	2,434 + 78.29A	17,140 + 28.41A	94,255 + 28.57A
Insulation add on	3,002 + 13.33A	3,363 + 28.10A	7,242 + 38.09A	16,520 + 26.34A	66,303 + 26.34A
Induced draft add on	2,039 + 1.90A	3,334 + 3.97A	-	2,493 + 5.07A	-

Note: A = net cloth area, m²

Table 6.6.2-2. Approximate Guide to Estimate Gross Cloth Area (Neveril et al., 1979).

Net Cloth Area m ² (ft ²)		Gross Cloth Area m ² (ft ²)
0.1	- 372 (1- 4,000)	Multiply by 2
372	- 1,115 (4,001- 12,000)	1.5
1,115	- 2,230 (12,001- 24,000)	1.25
2,230	- 3,346 (24,001- 36,000)	1.17
3,346	- 4,460 (36,001- 48,000)	1.125
4,460	- 5,576 (48,001- 60,000)	1.11
5,576	- 6,691 (60,001- 72,000)	1.10
6,691	- 7,807 (72,001- 84,000)	1.09
7,807	- 8,922 (84,001- 96,000)	1.08
8,922	-10,037 (108,001-132,000)	1.06
12,268	-16,729 (132,000-180,000)	1.05
16,729	on up (180,001 on up)	1.04

Table 6.6.2-3. Bag house prices (December 1981, U.S. Dollars).

Class	Type	Dacron	Orlon	Nylon	Nomex	Glass	Poly- propylene	Cotton
Standard	Mechanical shaker, <1,859m ² (20,000 ft ²)	5.71 ^b (0.53) ^c	9.84 (.08)	11.58 (.08)	18.10 (1.68)	7.46 (0.69)	9.84 (0.91)	6.83 (0.63)
	Mechanical shaker >1,859m ² (20,000 ft ²)	4.93 (0.46)	9.04 (0.84)	10.64 (0.99)	16.51 (1.53)	6.67 (0.62)	8.26 (0.77)	6.03 (0.56)
	Pulse jet ^a	9.04 (0.84)	14.77 (1.37)	-	20.64 (1.92)	-	10.64 (0.67)	-
	Reverse Air	4.97 (0.46)	9.04 (0.84)	10.64 (0.99)	16.51 (1.53)	6.67 (0.62)	8.26 (0.77)	6.03 (0.56)
Custom	Mechanical shaker	3.33 (0.31)	4.93 (0.46)	6.67 (0.62)	9.84 (0.91)	4.13 (0.38)	6.93 (0.46)	6.03 (0.56)
	Reverse air	3.33 (0.31)	4.93 (0.46)	6.67 (0.62)	9.84 (0.91)	4.13 (0.38)	6.93 (0.46)	6.03 (0.56)

Note: a = For heavy felt, multiply price by 1.5

b = \$/m²

c = \$/ft²

SECTION 6

REFERENCES

- American Air Filter Company, 1973. Bulletin 340B, Louisville, Kentucky.
- Billings, C. E., and J. E. Wilder, 1970. Handbook of Fabric Filter Technology, Volume I, Fabric Filter Systems Study. EPA-APTD 0690 (NTIS No. PB-200-648), U. S. Environmental Protection Agency, Research Triangle Park, North Carolina.
- Blythe, G. M., J. C. Dickerman, and M. E. Kelly, 1980. Survey of Dry SO₂ Control Systems. EPA 600/7-80-030. U. S. Environmental Protection Agency, Washington, DC 112 pages.
- Borgwardt, R. H., R. E. Harrington, and P. W. Spaite, 1968. Journal of the Air Pollution Control Association, 18:387.
- Butterworth, E., 1964. Manufacturing Chemistry, 35(1):66; (2):65.
- Cass, Reed W. and John E. Langley, 1977. Fractional Efficiency of an Electric Arc Furnace Baghouse. EPA-600/7-77-023, U. S. Environmental Agency, Washington, D.C.
- Cunningham, G. E., G. Broughton, and R. R. Kraybill, 1954. Industrial and Engineering Chemistry, 46:1196.
- Davies, C. N., 1952. Proc. Inst. Mech. Eng. 1B:185.
- Dennis, R., R. W. Cass, D. W. Cooper, R. R. Hall, and V. Hampl, 1977. Filtration Model for Coal Fly Ash with Glass Fabrics. EPA 600/7-77-084, U. S. Environmental Protection Agency, Research Triangle Park, North Carolina.
- Dennis, R., G. A. Johnson, L. Silverman, 1952. Chemical Engineering. 59:196.
- Dennis, R. and N. F. Surprenant, 1978. Particulate Control Highlights: Research on Fabric Filtration Technology. EPA-600/8-78-005d, U. S. Environmental Protection Agency, Industrial Environmental Research Laboratory, Research Triangle Park, North Carolina, 16 pp.
- Dennis, R., and J. E. Wilder, 1975. Fabric Filter Cleaning Studies. EPA-650/2-75-009, U. S. Environmental Protection Agency, Research Triangle Park, North Carolina.

- Dickerman, J. C. and K. L. Johnson, 1979. Technology Assessment Report for Industrial Boiler Applications: Flue Gas Desulfurization. EPA 600/7-79-178i, U. S. Environmental Protection Agency, Washington, DC. 664 pages.
- Frederick, E. R., 1961. Chemical Engineering 68(13):107.
- Furlong, D. A., R. L. Ostop, D. C. Drehmel, 1980. Selection, Preparation and Disposal of Sodium Compounds for Dry SO_x Scrubbers. In: Second Symposium on the Transfer and Utilization of Particulate Control Technology: Vol. 1. EPA 600/9-80-039a, U. S. Environmental Protection Agency, Research Triangle Park, North Carolina. pp. 425-431.
- Gorman, P. G., A. E. Vandergrift, and L. J. Shannon, 1975. Fabric Filters in Gas Cleaning for Air Quality Control, Marchello, J. M. and J. J. Kelly, editors. Marcel Dekker, Inc., New York, New York.
- Iinoya, K. and C. Orr, Jr., 1977. Filtration. In: Engineering Control of Air Pollution, Vol. IV. Academic Press, New York, New York, 149-185 pp.
- Iinoya, K. and N. Yamamura, 1956. Kagaku Kogaku, 29:163.
- Janssen, K. E., and R. L. Eriksen, 1979. Basin Electric Involvement with Dry Flue Gas Desulfurization. In: Symposium on Flue Gas Desulfurization-Las Vegas, Nevada, March 1979: Vol. II. EPA 600/7-79-167b. U. S. Environmental Protection Agency, Washington, DC. pp. 629-652.
- Kimura, N. and K. Iinoya, 1965. Kagaku Kogaku. 29:166; Kagaku Kogaku (Abbreviated English Edition). 3:193.
- Kimura, N. and K. Iinoya, 1970, J. Res. Ass. Powder Tech. 7:124.
- Kimura, N. and M. Shirato, 1970. Kagaku Kogaku. 34:984.
- Leith, D., S. N. Rudnick, and M. W. First, 1976. High Velocity, High Efficiency Aerosol Filtration. EPA 600/2-76-020, U. S. Environmental Protection Agency, Research Triangle Park, North Carolina. 181 pp.
- Loeffler, P., 1970. Staub, 30:518. Staub-Reinhalt. Luft 30(11):27.
- Lundgren, D. A. and K. T. Whitby, 1965. Industrial and Engineering Chemistry, Process Design and Development. 4:345.

- McKenna, J. D., and J. C. Mycock, and W. O. Lipscomb, 1975. Applying Fabric Filtration to Coal-Firing Industrial Boilers--A Pilot Scale Investigation. EPA-650/2-74-048a, U. S. Environmental Protection Agency, Washington, DC.
- Nakai, A. and K. Iinoya, 1972. J. Res. Ass. Powder Tech. 9:399.
- Robinson, J. W., R. E. Harrington, and P. W. Spaite, 1967. Atmospheric Environment, 1:499.
- Rudiger, S., 1971. Staub 31:439.
- Silverman, L., E. W. Conners, and D. M. Anderson, 1955. Industrial and Engineering Chemistry, 47:952.
- Smith, M., M. Melia, and N. Gregory, and K. Scalf 1980. EPA Utility FGD Survey: October - December, 1980, Vol. I. EPA 600/7-81-012a U. S. Environmental Protection Agency, Research Triangle Park, North Carolina. pp. 661.
- Solvach, W., 1969. Staub, 29:24.
- Tanaka, N., K. Makino, and M. Iinoya, 1973. Kagaku Kogaku, 37:718.
- Walsh, G. W., and P. W. Spaite, 1960. In: Annual Meeting of the ASME, New York, New York, December 1960.
- Whitby, K. T., D. A. Lundgren, A. R. McFarland, and R. C. Jordan, 1961. Journal of the Air Pollution Control Association, 11:503.
- Yung, S.C., R. D. Parker, R. G. Patterson, and S. Calvert, 1979. Evaluation of Granular Bed Filter for High Tempera- U. S. Environmental Protection Agency, Research Triangle Park, North Carolina.

SECTION 7

CYCLONES

7.1 INTRODUCTION

Particles suspended in a gas possess inertia which may be used to create centrifugal forces acting on the particle if the gas stream is forced to change direction. Centrifugal force is the primary mechanism of particle collection in cyclone separators and in most types of dust collection equipment loosely classed as "inertial separators".

The cyclone separator is widely used and cyclone theory is the basis for many inertial separator designs. They are relatively simple and inexpensive to fabricate, operate with moderate pressure losses, and if properly applied, give long trouble free service. Efficiency is generally good for dusts where particles are larger than about 5 μm in diameter. Cyclones are frequently used as final collectors where large particles are to be caught. They can also be used as precleaners for a more efficient collector such as an electrostatic precipitator, scrubber or fabric filter.

7.2 GENERAL DESIGN FEATURES

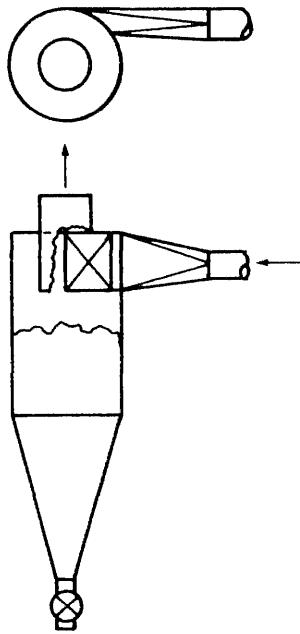
A cyclone collector is a structure without moving parts in which the velocity of an inlet gas stream is transformed into a confined vortex from which centrifugal forces tend to drive the suspended particles to the wall of the cyclone body.

The necessary elements of a cyclone consist of a gas inlet which produces the vortex; an axial outlet for cleaned gas; and a dust discharge opening. The various arrangements of these elements lead to a classification system of cyclone types as shown in Figure 7.2-1:

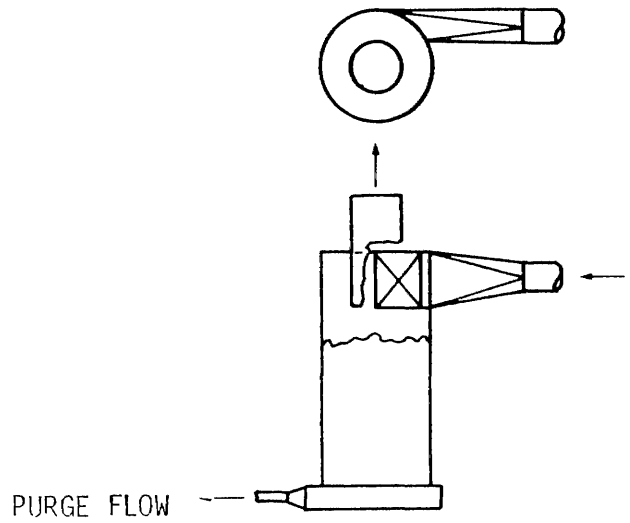
- A. The common cyclone, tangential inlet with axial dust discharge.
- B. Tangential inlet with peripheral dust discharge.
- C. Axial inlet through swirl vanes, with axial dust discharge.
- D. Axial inlet through swirl vanes, with peripheral dust discharge.

The present discussion will be limited to common cyclone (Figure 7.2-1A) which is the type most frequently used in industrial gas cleaning.

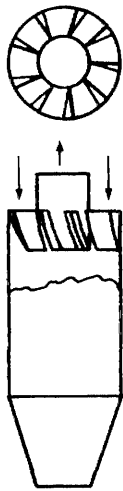
Cyclone separator geometry is described if each of the eight dimensions shown in Fig. 7.2-2 is known. However, it is often more convenient to state dimensions by expressing them in dimensionless form, as a multiple of diameter, D . The dimensions of



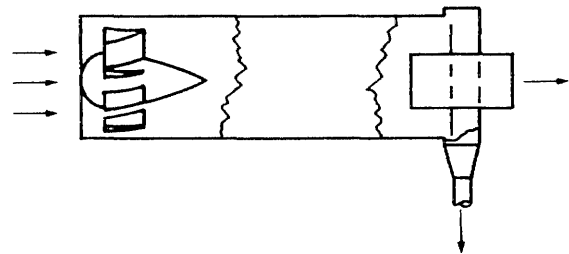
(A) Tangential inlet axial discharge.



(B) Tangential inlet peripheral discharge.



(C) Axial inlet axial discharge.



(D) Axial inlet peripheral discharge.

Figure 7.2-1. Types of cyclones in common use.

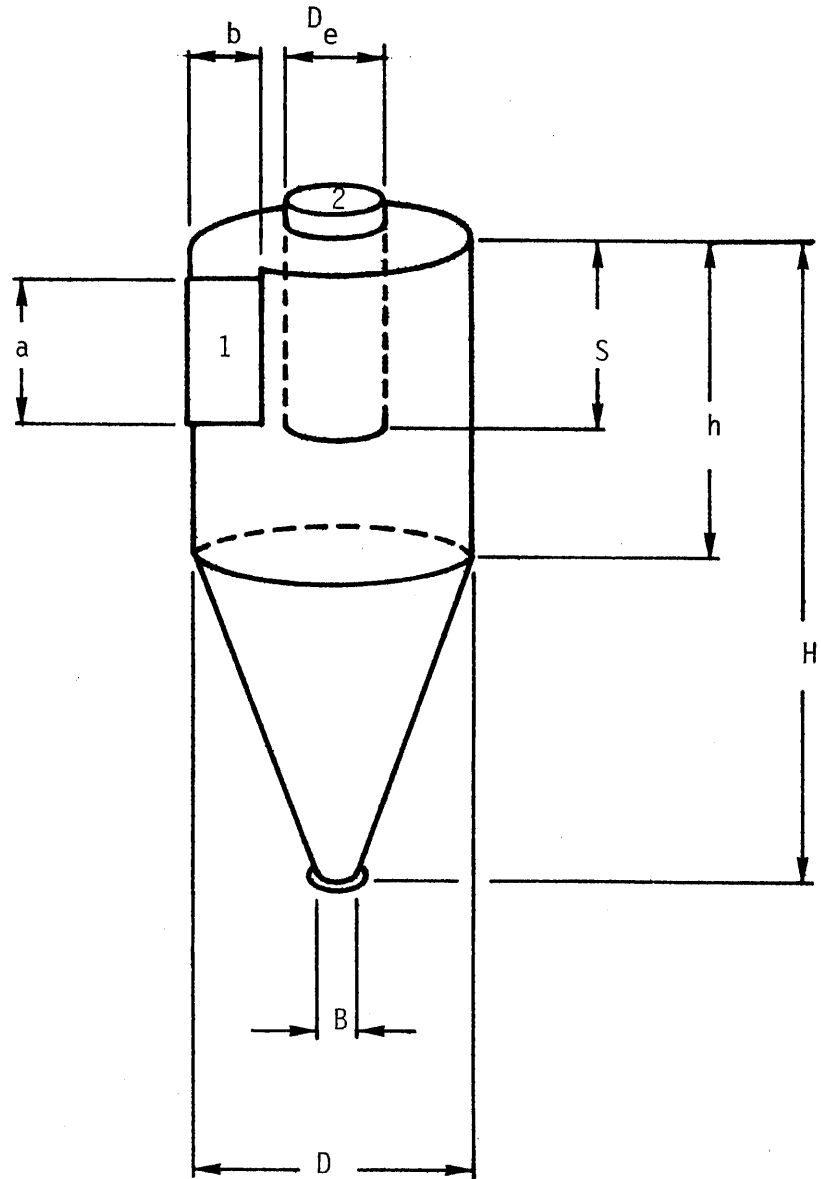


Figure 7.2-2. Cyclone geometry.

the cyclone are then specified by D and 7 dimension ratios, a/D , b/D , D_e/D , S/D , h/H , H/D and B/D . This permits a comparison of the geometric similarity of several cyclones through a consideration of their dimension ratios, without introducing absolute magnitude to the cyclone comparison.

A number of cyclone "standard designs" or sets of dimension ratios have been suggested in the literature. Several are listed in Table 7.2-1. Comparing the designs shows that the dimension ratios differ according to the purpose for which the cyclone is to be used. High efficiency cyclones tend to have smaller inlet area (a/D and b/D) and exit area (D_e/D) than do the high throughput designs. Gas exit duct length (S/D) is less in the high efficiency designs, probably because inlet height (a/D) is less. Exit duct length is always greater than inlet height in order to avoid the gas short circuiting the cyclone by passing directly from the inlet to the outlet without forming a vortex. General purpose standard designs appear to be a compromise between high efficiency and high throughput.

7.3 CYCLONE FUNDAMENTALS

7.3.1 Properties of the Vortex

The gas entering the tangential inlet near the top of the cylindrical body creates a vortex or spiral flow downward between the walls of the gas discharge outlet and the body of the cyclone. This vortex, called the "main vortex", continues downward even below the walls of the gas outlet, and at some region near the bottom of the cone, the vortex reverses its direction of axial flow but maintains its direction of rotation, so that a secondary or inner vortex core is formed traveling upward to the gas outlet as shown in Figure 7.3.1-1. The collected dust moves along the cyclone walls to the dust exit due to the downward movement of gas at the cyclone walls aided somewhat by gravity if the cyclone is stalled vertically.

Alexander (1949) observed that the gas vortex will have a stable turning point at some distance below the bottom of the exit duct which is less than $(H - S)$. He calls this the "natural length", L , of the cyclone and gives an empirical formula for it, as:

$$L = 2.3 D_e \left(\frac{D^2}{ab} \right)^{1/3} \quad (7.3.1-1)$$

It is noteworthy that this natural length is, according to Alexander, independent of the gas flow rate.

The diameter of the conical section at the turning point of the vortex, d , can be calculated from:

TABLE 7.2-1. CYCLONE STANDARD DESIGNS

Source	Recommended duty	D	a/D	b/D	D _e /D	S/D	h/D	H/D	B/D
Stairmand (1951)	High efficiency	1	0.5	0.2	0.5	0.5	1.5	4.0	0.375
Swift (1969)	High efficiency	1	0.44	0.21	0.4	0.5	1.4	3.9	0.4
Lapple (1951)	General purpose	1	0.5	0.25	0.5	0.625	2.0	4.0	0.25
Swift (1969)	General purpose	1	0.5	0.25	0.5	0.6	1.75	3.75	0.4
Stairmand (1951)	High throughput*	1	0.75	0.375	0.75	0.875	1.5	4.0	0.375
Swift (1969)	High throughput	1	0.8	0.35	0.75	0.85	1.7	3.7	0.4

*Scroll type gas entry used.

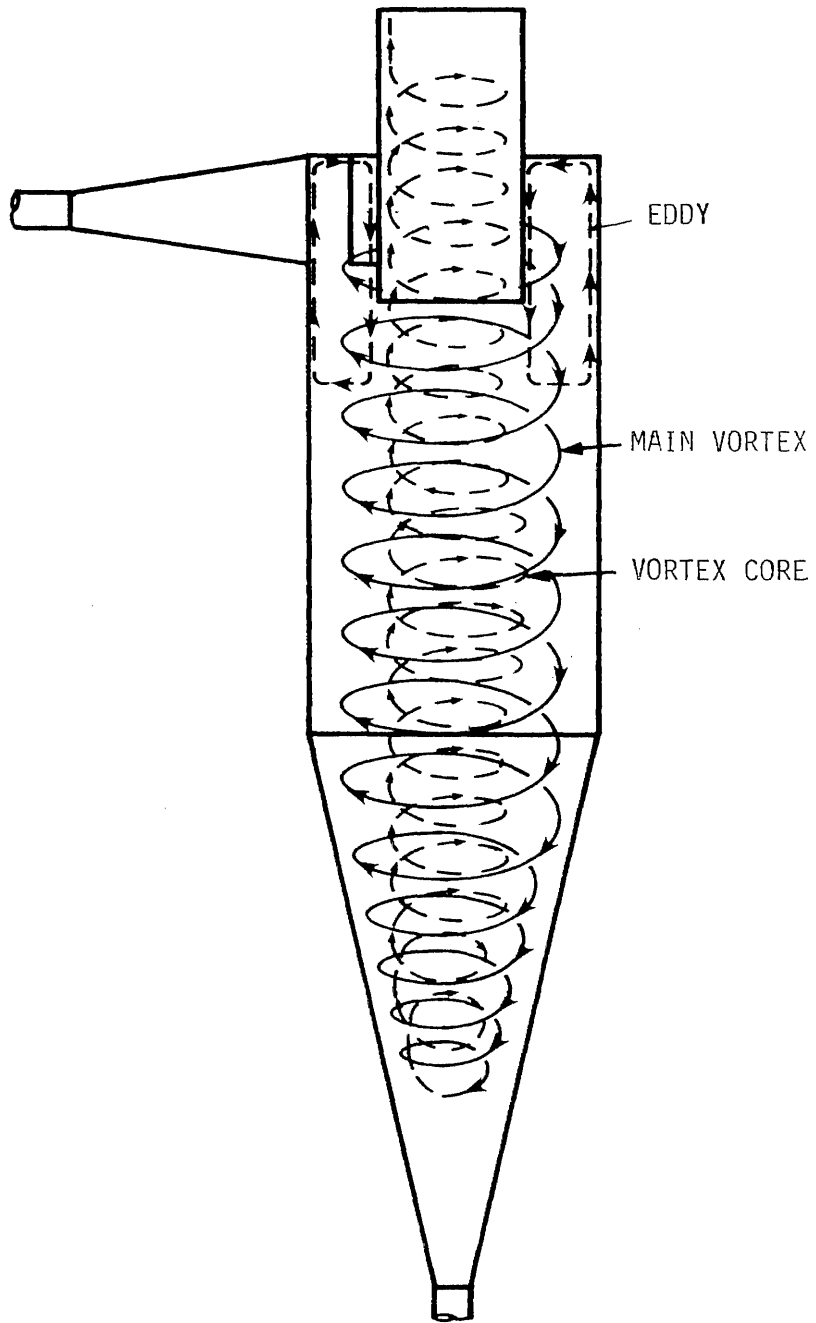


Figure 7.3.1-1. Vortex and eddy flows in a cyclone.

$$d = D - (D - B) \frac{S + L - h}{H - h} \quad (7.3.1-2)$$

The vortex core is generally smaller in diameter than the gas outlet. The radius of the core is between 0.2 and 0.4 times the radius of the gas outlet; and the radius of maximum tangential velocity is from 0.4 to 0.8 times the radius of the gas outlet, according to First (1950).

In the annular space between the cyclone body and the gas outlet, near the top of the body where the tangential inlet enters, the tangential gas velocity increases uniformly from the body wall to the outlet wall, and there is generally downward vortex flow. Because the radius of the outlet is greater than the radius of maximum velocity, the gas does not attain the maximum velocity in the annulus that it can attain later in the main body of the cyclone. In addition, there is upward gas flow along the body wall surface near the top of the cylinder. This upward flow, known as an eddy, carries gas (and dust particles) up along the body wall, inward across the top, and downward along the gas outlet wall. From this point dust particles are lost into the gas outlet. The longer the gas outlet projection into the body, the more pronounced the eddy; elimination of the gas outlet protrusion, however, does not eliminate the eddy. The axial inlet cyclone as shown in Figure 7.2-1 does not form this eddy.

Tangential gas velocity, v_t , has been found by Shepherd and Lapple (1939), First (1950), Alexander (1949), and others to be described by:

$$v_t r^n = \text{constant} \quad (7.3.1-3)$$

where r = radial distance from the vortex centerline, cm
 n = vortex exponent, dimensionless

In the ideal free vortex law, $n=1$; but experiment has shown that in a cyclone "n" may range between 0.5 and 0.9, depending on the size of the cyclone and the temperature. Figure 7.3.1-2 shows a chart of "n" values prepared by Caplan (1977) based on equations developed by Alexander (1949). This may be used to estimate a value of "n".

7.3.2 Pressure Drop

Numerous methods have been proposed for the calculation of cyclone pressure drop. Leith and Mehta (1973) have examined equations reported by Shepherd and Lapple (1940), First (1950), Alexander (1949), Stairmand (1949), and Barth (1956) and compared

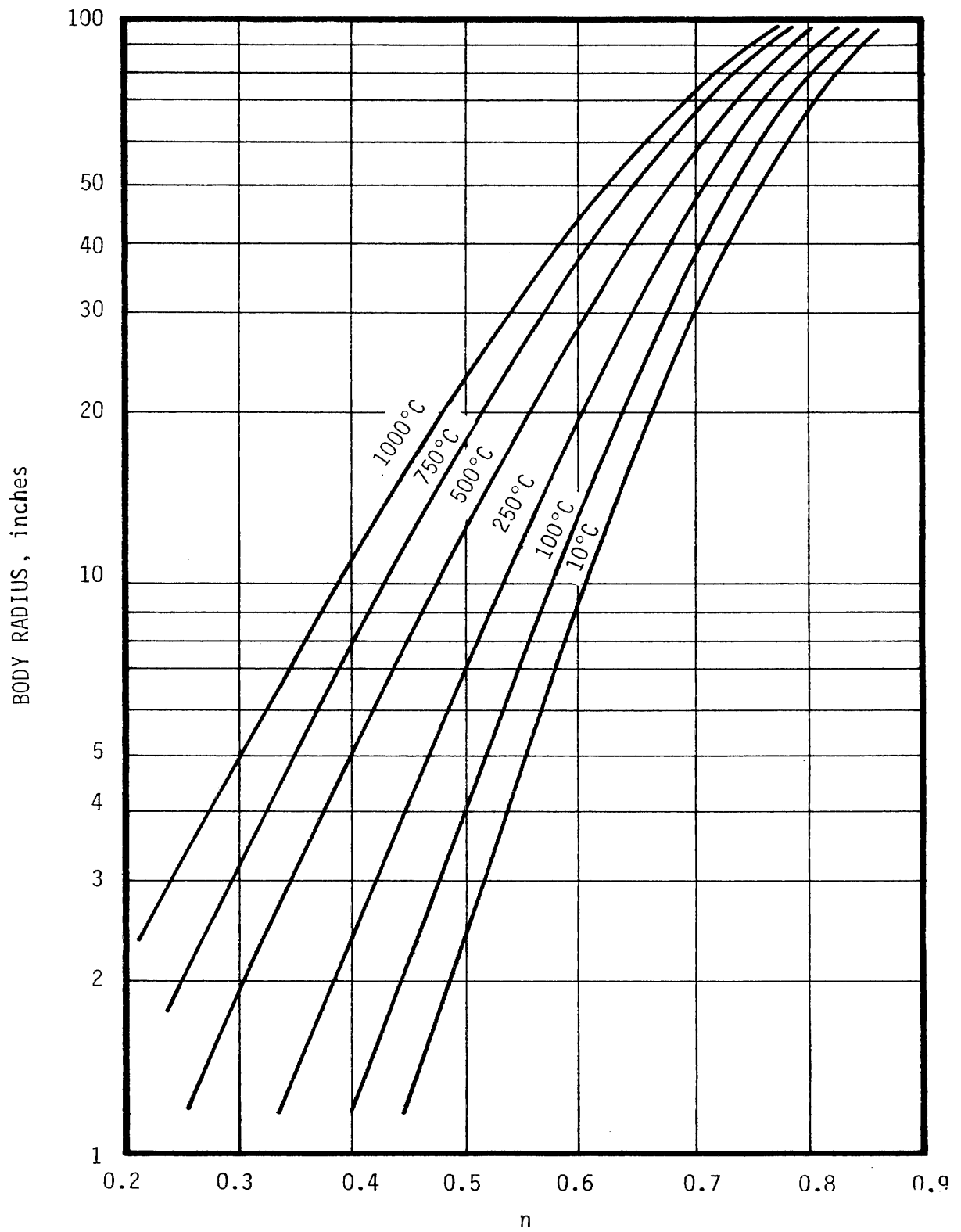


Figure 7.3.1-2. Values of n for theoretical calculations (Caplan, 1977)

data with computed results. From this they determined that the Barth, Stairmand, and Shepherd and Lapple methods are the best. However, the Barth and Stairmand methods are complex and require knowledge of all cyclone dimensions. The Shepherd and Lapple approach is simpler; it does not include all dimensions. However, the Shepherd and Lapple method appears to give results about as good as those produced by the more complicated calculation methods.

Pressure drop in a cyclone will be considered as that between points 1 and 2 in Figure 7.2-2. Shepherd and Lapple (1939) identified a number of factors contribute to the pressure difference between these points, including:

- (1) Loss due to expansion of the gas when it enters the cyclone chamber.
- (2) Loss as kinetic energy of rotation in the cyclone chamber.
- (3) Losses due to wall friction in the cyclone chamber.
- (4) Any additional frictional losses in the exit duct, resulting from the swirling flow above and beyond those incurred by straight flow.
- (5) Any regain of the rotational kinetic energy as pressure energy.

Most pressure drop theories consider factors two and three to be most important in determining the cyclone pressure drop. Shepherd and Lapple correlated experimental pressure drop results with the following equation:

$$\Delta H = K \frac{ab}{D_e^2} \quad (7.3.2-1)$$

where ΔH = number of inlet velocity heads lost, number
 K = constant for a given inlet velocity, dimensionless

"K" is equal to 16 for a cyclone with a standard tangential inlet and is equal to 7.5 for a cyclone with an inlet vane, i.e., where the inner wall of the tangential entry extends past the cyclone inner wall to a point halfway to the opposite wall.

Cyclone pressure loss is commonly reported as a number of inlet velocity heads, ΔH . Inlet velocity heads can be converted to pressure drop in terms of static pressure head, ΔP , by:

$$\Delta P = \frac{v_g^2 \rho_G \Delta H}{2g \rho_L} \quad (7.3.2-2)$$

where ΔP = pressure loss, cm W.C.

v_g = gas velocity through cyclone inlet, cm/s
 ρ_G = gas density, g/cm³
 ρ_L = density of water, g/cm³

7.3.3 Collection Efficiency

Leith and Licht (1971) developed a theoretical model for the calculation of collection efficiency. This theory was compared to theories reported by Barth (1956), Lapple (1951), Sproull (1970), and experimental data. Predictions from the Leith and Licht equation were shown to give the best approximation of experimental data (Leith and Licht, 1971). Their equation is:

$$\eta = 1 - \exp[-2(C K)^{1/(2n+2)}] \quad (7.3.3-1)$$

where "C" is a function of the cyclone dimension ratios (Figure 7.2-2) only:

$$C = \frac{\pi D^2}{ab} \left[2 \left(1 - \left(\frac{D_e}{D} \right)^2 \right) \left(\frac{S}{D} - \frac{a}{2D} \right) + \frac{1}{3} \left(\frac{S + L - h}{D} \right) \left(1 + \frac{d}{D} + \left(\frac{d}{D} \right)^2 \right) + \frac{h}{D} - \left(\frac{D_e}{D} \right)^2 \frac{L}{D} - \frac{S}{D} \right] \quad (7.3.3-2)$$

and

$$K = \frac{C' \rho_p d_p^2 v_g}{18\mu_G D} (n + 1) \quad (7.3.3-3)$$

where K = centrifugal inertial impaction parameter, dimensionless

Cyclones provide the lowest collection efficiency as well as the lowest initial cost for devices in general commercial use to control particule emissions. Typical particle collection efficiencies for cyclone collector installations are shown in Figure 7.3.3-1.

In general, efficiency will increase with increase in dust particle size or density, gas inlet velocity, cyclone length, and ratio of body diameter to gas outlet diameter. Conversely, efficiency will decrease with increase in gas viscosity or den-

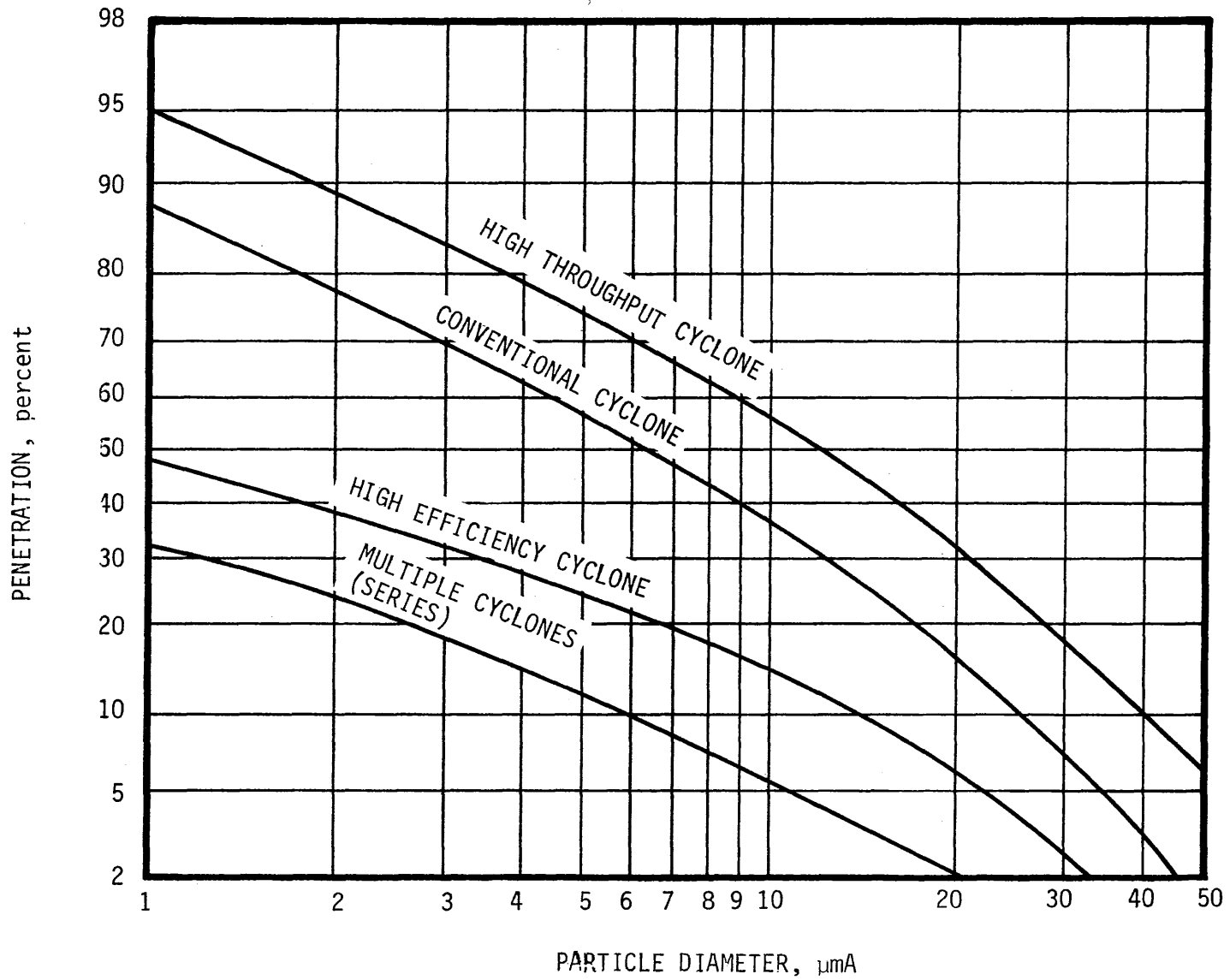


Figure 7.3.3-1. Typical grade penetration curves for cyclones. (Caplan, 1977).

sity, cyclone diameter, gas outlet diameter, and inlet width or inlet area. Figures 7.3.3-2 and 7.3.3-3 show the effect of velocity and cyclone diameter.

Unfortunately, changes in parameters which tend to increase collection efficiency also tend to increase pressure drop. The loss of pressure of the gas stream through the cyclone is of the order of one to four inlet velocity heads, with a resulting range of pressure drop from 1 to 20 cm W.C. Efficiency increases with increasing inlet velocity, but this increase is at lower rate than the pressure drop. In addition, for any practical installation there is a limiting value of inlet velocity above which turbulence causes a decrease in collection efficiency with further increase in inlet velocity.

The only practical upper limit to particle concentration occurs with the smaller body diameters of high efficiency cyclones, where a fine or sticky dust concentration of 20 to 35 g/m³ may cause plugging of the narrow passages. For ordinary cyclones, there is no practical upper limit to the dust concentration and the efficiency increases with an increasing dust concentration. Even though the collection efficiency increases with increasing dust concentration, the total weight rate of uncollected particles will be higher for higher inlet concentrations because the efficiency increase is not nearly as rapid as is the increase in particle concentration.

All theoretical equations were derived by assuming that once a particle reaches the wall of the cyclone, it is collected. This is in contrast to the observations of Morii et al. (1968) that large hard particles bounce off the cyclone walls back into the gas stream. It is also probable that some collected particles, primarily in the smaller size ranges, will be reentrained from the collector wall before being discharged through the dust exit duct. Smaller particles may be more susceptible to reentrainment as they are only collected with difficulty in the first place. It has been noted by Stairmand (1951) that cyclone efficiency increases if the cyclone walls are wetted, as wetting presumably hinders particle bounce and reentrainment.

No theoretical equation accounts for the increase in collection efficiency noted by Stairmand (1951) and Caplan (1968) associated with the drawing off a fraction of the gas throughput from the dust exit. The increase in efficiency associated with the base draw-off has been attributed to a reduction in dust reentrainment near the dust exit. Another effect of the draw off may be to induce the vortex to run the full length of the cyclone, rather than ending some distance above the bottom of the cyclone. A disadvantage of this practice is that the gas drawn off, typically 5-15 per cent of the gas throughput, has to be recycled to the cleaning equipment. The recycle results in a somewhat larger cleaning system being required, as well as the installation of otherwise unnecessary auxiliary fans.

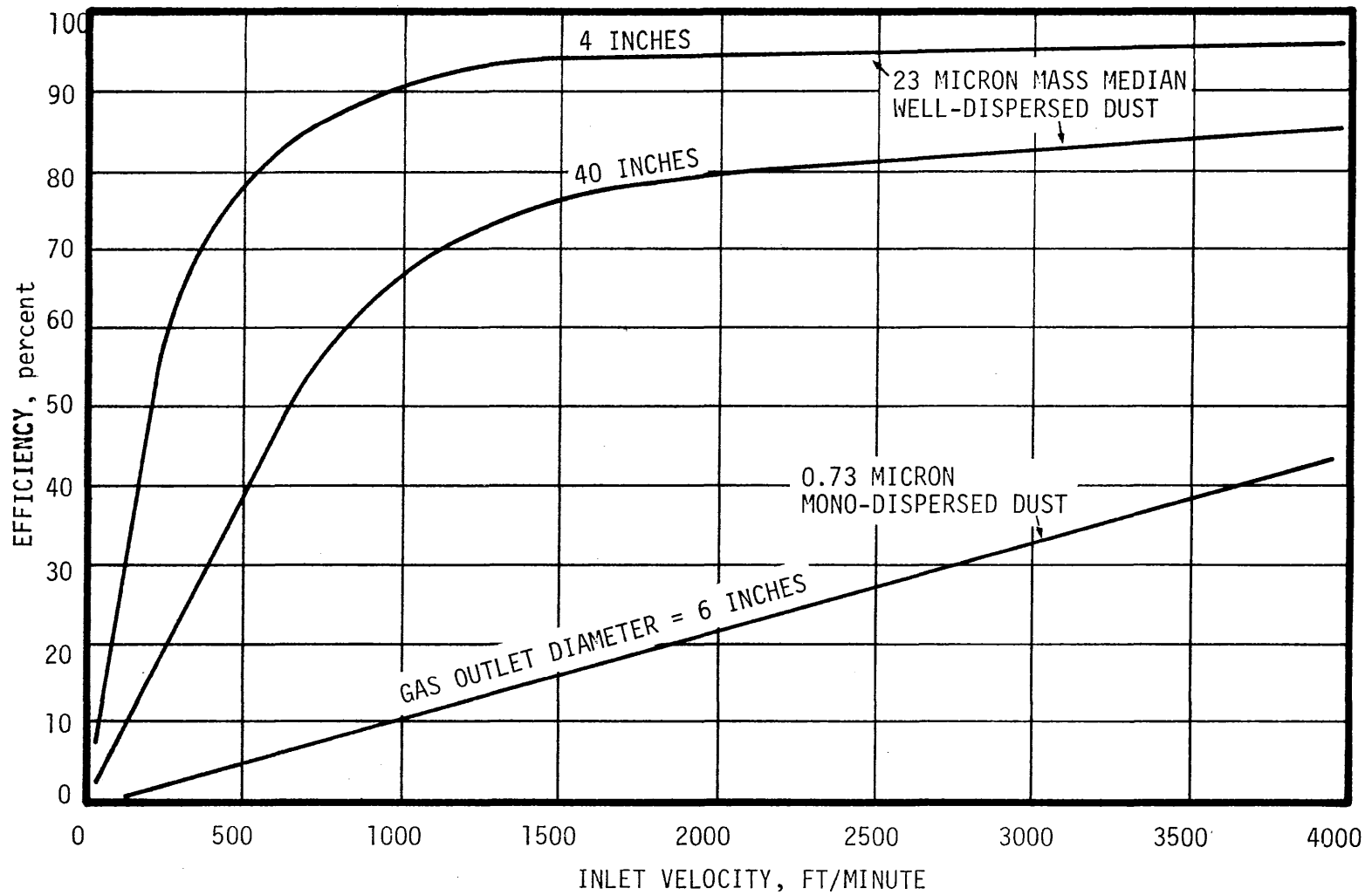


Figure 7.3.3-2. Variation of efficiency with inlet velocity. (Caplan, 1977)

7-14

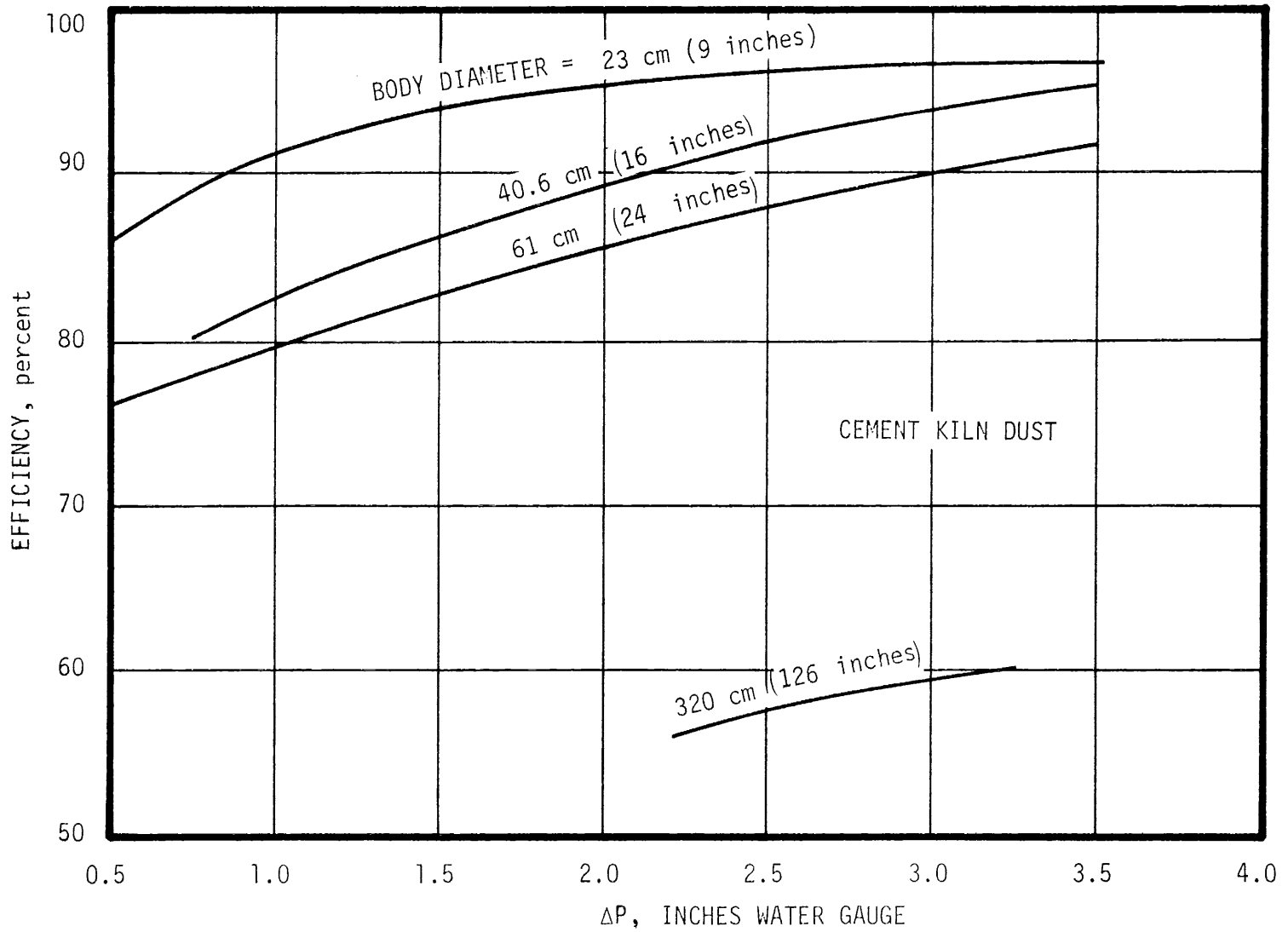


Figure 7.3.3-3. Variation of efficiency with pressure drop (Caplan, 1977).

7.3.4 Discharge of Separated Dust

The application of centrifugal force to drive particles out of the gas stream toward the walls of a cyclone collector results in a concentrated dust layer swirling slowly down the walls of the cyclone body. The purpose of the discharge is to retain the dust or liquid in a container and to prevent its reentrainment into the gas stream at the base of the vortex. The length and dimension ratios of the cyclone affect such reentrainment. Smoothness of the inner walls of the cyclone is essential to prevent small eddy currents which would bounce the dust layer out into the active zone of the vortex. Recirculation of gas or in-leakage of gas into the dust outlet will be harmful to attempt to discharge the dust without reentrainment, and conversely, a small purge flow of gas outward from the dust outlet will be helpful; similarly an air lock material discharge valve or dip leg is an aid to discharging dust without reentrainment.

Because the outlet duct for the gas discharge consists essentially of a cylinder to confine and conduct the vortex core out of the cyclone, any dust which escapes into this gas stream is still subjected to centrifugal forces and tends to be concentrated near the walls of the duct. Devices for skimming off the outside layer of this vortex can be employed to improve the overall efficiency of dust separation.

7.4 FACTORS INFLUENCING PERFORMANCE

7.4.1 Effect of Design Factors

7.4.1.1 Body Diameter and Dimension Ratios

In the study of design parameters which affect efficiency and pressure drop, a typical cyclone has been selected as the starting point. The dimensions of the various body elements, Figure 7.4.1-1, are based on the proportion of the dimension to the gas outlet diameter.

Starting with this design, a cyclone of higher efficiency and higher pressure drop could be designed by increasing the length of the cyclone, decreasing the inlet width, or increasing the ratio of body diameter to outlet diameter while at the same time providing a smaller body diameter.

The length of the cyclone body is of importance. An increase in length provides for a longer residence time of gas in the vortex and therefore for more revolutions or turns in the vortex. A very practical consideration involving the total length of the cyclone is that one of the most common defects leading to lower efficiency is reentrainment of dust into the vortex core from the region of the dust discharge port. The further the cyclone extends below the gas outlet, the greater the opportunity for reentrained dust to be precipitated out of the vortex core before it enters the gas outlet.

A number of investigators (Alexander, 1949; Ter Linden, 1949; Stairmand, 1951; and Schneider, 1950) have presented data

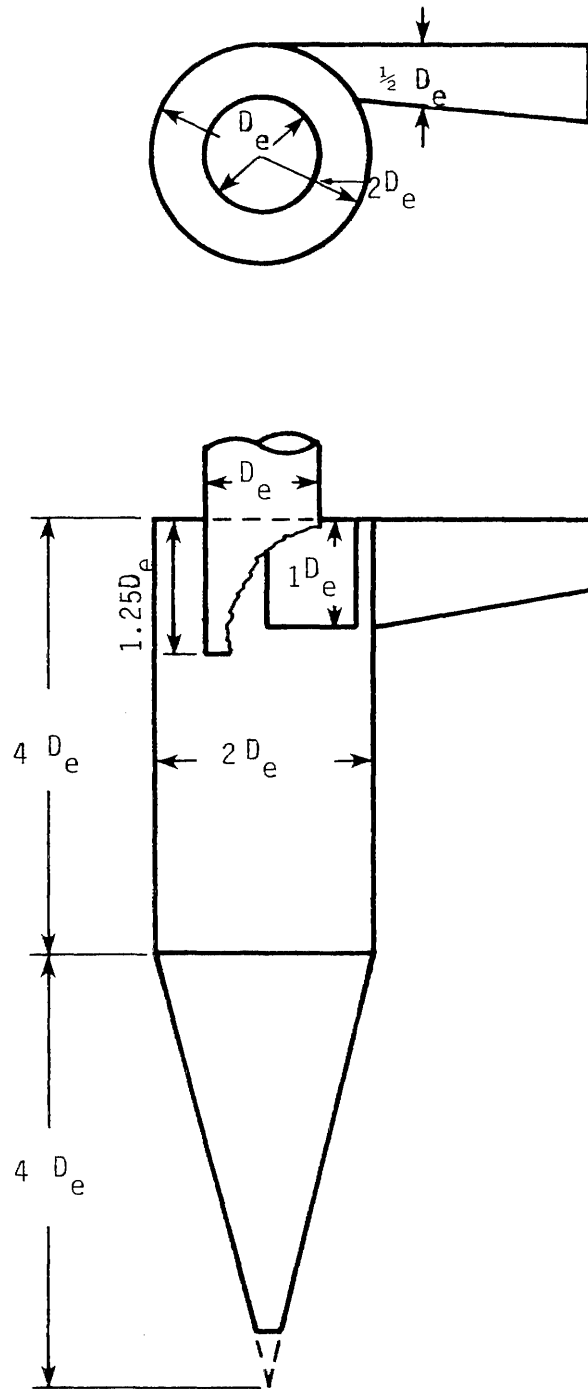


Figure 7.4.1-1. Typical cyclone dimension ratios.

or conclusions which are in substantial agreement that the height of the main vortex zone should be at least 5.5 times the gas outlet diameter, preferably more, perhaps up to 12 times the outlet diameter. The total length for the typical cyclone, Figure 7.4.1-1, of 8 times the outlet diameter seems to meet these criteria. Contrary to general statements previously made, increasing the length of the cyclone without changing any other dimension ratios will achieve an improvement in efficiency with no penalty in terms of increased pressure loss.

Increasing the ratio of the body diameter to the gas outlet diameter does show an increase in efficiency up to a ratio of about 3 with relatively small gain above that. On the other hand, there is a corresponding increase in pressure drop as this ratio increases so that the optimum ratio would appear to be between 2 and 3.

Theoretically, efficiency should continue to increase with a decrease in cyclone diameter, but this has not been proved in practice. In a very small cyclone, the gas outlet is dimensionally very close to the region where the dust is concentrated along the cyclone wall. Therefore any bouncing of large particles or local eddies caused by turbulence are more likely to result in accidental loss of dust to the gas outlet.

7.4.1.2 Cone Design

The definition of a cyclone makes no mention of a cone. If a cone is present its design is important, but it is not necessary for a cyclone to have a cone. Neither is a cone essential to cyclone theory, since the main vortex will transform to the upflowing vortex core in a long cylinder without a cone. The various types of cyclones without a cone will be discussed later under the subject of dust discharge. However, a cone does serve the practical function of delivering the dust to a central point for ease in disposal, and forces the main vortex to transform to the vortex core in a shorter total length than would occur in a straight cylinder.

The axis of a free vortex is frequently curved, a similar curvature or eccentricity of the vortex core has been observed in cyclone operation (Schulz, 1948) and may amount to as much as one-fourth the gas outlet diameter. Theoretically, the diameter at the apex of the cone should be greater than one-fourth the gas outlet diameter to prevent the vortex core from touching the wall of the cone and reentraining collected dust. For cyclones of larger sizes, a cone apex of such dimensions may be unreasonable. This merely reemphasizes the need for adequate total cyclone length so that any dust reentrained at the cone apex may be separated again before it reaches the gas outlet.

7.4.1.3 Inlet Design

The design of the cyclone inlet is of critical importance to both cyclone efficiency and pressure drop. Unfortunately, little design data are available for the axial inlet type, since most cyclones of this design are proprietary. However, there has been much effort to experiment with the design of the tangential inlet to improve cyclone performance. The different types of common tangential inlets are shown in Figure 7.4.1-2.

The helical inlet design is provided to impart a downward velocity to the gas to avoid interference between the incoming gas and the mass of gas already rotating in the annulus. Existing test data are conflicting as to whether or not this design actually does provide a lower pressure drop, and there is some indication that a lower efficiency is obtained. Most commercial cyclones do not have a helical inlet.

As the inlet gas enters the annular space between the cyclone body wall and the wall of the gas outlet duct, it undergoes a squeeze between the body wall and the rotating air mass already in the annulus. The involute inlet design has been developed to minimize the interference between these gas streams. Use of multiple involute inlets has the further advantage that for the same inlet area and height, the inlet width is reduced.

The multiple inlet designs are found in small "high efficiency" cyclones where the inlet gas is taken from a plenum serving all inlets simultaneously. If practical, a bell-mouth inlet from the plenum to the cyclone inlets will reduce pressure loss and possibly improve efficiency.

The acceleration of gas associated with the previously described squeeze of gas entering the annulus is an important part of the total pressure loss of the cyclone. Inlet vanes (Figure 7.4.1-2A) have been tried as a method of reducing this pressure loss. Non-expanding inlet vanes result in one-half the pressure drop of the same cyclone without vanes, expanding vanes result in one-fourth the pressure drop. However, both of these types of inlet vanes decreased dust collection efficiency by preventing the formation of a vortex in the upper part of the annulus.

The approach duct to a common cyclone is usually round, and if a proper inlet height-to-width ratio is to be obtained, the round duct must be transformed to a rectangular inlet. Such transformation should be gradual, if possible with a maximum included angle of 15° or less, in order to minimize shock losses when inlet velocity is increased from duct velocity. Similarly, if the inlet velocity is lower than the duct velocity, a gradual transformation will result in maximum static pressure regain. To conserve space, an involute inlet can be used as shown in Figure 7.4.1-2C.

The orientation of the inlet duct is also important. If the inlet is downwardly inclined from the horizontal to a vertical axis cyclone, the pressure drop is increased and the efficiency is decreased (Larcombe, 1947).

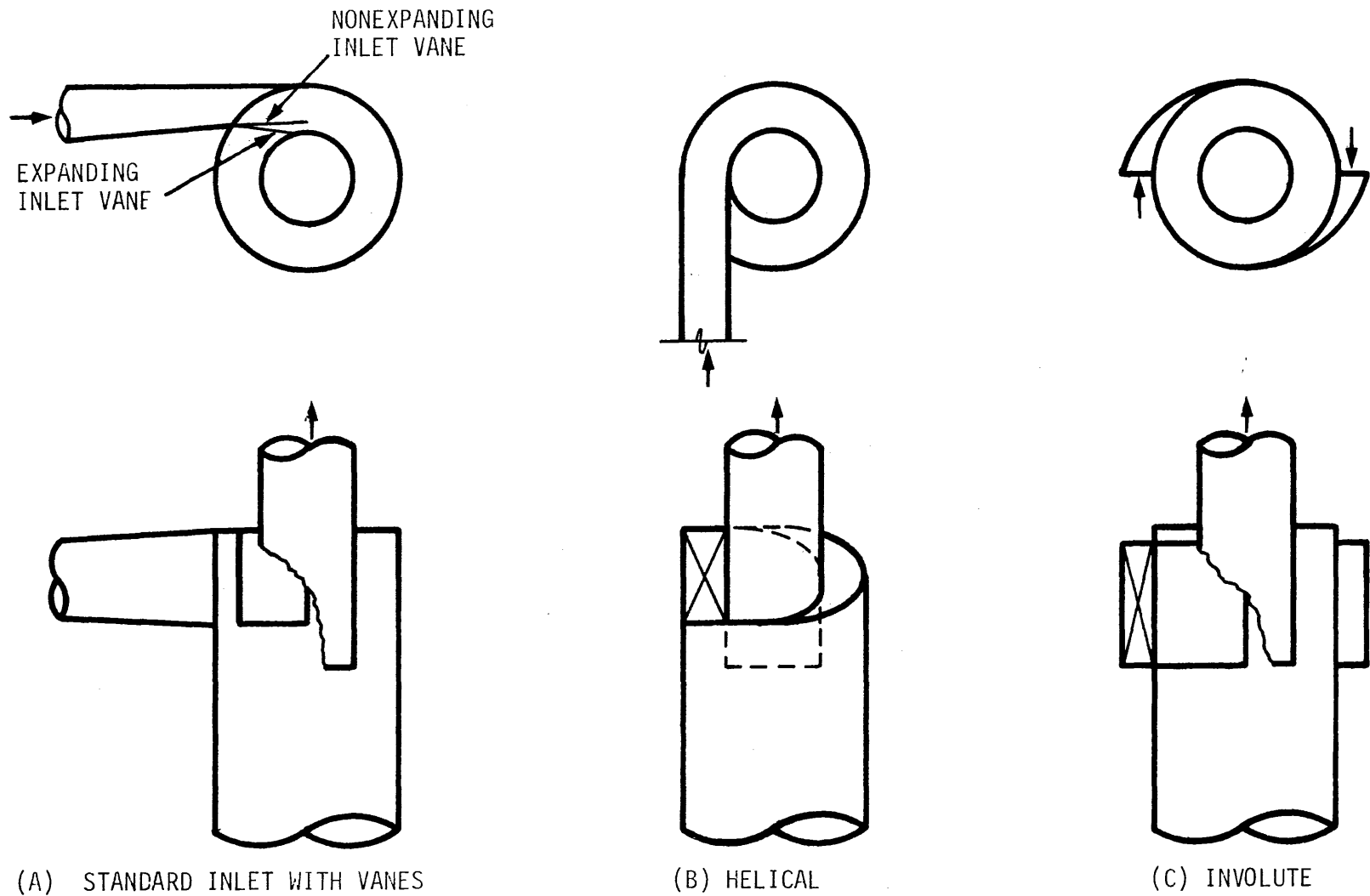


Figure 7.4.1-2. Types of tangential inlets.

7.4.1.4 Dust Discharge

It is essential in any cyclone design to remove the separated dust from the cyclone cone or body as immediately, completely, and continuously as possible. Many different schemes have been developed for accomplishing these results. The simplest system is a hopper or dust bin closed at the bottom and open at the top to the cyclone discharge. There will be a vortex in the bin as well as in the core. If this upflow is excessive, the normal discharge of dust is prevented. The vortex in the connection between the cyclone cone and dust bin can be suppressed by straightening vanes in the dust discharge pipe, or by baffles (disks or cones) installed about two dust discharge diameters above the apex of the cone so that there is approximately a 8 cm annular space between the edge of the baffle and the cone wall. An axial disk near the dust discharge is a trend toward the peripheral dust discharge cyclone design discussed later.

Another common method of minimizing upflow through the dust discharge pipe is to use some type of valve to prevent such flow. For most dust collection systems, where the negative pressure at the bottom of the cyclone is in the range of 10 cm W.C., ordinary rotary valves are sufficiently gas-tight. If the negative pressure is higher, however, much better valving is required--usually a double set of valves which are capable of providing airtight closure in the presence of solids. Choke discharge screw conveyors may also be used at the bottom of a cyclone.

Since an inward flow of gas at the dust discharge is harmful, one method of correcting this situation is to install the cyclone at such a location in the system that it is under positive pressure with respect to the atmosphere or to the dust retention bin. Although this solves the problem of gas inflow at the dust discharge, it causes two other problems which may be of equal importance. First, the dust retention bin and disposal system may itself become a source of air pollution; second, such an arrangement requires the entire dust load to be handled by the fan, in many cases with excessive erosion or fan unbalance.

7.4.1.5 Gas Outlet Design

The eddy currents in the annulus of the cyclone require that the gas outlet have an extension into the body of the cyclone in order to minimize loss of dust through the gas outlet. The optimum length of the gas outlet extension has been determined to be about one gas outlet diameter (Ter Linden, 1949). It is also generally assumed that this extension should terminate slightly below the bottom of the gas inlet. The shorter the outlet extension into the cyclone, the lower the pressure drop attained. No outlet extension results in the lowest pressure loss, but dust collection efficiency under such circumstances will generally be unsatisfactory.

7.4.1.6 Effect of Internal Roughness

An extensive experimental and theoretical investigation of cyclone design and performance (First, 1950) resulted in the conclusion that the wall friction in the cyclone was a negligible portion of the pressure drop. The pressure drop is due almost entirely to the vortex, and to the design of the inlet and gas outlet. Increased roughness of the internal wall of the cyclone, probably by the inducement of local eddy currents and increased local wall friction, reduces vortex intensity, with the overall result that cyclone pressure drop is reduced. Dust collection efficiency is also reduced.

7.4.2 Effect of Dust Properties

The properties of the dust to be collected represent the most important variable in cyclone efficiency, and are probably the most difficult to evaluate. Many physical properties of the dust will affect the efficiency, but the only ones that have been investigated quantitatively are particle size and particle density. Other physical and chemical properties which make the dust hard or easy to handle will also affect the practical aspects of cyclone operation in terms of erosion and fouling in cyclones.

Erosion in cyclones is caused by the impingement and rubbing of dust particles on the cyclone wall. Erosion is worse with high dust loadings, high inlet velocities, and large or hard dust particles. Any defect in cyclone design or operation which tends to concentrate dust moving at high velocity will accelerate erosion.

The areas most subject to erosive wear are those along welded seams or mismatched flange seams, near the bottom of the cone; and opposite the inlet. Surface irregularities at welded joints, and the annealing softening of metal adjacent to the weld will induce rapid wear in the weld region. Welded seams should be kept to a minimum, and heat treated if necessary to maintain the hardness of the metal adjacent to the weld.

The importance of proper dust discharge has been stressed previously in discussions of efficiency. It is similarly important in preventing erosion. If dust is not effectively and continuously discharged from the bottom of the cone, a high circulating dust load is maintained in that region, leading to excessive wear of the cone. If the dust outlet should plug, the entire circulating dust load is conducted through the cyclone, including the gas discharge pipe, and it may cause erosive wear at any point.

Excessive wear of the cyclone shell opposite the inlet may occur, particularly if large particles are handled. This can be cured by the provision of removable wear plates of abrasive-resistant metal or rubber designed so as to be flush with the inside surface of the shell.

Combinations of dust loading and velocity which will, if exceeded, induce erosion have been shown in the following tabulation (Stern et al. 1955).

Dust Concentration (g/m ³)	Velocity (m/min)
0.7	2,100
7.0	1,200
7,000	120

It has also been determined that dust particles smaller than about 10 μ m do not cause appreciable erosion.

It is possible to design a cyclone to reduce erosion by increasing the diameter of the cyclone body without increasing the diameter of the gas outlet. This results in reduced velocity at the body wall without reducing maximum velocities and separating force of the vortex. It also results in increased pressure drop. Consequently, at high loadings of abrasive dust, large-diameter cyclones are required to control erosion. For more moderate conditions, small-diameter cyclones have an advantage since they usually do not have seams or welds.

Fouling of cyclones results in decreased efficiency, increased erosion, and increased pressure drop. Fouling is generally found to occur either by plugging of the dust outlet or by the buildup of materials on the cyclone wall.

Dust outlets become plugged by large pieces of extraneous material in the system, by the overflowing of the dust bin, or by the spalling of material caked upon the walls of the cyclone. The valves used to discharge dust from the collection bin should not be smaller than 10 cm in most applications, and in all except large pneumatic conveying or fluidized bed applications need not be larger than 35 cm. A vertical axis cyclone is somewhat less subject to plugging of the dust outlet because gravity helps to remove large objects through the discharge.

It is of utmost importance to prevent overflowing of dust hoppers, particularly under multiple banks of small-diameter cyclones. If a hopper has filled sufficiently to plug the outlets and later has been emptied, the dust plugs may remain in the outlets. In large-diameter cyclones, cleanout openings can be provided, but this is not practical for large banks of small-diameter tubes. The buildup of sticky materials on the wall of the cyclone is primarily a function of the dust. In general, the finer and softer the dust, the greater the tendency to cake on the wall. Chemical and physical properties will also affect this behavior. Condensation of moisture on the walls of the cyclone will also contribute to the accumulation of material. In many cases, buildup of sticky material on the walls can be mini-

mized by keeping the inlet velocity above 15 m/s. Smoothness of the cyclone walls is also important, and some applications have even used electropolished walls to minimize the buildup of powdered milk or coffee dust.

The cure for excessive wall buildup frequently must be tailored to meet the particular circumstance. In one case, the removal of an inertial precleaner so as to permit the coarser material to also traverse the cyclone walls may present a cure; in another, periodically inducing a reverse gas flow from the dust bin by the introduction of compressed air to the bin may be successful. If wall condensation is the cause, it must be eliminated by insulation or other appropriate methods. In some cases, the use of water or other fluids is necessary to wash accumulations out of the tubes. As far as the design is concerned, the important features to minimize fouling are good removal of dust from the dust discharge, adequate size of dust bin discharge, prevention of dust bin overflowing, choice of proper inlet velocity, and prevention of wall condensation.

SECTION 7

REFERENCES

- Alexander, R. McK., 1949. Fundamentals of Cyclone Design and Operation. Proc. Australas Inst. Min. Met. (New Series). 152-3:203-228.
- Barth, W., 1956. Design and Layout of the Cyclone Separator on the Basis of New Investigations. Brenn. Warme Kraft. 8:1-9
- Caplan, Knowlton J., 1977. Source Control by Centrifugal Force and Gravity. In: Air Pollution Third edition, Vol. IV (edited by A. C. Stern). Academic Press, New York, New York. pp. 97-146.
- First, M. W., 1950. Fundamental Factors in the Design of Cyclone Dust Collectors. Doctoral Thesis. Harvard University.
- Lapple, E. C., 1951. Processes use many collector types. Chemical Engineering. 58:144-151.
- Larcombe, H. L. M., 1947. Mining Magazine. 77:137-148, 208-217, 273-278, and 356-347.
- Leith, David and Wm. Licht, 1971. The Collection Efficiency of Cyclone Type Partricle Collectors - A New Theoretical Approach. Presented at 64th Annual Meeting American Institute of Chemical Engineers - December, 1971. Paper 13a.
- Leith, David and Dilip Mehta, 1973. Cyclone Performance and Design. Atmospheric Environment. 7:527-549.
- Morii, Y., A. Sukanuma, and S. Tanaka, 1968. On Collection Efficiency of Gas Cyclone on Coarse Particle Range. Journal of Chemical Engineering Japan. 1:82-86.
- Schneider, F. G., 1950. General Electric Review. 53:22-29.
- Schulz, F., 1948. Engineering Digest. 5:49.
- Shepherd, C. B. and C. E. Lapple, 1939. Flow Pattern and Pressure Drop in Cyclone Dust Collectors. Industrial and Engineering Chemistry. 31:972-984.
- Shepherd, C. B. and C. E. Lapple, 1940. Flow Pattern and Pressure Drop in Cyclone Dust Collectors. Industrial Engineering Chemistry. 32:1246-1248.

Sproull, W. T., 1970. Air Pollution and Its Control. Exposition Press, New York.

Stairmand, C. J., 1949. Pressure Drop in Cyclone Separators. Engineering. 16B:409-411.

Stairmand, C. J., 1951. the Design and Performance of Cyclone Separators. Transactions Institution of Chemical Engineers. 29:356-383.

Swift, P., 1969. Dust Control in Industry. Steam Heat Engineer. 38:453-456.

Ter Linden, A. J., 1949. Proceedings Institute of Mechanical Engineers. 160:233.

SECTION 8

FUEL COMBUSTION SOURCES

8.1 INTRODUCTION

The purpose of this section is to present information on the fine particle emissions from stationary fuel combustion installations. This information will serve as a basis for selecting or recommending fine particle control technology. The following categories of fuel combustion sources were found to be the major contributors of fine particle emissions in California (Minicucci et al. 1980; ARB, 1980).

1. Residual Fuel Oil
 - a. Field-Erected Boilers
 - b. Package Boilers
2. Crude Oil
 - a. Package Boilers
3. Distillate Fuel Oil
 - a. Package Boilers
4. Coal
 - a. Field-Erected Boilers

There are no coal-fired utility boilers in California at this time, but they are included here because it is expected that certain oil-fired utility boilers will be converted to coal during the next five years (ARB, 1980). Therefore, combustion of low and medium sulfur coals is expected to become a major source.

Particles appear in the effluent gas from fuel combustion processes because of 1. entrainment of non-combustible and non-volatile components, 2. condensation of low vapor pressure compounds in the fuel, and 3. condensation of low vapor pressure compounds formed in the combustion process. The size and type of the combustion installation affects the size distribution and concentration of particles in the flue gas. Larger installations, such as those found in electric utilities, often have more elaborate fuel preparation procedures (more thorough atomization, for example) (Monroe, 1973; Babcock and Wilcox Co., 1978). Large installations are also more closely monitored. Smaller industrial and commercial boilers are less elaborate and often operate unattended.

Steam generators must be field-erected when steam pressures higher than 1,500 psig are required, steam flow rates in excess of 500,000 lb/hr are specified, or steam-side process features such as reheat cycles are desired (Babcock and Wilcox Co., 1978). These boilers are usually custom-designed for the purchaser. The boiler is shipped in modules or pieces and assembled at the installation site. Large utility boilers are usually of this type.

Package boilers are manufactured in complete units and shipped to the purchaser for installation (Babcock and Wilcox Co., 1978). They are available with maximum capacities of 200,000 lb/hr of steam for rail shipping, and 500,000 lb/hr for barge shipping. Package boilers are available with either fire-tube or water-tube construction. In water-tube boilers the boiling fluid circulates around the walls of the combustion zone. In fire-tube boilers the combustion products are directed through tubes which are immersed in the boiling fluid. Most newer package boilers are of the water-tube design (Vandegrift et al. 1970). No distinction will be made below between the two firing methods since the particle emission characteristics are similar.

8.2 OIL FUEL

Several grades of fuel oil are used in California. The three most important oil fuels from a particle emission standpoint are distillate fuel oil, residual fuel oil, and crude oil. The uses and identifications of these fuels appear in Table 8.2-1.

The differences in the methods of combustion and their effect on particulate emissions for these three types of oil fuel are explored in Section 8.2.1.

8.2.1 Process Description

In general the process steps required for the combustion of any fuel are the following (Babcock and Wilcox Co., 1978):

1. The preparation and feeding of fuel and air.
2. Heat exchange with the heat transfer medium.
3. Separation and disposal of unburned fuel and ash.
4. The venting of the combustion gases.

Oil fuel must be divided into small drops (atomized) to provide interfacial surface area for rapid ignition and combustion (Babcock and Wilcox Co., 1978). Poor atomization (fuel drops too large) can lead to increased particulate emissions due to incompletely combusted drops (Walsh and Danielson, 1973a; Monroe, 1973). Residual fuel generally requires preheating to reduce the fuel viscosity for thorough atomization. Atomization may be done mechanically, or with air or steam. No distinction will be made in Section 8.2.2 below between atomization methods.

The burner arrangement affects the rate of combustion and fouling of the heat exchange surfaces inside the boiler. The most common burner arrangements are listed below (Corey, 1973):

1. Wall-Fired. All the burners are situated on one wall of the boiler. The combustion gas flow may be vertical or horizontal.

TABLE 8.2-1. OIL FUEL IDENTIFICATION AND USES^{a,b,c}

<u>Fuel Type</u>	ASTM D396 <u>Grades</u>	<u>Use</u>
Distillate	1, 2	Home heating oil. Small commercial and industrial furnaces and boilers.
Residual	5, 6*	Large commercial and industrial furnaces. Electric utility boilers.
Crude	-	Oil field tertiary oil recovery.

*Several areas in California have regulations limiting the sulfur contents of fuel oils to a lower value than the ASTM specification. Examples are SCAQMD (Rule 431.2) and SDAPACD (Rule 62).

^aAmero, 1973

^bBabcock and Wilcox Co., 1978

^cWalsh and Shaffer, 1973

2. Horizontally Opposed. The burners are situated on opposite walls. The hot combustion gas is concentrated in the central region of the firebox.
3. Corner-Fired. The burners are aimed to form a vortex of combustion gas in the firebox. The swirling gas reduces the deposition of condensibles and fly ash on the tube surfaces.

Field-erected boilers fired with residual oil are usually of the wall-fired configuration. Tangential (corner) firing is infrequent but is becoming more widespread (Vandegrift, et al., 1970).

8.2.2 Source Characteristics

Figures 8.2.2-1 through 8.2.2-4 show particle size distributions for oil-fired boilers. Tables 8.2.2-1 through 8.2.2-3 show gas and solids emission characteristics for oil-fired boilers. The information in the tables is for wall-fired boilers only. Soot blowers are used on oil-fired utility boilers to remove deposits on the tube surfaces. Their use increases the particle concentration in the effluent gases (Babcock and Wilcox, 1978). The effects of soot blowing have been included in Figure 8.2.2-1 and Table 8.2.2-3.

8.2.3 Control Technology

Most oil-fired utility boilers in California do not have particle emission control equipment at present (Minicucci et al. 1979) because of:

1. Low fuel sulfur content. Utilities are only allowed to burn low sulfur fuel in major metropolitan areas of California (SCAQMD, 1978; SDAPCD, 1978). Since fine particle emissions are proportional to the fuel sulfur content (Taback et al. 1976), limiting the fuel sulfur content reduces fine particle emissions.
2. Low fuel ash content. Fuel oils generally have an ash content of less than 1% (Amero, 1973; Walsh and Shaffer, 1973).
3. Ease of process control. Opacity and particle mass concentration can generally be controlled by varying the fuel-to-air ratio, boiler load, stack temperature, or fuel atomization pressure (Monroe, 1973; Walsh and Danielson, 1973; Babcock and Wilcox Co., 1978). These variables are easily controlled with oil-firing of utility boilers.

Even a smaller fraction of the industrial, and commercial boilers have fine particle control devices (Minicucci et al. 1980).

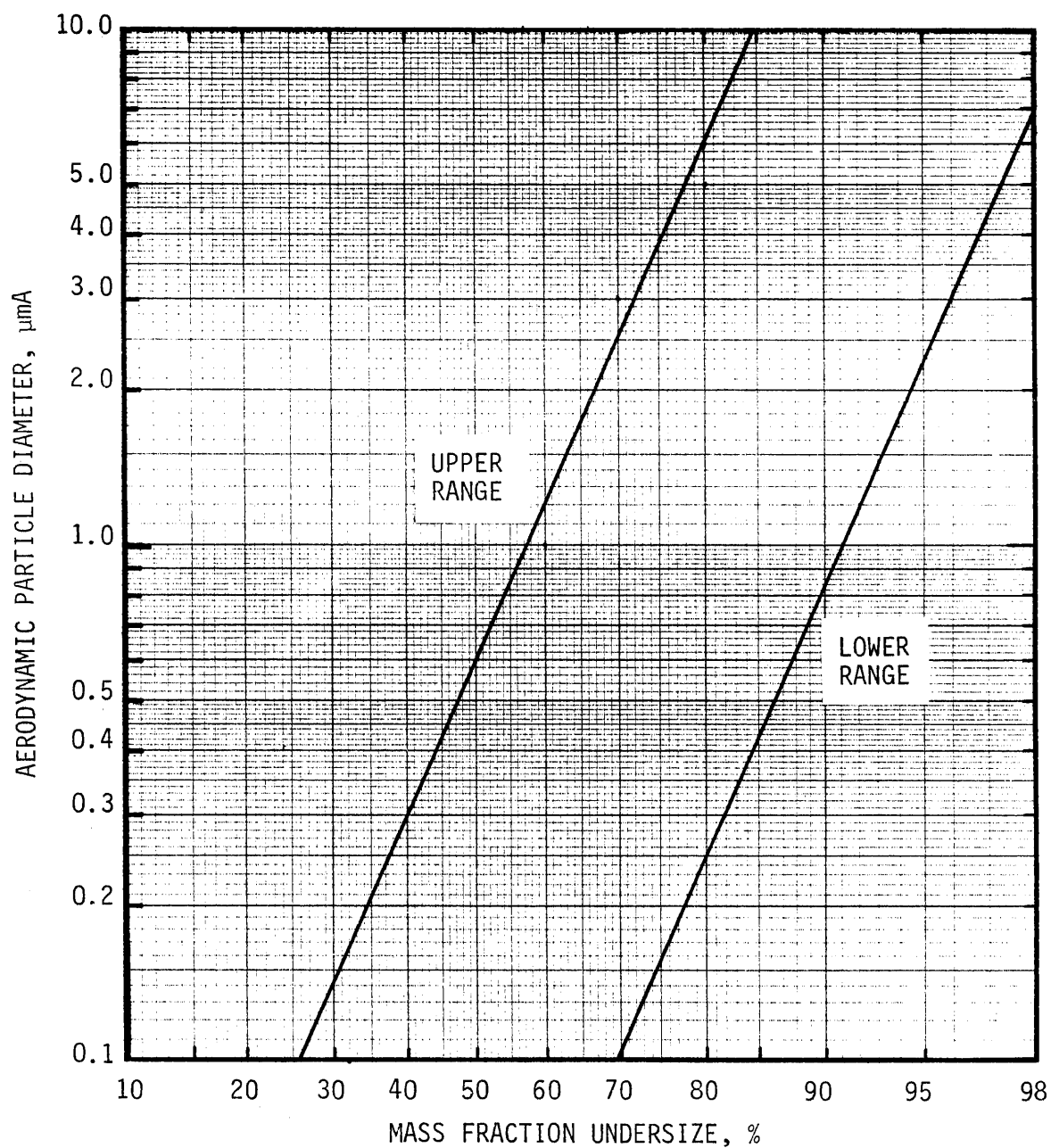


Figure 8.2.2-1. Particle size distribution for the flue gas of uncontrolled residual oil-fired utility boilers (Taback et al., 1979).

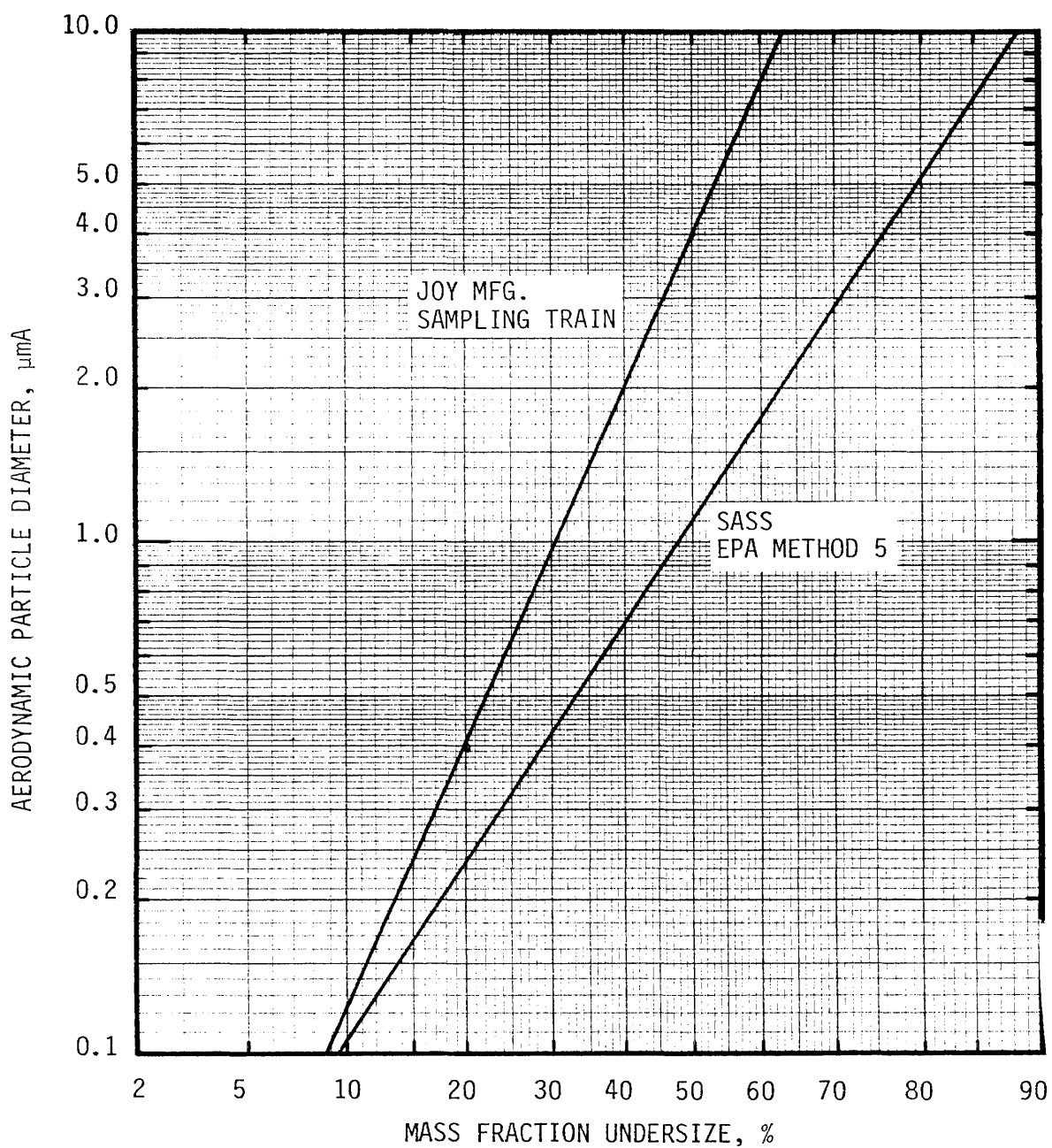


Figure 8.2.2-2. Particle size distributions for the flue gas of an uncontrolled residual oil-fired industrial boiler (Taback et al., 1979).

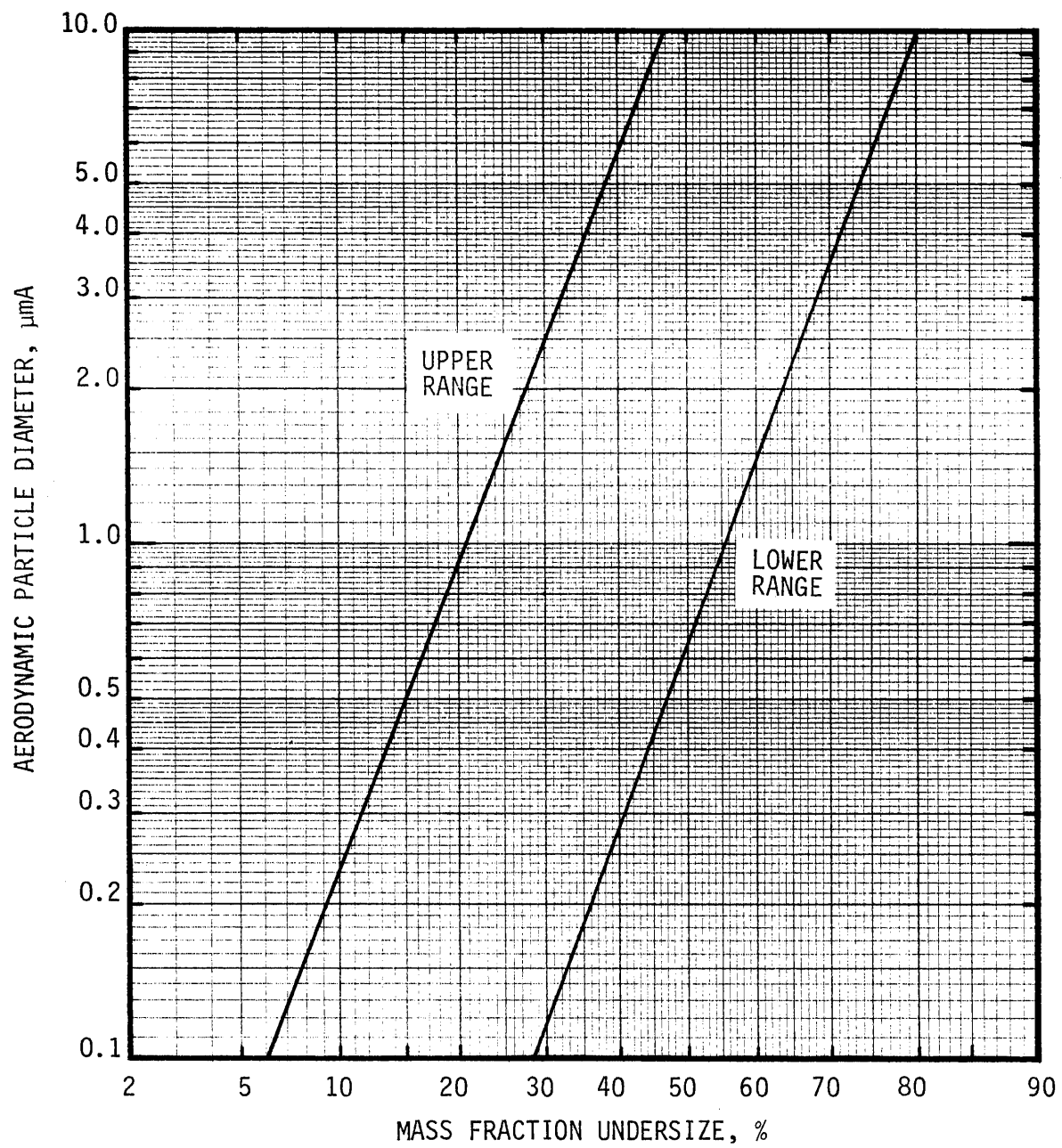


Figure 8.2.2-3. Particle size distribution for the flue gas from crude-oil fired package boilers (Taback et al., 1979).

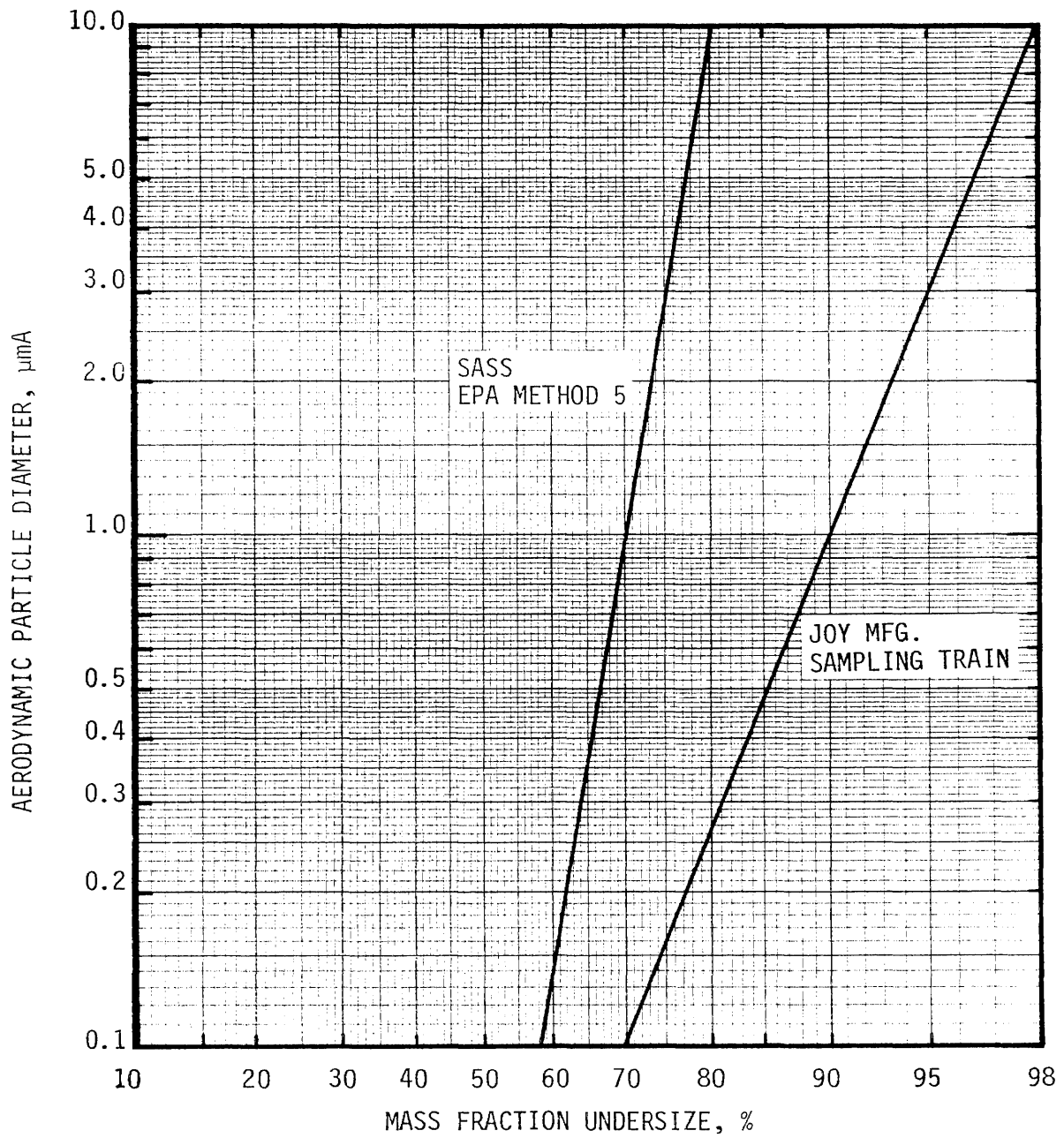


Figure 8.2.2-4. Particle size distributions for the flue gas of a distillate fuel-oil fired industrial boiler (Taback et al., 1979).

TABLE 8.2.2-1. PARTICLE CHARACTERISTICS FOR OIL-FIRED BOILERS

Process	Mass Concentration, mg/Nm ³				Particle Density g/cm ³	Particle Resistivity ohm-cm
	Uncontrolled		Controlled			
	Total	<3 μm	Total	<3 μm		
Residual Fuel Oil; Field Erected Boilers	10 ^a -130 ^b 300-400 ^c *	7-120 ^{a,b}	-	-	2 ^b -2.5 ^c	-
Residual Fuel Oil; Package Boilers	30-1,000 ^{a,c,d}	20-700 ^a	-	-	-	-
Crude Oil; Package Boilers	200-400 ^{a,e}	80-240 ^a	~200 ^e	-	-	-
Distillate Fuel Oil; Package Boilers	20-25 ^a	14-23 ^a	-	-	-	-

6-8

^aTaback et al. (1979)

^bFPEIS, Test Series No. 17, 1975

^cVandegrift et al. (1970)

^dFPEIS, Test Series Nos. 14, 59, 60, 61, 62

^eTaback et al. (1980)

*Soot blowing

TABLE 8.2.2.-2. PARTICLE CHEMICAL COMPOSITION FOR OIL-FIRED BOILER FLUE GAS^a

Composition, Wt. %

<u>Component</u>	<u>Residual Oil Field Erected Boilers</u>	<u>Oil Package Boilers</u>	<u>Crude Oil Package Boiler</u>	<u>Distillate Oil Package Boiler</u>
Ca	10	1		
Fe		1	3	
Ni	5	1		
S (as Sulfate)	28	30	44	25
C	22	40	23	15
N (as Nitrate)				4
Other (O ₂ , Si, Mg, Al, Na)	33	27	30	56

^aTaback et al. (1979)

TABLE 8.2.2-3. GAS CHARACTERISTICS FOR OIL-FIRED BOILERS

<u>Process</u>	<u>Production Rate</u>	<u>Gas Flowrate Nm³/kg (unless otherwise noted)</u>	<u>Temperature °C</u>	<u>Chemical Composition, % vol, dry (unless otherwise noted)</u>
Residual Fuel Oil Field-Erected Boilers	3-28 ^{a*} kg/s (10-100 MT/hr) (50-500 MW _e)	10-25 ^b	100 ^b -150 ^a	CO ₂ 6-15 ^{b*} O ₂ 1-13 N ₂ Balance, dry SO ₂ 120-2,200 ppmv SO ₃ 2-75 ppmv NO _x 15-900 ppmv H ₂ O 7-10 (Wet basis)
Residual Fuel Oil Package Boilers	6x10 ⁻⁴ -3 ^{a*} kg/s (2.5-12,000 ℓ/hr) (0.1-500 GJ/hr)	9-32 ^{b,c}	120-380 ^b	CO ₂ 3-12 ^{b,c*} O ₂ 5-16 ^{b,c} CO 1,000-20,000 ^b ppmv NO _x 20-400ppmv N ₂ Balance, dry H ₂ O 3-13(Wet basis)
Crude Oil Package Boilers	0.35-0.4 ^{d*} kg/s (1,300-1,500 ^{d*} ℓ/hr) (4.5 m ³ product/m ³ fuel) (53 GJ/hr)	13-15 ^d	200-320 ^d	CO ₂ 12-13 ^d O ₂ 2.5-5 SO ₂ ~500ppmv NO 1,000ppmv N ₂ Balance, dry H ₂ O 8.5-9.5(Wet basis)

TABLE 8.2.2-3. GAS CHARACTERISTICS FOR OIL-FIRED BOILERS (cont.)

<u>Process</u>	<u>Production Rate^a</u>	<u>Gas Flowrate Nm³/kg (unless otherwise noted)</u>	<u>Temperature °C</u>	<u>Chemical Composition, % vol, dry (unless otherwise noted)</u>
Distillate Fuel Oil; Package Boilers	5x10 ⁻⁴ -0.25 kg/s (2.5-1,200 ℓ/hr) (0.1-50 GJ/hr)	7.5-11 ^{a,c}	200-300 ^{a,e}	CO ₂ 9-12 ^{e*} O ₂ 2-9 SO ₂ 100-200ppmv N ₂ Balance, dry H ₂ O 8-12(Wet basis)

^aAuthor (BLH) estimate

^bVandegrift et al. (1970)

^cFPEIS, Test Series Nos. 14, 59, 60, 61,
62, 67, 170

^dTaback et al. (1980)

^eTaback et al. (1979)

*Entries in this column are from the same reference unless otherwise noted.

At present less than half of the steam generators used for Thermally Enhanced Oil Recovery (TEOR) in California are equipped with sulfur dioxide scrubbing devices (Nimelstein, 1980; Patkar and Kothari, 1980). TEOR scrubbers generally use gaseous caustic soda (sodium hydroxide) as an absorbent. Few data are available on the particle emissions from these scrubbers. Taback (1980) reports overall particle collection efficiencies of 40% for a TEOR scrubber.

8.3 COAL FUEL

The combustion of coal is a major source of fine particles throughout the U.S. (Shannon et al., 1971). Most utilities in California presently use low sulfur fuel oil or residual oil. Within the next five years, California utilities may start switching to burning low to medium sulfur coal in their boilers (Minicucci et al., 1980). Therefore, fine particle emission data and control technology for coal combustion are included in this report.

8.3.1 Process Description

The process steps for coal combustion are the same as for oil combustion (see Section 8.2), but the methods for carrying them out are different. The common methods of fuel preparation are as follows (Babcock and Wilcox Co., 1978):

1. Mechanical stoking.
2. Coarse grinding, tangential firing with air in external cyclone furnaces.
3. Fine grinding (pulverization) and pneumatic conveying into the boiler with the primary combustion air.

The last type is the most commonly used (Vandegrift et al., 1970), and will be the only one characterized below.

8.3.2 Source Characteristics

Coal-fired boilers may have burners which are horizontally opposed, wall-fired, or corner-fired (see section 8.2.1). The differences in the emissions characteristics of these firing methods is within the confidence limits of the data presented in Figure 8.3.2-1 and Tables 8.3.2-1, 8.3.2-2 and 8.3.2-3. Therefore, no distinction is made between the burner arrangements.

8.3.3 Control Technology

Many strategies are used for the control of particulate emissions from coal-fired utility boilers. They include (Vandegrift, et al., 1970):

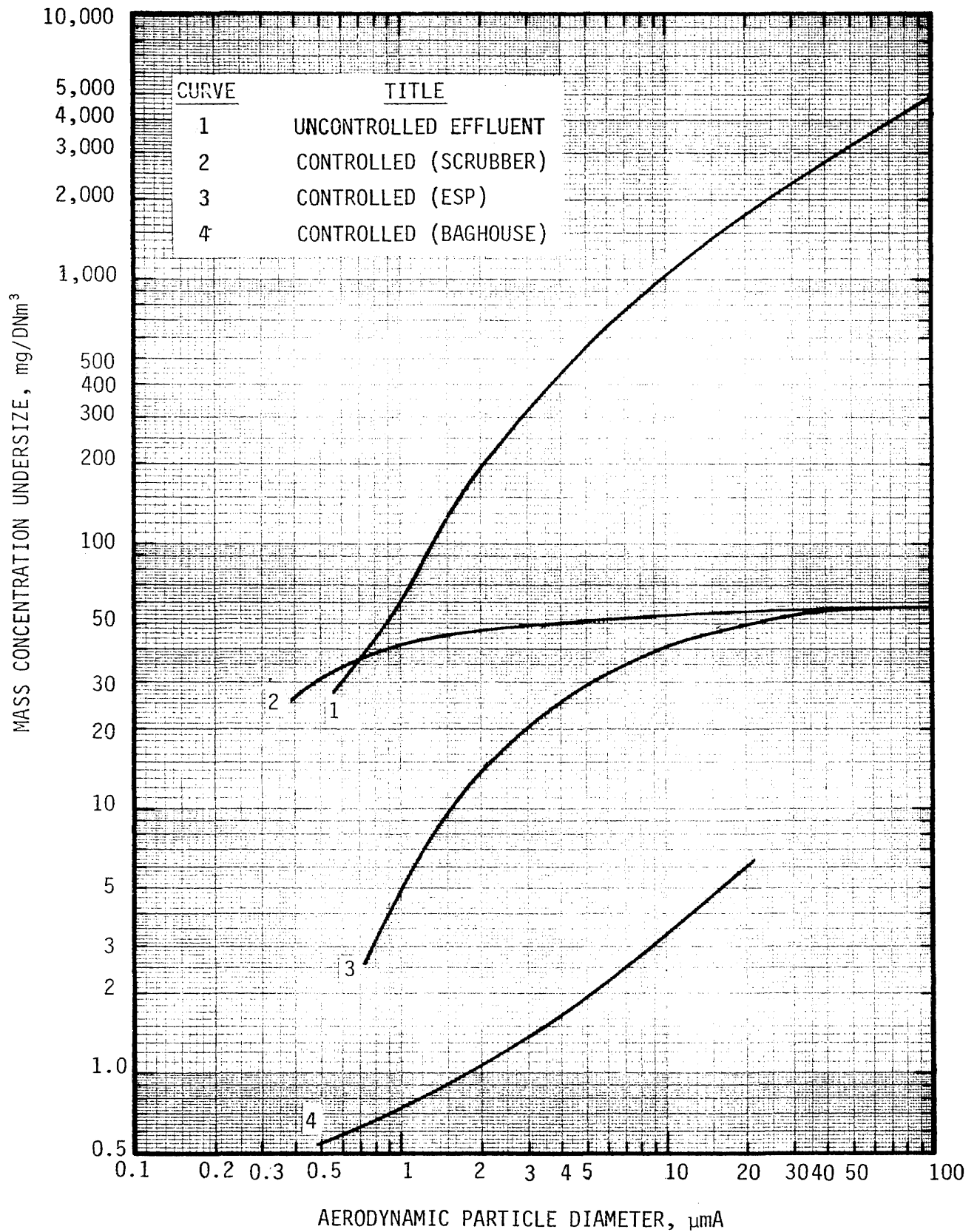


Figure 8.3.2-1. Typical particle size distributions for the flue gas from controlled and uncontrolled coal-fired utility boilers (FPEIS Test Series No. 81, 1976; Test Series No. 56, 1977; Test Series No. 35, 1975).

TABLE 8.3.2-1. PARTICLE CHARACTERISTICS FOR COAL-FIRED BOILERS

Process	Mass Concentration, mg/Nm ³				Particle Density g/cm ³	Particle Resistivity ohm-cm
	Uncontrolled		Controlled			
	Total	<3 μm	Total	<3 μm		
Coal Fuel Field-Erected Boilers	1,000- ^{a,b,c,d} 20,000	~300 ^{b,c,d}	100-500 ^{a,b,c,d}	Scrubber ~50 ^b ESP ~20 ^c Filter ~2 ^d	2-3 ^{a,b,c,d}	10 ¹⁰ -10 ¹² ^b

^aVandegrift et al. (1970)

^bFPEIS, Test Series Nos. 25, 69, 89, 115, 119-122, 125, 128, 131-133, 189: Selected Runs

^cFPEIS, Test Series Nos. 15, 16, 50, 51, 56, 57, 68, 116, 130, 171: Selected Runs

^dFPEIS, Test Series Nos. 11, 35, 71: Selected Runs

TABLE 8.3.2-2.

PARTICLE CHEMICAL COMPOSITION FOR COAL-FIRED
UTILITY BBOILER FLUE GAS^a

<u>Component</u>	<u>Composition, Wt. %</u>
SiO ₂	17 - 64
Fe ₂ O ₃	2 - 36
Al ₂ O ₃	9 - 58
CaO	0.1 - 22
MgO	0.1 - 5
Na ₂ O	0.3 - 4

^aVandegrift et al. (1970)

TABLE 8.3.2-3. GAS CHARACTERISTICS FOR COAL-FIRED BOILERS

<u>Process</u>	<u>Production Rate</u>	<u>Gas Flowrate Nm³/kg (unless otherwise noted)</u>	<u>Temperature °C</u>	<u>Chemical Composition,^{b*} % vol, dry (unless otherwise noted)</u>
Coal Fuel Field-Erected Boilers	10-110 ^a kg/s (40-400 MT/hr) (100-1,000 MW _e)	10-13 ^b	120-200 ^b	CO ₂ 12.5-12.6 O ₂ 6.2-6.2 CO 13-17ppmv NO _x 160-220ppmv SO ₂ 200-1,500 ^a ppmv SO ₃ 10 ^a -70 ^b ppmv N ₂ Balance, dry H ₂ O 6 ^b -10 ^a

^aAuthor (BLH) estimate

^bVandegrift et al. (1970)

*All entries below are from the same reference unless otherwise noted.

1. Fuel Beneficiation
2. Electrostatic Precipitation
3. Fabric Filtration
4. Wet Scrubbing
5. Cyclones

Fuel beneficiation (coal washing) is usually done at the mine site. Processes such as physical washing, solvent extraction, and heavy media separation can reduce the coal ash content by 30-50% (Minicucci et al., 1980).

Electrostatic precipitators are widely used on coal-fired boilers (Oglesby and Nichols, 1970). ESP's have generally proved reliable, long-lived, economical, and effective. Typical efficiencies are greater than 99%.

Fabric filtration of coal-fired boilers fly ash is widely practiced, efficient, and reliable. Collection efficiencies greater than 99% have been reported.

Wet scrubbers are being installed more frequently today because they may be used for the removal of both sulfur oxides and particles from flue gases. Many such installations exist, but their reliability and efficiency records have been mixed (Smith et al., 1979). Minicucci et al. (1980) reported that Venturi scrubbers generally have a particle removal efficiency of greater than 98% and have high reliability. Mobile bed scrubbers and spray towers have lower efficiencies (>95%) and poorer reliability records.

Cyclones are generally not effective on smaller particles (see Section 7). The use of cyclones alone is infrequent.

8.4 CALCULATIONS

A list of the performance calculations for fuel combustion sources is shown in Table 8.4-1. The calculation results are summarized in Table 8.4-2 through 8.4-6. A duty factor of 0.7 was used in estimating the operating costs.

The calculations for oil fuel were based on the upper range particle size distributions because the particle control device cannot achieve the minimum 50% collection for particles smaller than 3 μm diameter when the lower range particle size distributions were used. Calculations for coal-fired utility boilers were based on the uncontrolled effluent. The particle resistivity was assumed to be 1×10^9 Ohm-m when it is controlled with an ESP and to be 5×10^9 Ohm-m when it is controlled with a pulse charging ESP.

The particle diameter of the emission from oil burning sources is small and the particle concentration is low. High energy is needed to attain the required efficiency. For some conventional devices, such as the Venturi scrubber, efficiency higher than 50% cannot be attained no matter how high the scrubber pressure drop is.

TABLE 8.4-1. LIST OF PERFORMANCE CALCULATIONS

EMISSION SOURCE	CONTROL DEVICE								
	ESP	ESP with SoRI Precharger	Pulse Charging ESP	Filter	Electrified Filter	Calvert Collision Scrubber	Venturi	Charged Particles/ Charged Spray Scrubber	F/C Scrubber
Residual Oil-fired Utility Boiler	x	x		x	x	x	x	x	
Residual Oil-fired Industrial Boiler	x	x		x	x	x	x	x	
Crude Oil-fired Package Boiler	x	x		x	x	x	x	x	
Distillate Oil-Fired Industrial Boiler	x	x		x	x	x	x	x	
Coal-fired Utility Boiler	x	x	x	x	x	x	x	x	

TABLE 8.4-2

CONTROL TECHNOLOGY FOR STATIONARY SOURCES OF AIR POLLUTION

INDUSTRY:

SECTION:

PROCESS	EMISSION SOURCE	PL CONTROL TECHNOLOGY	CAPITAL, OPERATING, ANNUALIZED COSTS, \$	EFFY (%)	REL (%)	ENERGY USE	ENVIR IMPACT	REMARKS	REF
Oil- combustion	Residual oil- fired boiler	PM Scrubber Calvert Collision Scrubber	6,440/m ³ /s	81.5		2	4.0kW/m ³ /s	E=75% for d _{pa} < 3 μm at a scrubber pres- sure drop of 15cm W.C.	
			5,270/m ³ /s						
			6,320/m ³ /s						
Oil combustion	Residual oil- fired boiler	PM Scrubber Venturi	80,670/m ³ /s	63.5		1	60kW/m ³ /s	E=75% for d _{pa} < 3 μm at a pressure drop of 350 W.C.	
			39,631/m ³ /s						
			52,760/m ³ /s						
Oil combustion	Residual oil- fired boiler	PM Filter Electrostatically augmented filter		95.1		4		E=93.2% for d _{pa} < 3 μm at full ESP power	
Oil combustion	Residual oil- fired boiler	PM Scrubber CP/CD spray scrubber		99.6		5		E=99.5% for d _{pa} < 3 μm 3-stage scrubber with L/G=4x10 ⁻³ m ³ /m ³ per stage.	

TABLE 8.4-2

CONTROL TECHNOLOGY FOR STATIONARY SOURCES OF AIR POLLUTION

INDUSTRY: Utility

SECTION:

PROCESS	EMISSION SOURCE	PL CONTROL	TECHNOLOGY	CAPITAL, OPERATING, ANNUALIZED		EFFY REL (%)	REL (%)	ENERGY S USE	ENVIR IMPACT	REMARKS	REF
				COSTS, \$							
Oil combustion	Residual oil-fired boiler	PM	Filter	18,700/m ³ /s	93.9	1	8kW/m ³ /s	E=91.5% for d _{pa} < 3μA. Air/cloth = 0.93m/min.			
				4,497/m ³ /s							
				6,694/m ³ /s							
Oil combustion	Residual oil-fired boiler	PM	Filter	13,024/m ³ /s	67.7	1	8kW/m ³ /s	E=55.5% for d _{pa} < 3μA. Air/cloth = 3.1 m/min.			
				3,986/m ³ /s							
				5,516/m ³ /s							
Oil combustion	Residual oil-fired boiler	PM	ESP	7,341/m ³ /s	58.0	1	1.9kW/m ³ /s	E=50% for d _{pa} < 3μA. Corona power = 25w/m ³ /s. SCA = 25m ² /m ³ /s.			
				1,255/m ³ /s							
				2,118/m ³ /s							
Oil combustion	Residual oil-fired boiler	PM	ESP	7,342/m ³ /s	80.0	1	2.2kW/m ³ /s	E=75% for d _{pa} <3μA. Corona power = 128W/m ³ /s SCA = 25m ² /m ³ /s.			
				1,370/m ³ /s							
				2,232/m ³ /s							

8-21

TABLE 8.4-2

CONTROL TECHNOLOGY FOR STATIONARY SOURCES OF AIR POLLUTION

INDUSTRY: Utility

SECTION:

PROCESS	EMISSION SOURCE	PL	CONTROL TECHNOLOGY	CAPITAL, OPERATING, ANNUALIZED		EFFY REL (%)	ENERGY USE	ENVIR IMPACT	REMARKS	REF
				COSTS, \$						
Oil combustion	Residual oil-fired boiler	PM	ESP	12,259/m ³ /s	92.0	1	2.5kW/m ³ /s		E=90% for d _{pa} <3μmA. Corona power = 197W/m ³ /s. SCA = 50m ² /m ³ /s.	
				1,700/m ³ /s						
				3,140/m ³ /s						
Oil combustion	Residual oil-fired boiler	PM	ESP ESP w/SoRI precharger		78.0	4			E=75% for d _{pa} <3μmA. Corona power=30.5W/m ³ /s SCA = 25m ² /m ³ /s. Precharger power = 14.9W/m ³ /s	
Oil combustion	Residual oil-fired boiler	PM	ESP ESP w/SoRI precharger		91.5	4			E=90% for d _{pa} <3μmA. Corona power=219W/m ³ /s SCA = 25m ² /m ³ /s. Precharger power = 84W/m ³ /s	

8-22

TABLE 8.4-3

CONTROL TECHNOLOGY FOR STATIONARY SOURCES OF AIR POLLUTION

INDUSTRY: Any Industry

SECTION:

PROCESS	EMISSION SOURCE	PL	CONTROL TECHNOLOGY	CAPITAL, OPERATING, ANNUALIZED		EFFY REL (%)	ENERGY S USE	ENVIR IMPACT	REMARKS	REF
				COSTS, \$						
Oil combustion	Residual oil-fired industrial boiler	PM	Scrubber	7,208/m ³ /s	88.5	2	3.5kW/m ³ /s	E=75% for d _{pa} <3μm at scrubber pressure drop of 12 cm W.C. Efficiency higher than 90% cannot be attained.		
			Calvert	7,280/m ³ /s						
			Collision Scrubber	8,454/m ³ /s						
Oil combustion	Residual oil-fired industrial boiler	PM	Scrubber	18,430/m ³ /s	77.0	1	9.6kW/m ³ /s	E=50% for d _{pa} <3μm at Δp=53 cm W.C. Efficiency higher than 75% cannot be attained.		
			Venturi	10,059/m ³ /s						
				13,059/m ³ /s						
Oil combustion	Residual oil-fired industrial boiler	PM	Filter		98.5	4		E=96.7% for d _{pa} <3μm at full ESP power.		
Oil combustion	Residual oil-fired industrial boiler	PM	Scrubber		99.7	5		E=99.4% for d _{pa} <3μm. 3-stage scrubber with L/G=4 x 10 ⁻⁴ m ³ /m ³ per stage.		
			CP/CD Spray Scrubber							

8-23

TABLE 8.4-3

CONTROL TECHNOLOGY FOR STATIONARY SOURCES OF AIR POLLUTION

INDUSTRY: Any Industry

SECTION:

PROCESS	EMISSION SOURCE	PL	CONTROL TECHNOLOGY	CAPITAL, OPERATING, ANNUALIZED		EFFY REL (%)	ENERGY S USE	ENVIR IMPACT	REMARKS	REF
				COSTS, \$						
Oil combustion	Residual oil-fired industrial boiler	PM	Filter	26,494/m ³ /s	97.8	1	9.6kW/m ³ /s	E=95.7% for d _{pa} < 3μm. Air/cloth = 0.93 m/min.		
				7,519/m ³ /s						
				10,632/m ³ /s						
Oil combustion	Residual oil-fired industrial boiler	PM	Filter	17,648/m ³ /s	86.1	1	8.4kW/m ³ /s	E=70.8% for d _{pa} < 3μm. Air/cloth = 3.1 m/min.		
				6,406/m ³ /s						
				8,479/m ³ /s						
Oil combustion	Residual oil-fired industrial boiler	PM	Filter	19,584/m ³ /s	79.5	1	11,0kW/m ³ /s	E=56.8% for d _{pa} < 3μm. Air/cloth = 5.5 m/min.		
				7,402/m ³ /s						
				9,703/m ³ /s						
Oil combustion	Residual oil-fired industrial boiler	PM	ESP	16,482/m ³ /s	64.0	1	2.2kW/m ³ /s	E=50% for d _{pa} < 3μm. Corona power = 6.6w/m ³ /s. SCA = 50m ² /m ³ /s.		
				2,934/m ³ /s						
				4,870/m ³ /s						

8-24

CONTROL TECHNOLOGY FOR STATIONARY SOURCES OF AIR POLLUTION

INDUSTRY: Any Industry

SECTION:

PROCESS	EMISSION SOURCE	PL	CONTROL TECHNOLOGY	CAPITAL, OPERATING, ANNUALIZED		EFFY REL (%)	ENERGY S USE	ENVIR IMPACT	REMARKS	REF
				COSTS, \$						
Oil combustion	Residual oil-fired industrial boiler	PM	ESP	16,482/m ³ /s	83.0	1	2.3kW/m ³ /s	E=75% for d _{pa} <3μmA. Corona power = 49.8W/m ³ /s. SCA = 50m ² /m ³ /s.		
				3,005/m ³ /s						
				4,941/m ³ /s						
Oil combustion	Residual oil-fired industrial boiler	PM	ESP	16,482/m ³ /s	94.4	1	3.0kW/m ³ /s	E=90% for d _{pa} <3μmA. Corona power = 292W/m ³ /s SCA = 50m ² /m ³ /s.		
				3,292/m ³ /s						
				5,228/m ³ /s						
Oil combustion	Residual oil-fired industrial boiler	PM	ESP ESP w/SoRI Precharger		85.0	4		E=75% for d _{pa} <3μmA. Corona power=10.2W/m ³ /s. SCA = 25m ² /m ³ /s. Precharger power = 84W/m ³ /s		
Oil combustion	Residual oil-fired industrial boiler	PM	ESP ESP w/SoRI Precharger		94.4	4		E=90% for d _{pa} <3μmA. Corona power=10.9W/m ³ /s. SCA = 50m ² /m ³ /s. Precharger power = 84W/m ³ /s.		

8-25

CONTROL TECHNOLOGY FOR STATIONARY SOURCES OF AIR POLLUTION

INDUSTRY: Any Industry

SECTION:

PROCESS	EMISSION SOURCE	PL	CONTROL TECHNOLOGY	CAPITAL, OPERATING, ANNUALIZED		EFFY (%)	REL (%)	ENERGY S USE	ENVIR IMPACT	REMARKS	REF
				COSTS, \$							
Oil combustion	Crude-oil fired package boiler	PM	Scrubber Calvert Collision Scrubber			88.5		2		E=75% for $d_{pa} < 3\mu\text{m}$ A at a scrubber pressure drop of 12 cm W.C.	
Oil combustion	Crude-oil fired package boiler	PM	Scrubber Venturi	29,950/m ³ /s		83.5		1	10.8kW/m ³ /s	E=50% for $d_{pa} < 3\mu\text{m}$ A at a scrubber pressure drop of 60 cm W.C.	
				29,654/m ³ /s							
				34,528/m ³ /s							
Oil combustion	Crude-oil fired package boiler	PM	Filter Electrostatically Augmented Filter			98.5		4		E=96.6% for $d_{pa} < 3\mu\text{m}$ A at full ESP power.	
Oil combustion	Crude-oil fired package boiler	PM	Scrubber Charged Particle/Charged Drop Spray Scrubber			99.8		5		E=99.4% for $d_{pa} < 3\mu\text{m}$ A. 3-stage with L/G = $4 \times 10^{-4} \text{m}^3/\text{m}^3$ per stage.	

8-26

CONTROL TECHNOLOGY FOR STATIONARY SOURCES OF AIR POLLUTION

INDUSTRY: Any Industry

SECTION:

PROCESS	EMISSION SOURCE	PL	CONTROL TECHNOLOGY	CAPITAL, OPERATING, ANNUALIZED		EFFY REL (%)	ENERGY USE	ENVIR IMPACT	REMARKS	REF
				COSTS, \$	(%)					
Oil combustion	Crude-oil fired package boiler	PM	Filter	52,025/m ³ /s	98.2	1	9.6kW/m ³ /s		E=95.7% for d _{pa} < 3μm. Air/cloth = 0.93 m/min.	
				19,587/m ³ /s						
				25,698/m ³ /s						
Oil combustion	Crude-oil fired package boiler	PM	Filter	40,878/m ³ /s	90.3	1	8.4kW/m ³ /s		E=71.1% for d _{pa} < 3μm. Air/cloth = 3.1 m/min.	
				18,381/m ³ /s						
				23,183/m ³ /s						
Oil combustion	Crude-oil fired package boiler	PM	Filter	42,384/m ³ /s	85.7	1	11.0kW/m ³ /s		E=57.4% for d _{pa} < 3μm. Air/cloth = 5.5 m/min.	
				19,361/m ³ /s						
				24,339/m ³ /s						
Oil combustion	Crude-oil fired package boiler	PM	ESP	16,372/m ³ /s	70.0	1	2.0kW/m ³ /s		E=50% for d _{pa} <3μm. Corona power = 29.5W/m ³ /s. SCA = 25m ² /m ³ /s.	
				9,622/m ³ /s						
				11,545/m ³ /s						

8-27

CONTROL TECHNOLOGY FOR STATIONARY SOURCES OF AIR POLLUTION

INDUSTRY: Any Industry

SECTION:

PROCESS	EMISSION SOURCE	PL	CONTROL TECHNOLOGY	CAPITAL, OPERATING, ANNUALIZED		EFFY (%)	REL (%)	ENERGY USE \$	ENVIR IMPACT	REMARKS	REF
				COSTS, \$							
Oil combustion	Crude-oil fired package boiler	PM	ESP	22,956/m ³ /s	86.0	1	2.3kW/m ³ /s	E=75% for d _{pa} <3μm. Corona power = 50W/m ³ /s. SCA = 50m ² /m ³ /s.			
				10,017/m ³ /s							
				12,714/m ³ /s							
Oil combustion	Crude-oil fired package boiler	PM	ESP	22,956/m ³ /s	95.0	1	3.0kW/m ³ /s	E=90% for d _{pa} <3μm. Corona power = 292W/m ³ /s. SCA = 50m ² /m ³ /s.			
				10,311/m ³ /s							
				13,007/m ³ /s							
Oil combustion	Crude-oil fired package boiler	PM	ESP ESP w/SoRI Precharger		86.0	4		E=75% for d _{pa} <3μm. Corona power=5.4W/m ³ /s. SCA = 50m ² /m ³ /s. Precharger power = 14.9W/m ³ /s.			
Oil combustion	Crude-oil fired package boiler	PM	ESP ESP w/SoRI Precharger		94.6	4		E=90% for d _{pa} <3μm. Corona power=52W/m ³ /s. SCA = 50m ² /m ³ /s. Precharger power = 14.9W/m ³ /s.			

8-28

TABLE 8.4-5

CONTROL TECHNOLOGY FOR STATIONARY SOURCES OF AIR POLLUTION

INDUSTRY: Any Industry

SECTION:

PROCESS	EMISSION SOURCE	PL	CONTROL TECHNOLOGY	CAPITAL, OPERATING, ANNUALIZED		EFFY REL (%)	ENERGY USE	ENVIR IMPACT	REMARKS	REF
				COSTS, \$	(%)					
Oil combustion	Distillate oil-fired industrial boiler	PM	Filter Electro-statically Augmented Filter		77.7	4			E=76.6% for $d_{pa} < 3\mu\text{m}$ at full ESP power.	
Oil combustion	Distillate oil-fired industrial boiler	PM	Scrubber CP/CD Spray Scrubber		99.9	5			E=99.8% for $d_{pa} < 3\mu\text{m}$. 3-stage scrubber with L/G = $4 \times 10^{-4} \text{m}^3/\text{m}^3$ per stage.	
Oil combustion	Distillate oil-fired industrial boiler	PM	Filter	73,225/m ³ /s 38,060/m ³ /s 46,661/m ³ /s	68.8	1	9.6kW/m ³ /s		E=58.6% for $d_{pa} < 3\mu\text{m}$. Air/cloth = 0.93 m/min.	
Oil combustion	Distillate oil-fired industrial boiler	PM	ESP	39,180/m ³ /s 21,351/m ³ /s 25,954/m ³ /s	90.0	1	2.4kW/m ³ /s		E=90% for $d_{pa} < 3\mu\text{m}$. Corona power = 24W/m ³ /s. SCA = 75m ² /m ³ /s.	

8-29

CONTROL TECHNOLOGY FOR STATIONARY SOURCES OF AIR POLLUTION

INDUSTRY: Any Industry

SECTION:

8-30

PROCESS	EMISSION SOURCE	PL	CONTROL TECHNOLOGY	CAPITAL, OPERATING, ANNUALIZED COSTS, \$	EFFY REL (%)	ENERGY S USE	ENVIR IMPACT	REMARKS	REF
Oil combustion	Distillate oil-fired industrial boiler	PM	ESP	39,180/m ³ /s 21,328/m ³ /s 25,930/m ³ /s	75.0	1	2.4kW/m ³ /s	E=75% for d _{pa} <3μm. Corona power = 4.6W/m ³ /s. SCA = 75m ² /m ³ /s.	
Oil combustion	Distillate oil-fired industrial boiler	PM	ESP	39,180/m ³ /s 21,323/m ³ /s 25,925/m ³ /s	50.0	1	2.4kW/m ³ /s	E=50% for d _{pa} <3μm. Corona power = 1.4W/m ³ /s. SCA = 75m ² /m ³ /s.	
Oil combustion	Distillate oil-fired industrial boiler	PM	ESP ESP w/SoRI Precharger		80.0	4		E=75% for d _{pa} <3μm. Corona power=6.8W/m ³ /s. SCA = 25m ² /m ³ /s. Precharger power = 14.9W/m ³ /s.	
Oil combustion	Distillate oil-fired industrial boiler	PM	ESP ESP w/SoRI Precharger		92.0	4		E=90% for d _{pa} <3μm. Corona power=102W/m ³ /s. SCA = 25m ² /m ³ /s. Precharger power = 14.9W/m ³ /s.	

TABLE 8.4-6

CONTROL TECHNOLOGY FOR STATIONARY SOURCES OF AIR POLLUTION

INDUSTRY: Utility

SECTION:

PROCESS	EMISSION SOURCE	PL	CONTROL TECHNOLOGY	CAPITAL, OPERATING, ANNUALIZED		EFFY (%)	REL (%)	ENERGY S USE	ENVIR IMPACT	REMARKS	REF
				COSTS, \$							
Coal combustion	Coal-fired boiler	PM	Scrubber	8,900/m ³ /s	99.3	2	6.2kW/m ³ /s	E=90% for d _{pa} <3μmA at a scrubber pressure drop of 28 cm W.C.			
			Calvert	10,208/m ³ /s							
			Collision Scrubber	11,656/m ³ /s							
Coal combustion	Coal-fired boiler	PM	Scrubber	14,697/m ³ /s	99.3	1	9.4kW/m ³ /s	E=90% for d _{pa} <3μmA at a scrubber pressure drop of 52 cm W.C.			
			Venturi	11,211/m ³ /s							
				13,606/m ³ /s							
Coal combustion	Coal-fired boiler	PM	Filter		99.98	4		E=99.95% for d _{pa} <3μmA at full ESP power.			
			Electrostatically Augmented Filter								
Coal combustion	Coal-fired boiler	PM	Scrubber		99.96	5		E=99.3% for d _{pa} <3μmA. 3-stage with L/G = 4 X 10 ⁻⁴ m ³ /m ³ per stage.			
			CP/CD Spray Scrubber								

8-31

TABLE 8.4-6

CONTROL TECHNOLOGY FOR STATIONARY SOURCES OF AIR POLLUTION

INDUSTRY: Utility

SECTION:

PROCESS	EMISSION SOURCE	PL	CONTROL TECHNOLOGY	CAPITAL, OPERATING, ANNUALIZED		EFFY (%)	REL (%)	ENERGY S USE	ENVIR IMPACT	REMARKS	REF
				COSTS, \$							
Coal combustion	Coal-fired boiler	PM	Filter	20,439/m ³ /s	99.96	1	8.7kW/m ³ /s	E=99.93% for d _{pa} < 3μm. Air/cloth = 0.93 m/min.			
				8,745/m ³ /s							
				11,145/m ³ /s							
Coal combustion	Coal-fired boiler	PM	Filter	13,368/m ³ /s	98.1	1	8.2kW/m ³ /s	E=95.3% for d _{pa} < 3μm. Air/cloth = 3.1 m/min.			
				7,914/m ³ /s							
				9,485/m ³ /s							
Coal combustion	Coal-fired boiler	PM	Filter	15,637/m ³ /s	96.5	1	10.9kW/m ³ /s	E=89.6% for d _{pa} < 3μm. Air/cloth = 5.5 m/min.			
				9,008/m ³ /s							
				10,844/m ³ /s							
Coal combustion	Coal-fired boiler	PM	ESP	19,126/m ³ /s	98.7	1	2.5kW/m ³ /s	E=90% for d _{pa} < 3μm. Corona power = 89W/m ³ /s. SCA = 75m ² /m ³ /s.			
				5,858/m ³ /s							
				8,105/m ³ /s							

8-32

TABLE 8.4-6

CONTROL TECHNOLOGY FOR STATIONARY SOURCES OF AIR POLLUTION

INDUSTRY: Utility

SECTION:

PROCESS	EMISSION SOURCE	PL	CONTROL TECHNOLOGY	CAPITAL, OPERATING, ANNUALIZED		EFFY REL (%)	REL (%)	ENERGY ENVIR		REMARKS	REF
				COSTS, \$				S	USE IMPACT		
Coal combustion	Coal-fired boiler	PM	ESP	19,126/m ³ /s		95.0		1	2.3kW/m ³ /s	E=75% for d _{pa} < 3μm. Corona power = 14W/m ³ /s. SCA = 75m ² /m ³ /s.	
				5,632/m ³ /s							
				7,879/m ³ /s							
Coal combustion	Coal-fired boiler	PM	ESP	19,126/m ³ /s		88.5		1	2.3kW/m ³ /s	E=50% for d _{pa} < 3μm. Corona power = 3.5W/m ³ /s. SCA = 75m ² /m ³ /s.	
				5,353/m ³ /s							
				7,600/m ³ /s							
Coal combustion	Coal-fired boiler	PM	ESP Pulse Charging	14,873/m ³ /s		86.0		3	2.3kW/m ³ /s	E=50% for d _{pa} <3μm. Ash resistivity = 5x10 ⁹ Ohm-m. Corona power = 2.3W/m ³ /s. SCA = 75m ² /m ³ /s.	
Coal combustion	Coal-fired boiler	PM	ESP Pulse Charging	14,873/m ³ /s		94.6		3	2.3kW/m ³ /s	E=75% for d _{pa} <3μm. Ash resistivity = 5x10 ⁹ Ohm-m. Corona power = 9.0W/m ³ /s. SCA = 75m ² /m ³ /s.	

8-33

TABLE 8.4-6

CONTROL TECHNOLOGY FOR STATIONARY SOURCES OF AIR POLLUTION

INDUSTRY: Utility

SECTION:

PROCESS	EMISSION SOURCE	PL	CONTROL TECHNOLOGY	CAPITAL, OPERATING, ANNUALIZED	EFFY (%)	REL (%)	ENERGY ENVIR		REMARKS	REF
				COSTS, \$			S	USE		
Coal combustion	Coal-fired boiler	PM	ESP Pulse Charging	14,873/m ³ /s	98.6		3		E=90% for d _{pa} <3μmA. Ash resistivity = 5x10 ⁹ ohm-m. Corona power = 64W/m ³ /s. SCA = 75m ² /m ³ /s.	
Coal combustion	Coal-fired boiler	PM	ESP ESP w/SoRI Precharger		95.7		4		E=75% for d _{pa} <3μmA. Corona power=4.7W/m ³ /s. SCA = 50m ² /m ³ /s. Precharger power = 14.9W/m ³ /s.	
Coal combustion	Coal-fired boiler	PM	ESP ESP w/SoRI Precharger		98.5		4		E=90% for d _{pa} <3μmA. Corona power=262W/m ³ /s. SCA = 50m ² /m ³ /s. Precharger power = 14.9W/m ³ /s.	

8-34

The particles from coal-fired utility boilers are large. All devices are capable of removing 90% of the fine particles with low energy requirement. However, even with 90% removal of the fine particles, the emission is still in violation of the emission standard.

SECTION 8

REFERENCES

Amero, Robert C., 1973. Liquid Petroleum Fuels. From Section 9 of Perry's Chemical Engineer's Handbook, 5th edition, McGraw-Hill, New York, New York.

Babcock and Wilcox Co., 1978. Steam: Its Generation and Use, 35th Edition. Babcock and Wilcox Co., New York, New York.

Corey, Richard C. (1973). Combustion of Solid Fuels. In Section 9 of Perry, J. H. and Chilton, C. H., editors Chemical Engineer's Handbook, 5th Edition, McGraw-Hill, New York, New York.

FPEIS References for Coal-Fired Utility Boilers with ESP's.

Fine Particle Emission Information System (FPEIS) Series Report, Test Series No. 25, 1975, by R. E. Lee, et al., EPA/NERC RTP,NC.

FPEIS, Test Series No. 69, 1977, by S. P. Schliesser, Acurex Corp., EPA Contract 68-02-2646.

FPEIS, Test Series No. 81, 1976, by J. P. Gooch, et al., Southern Research Institute (SoRI), Report No. SoRI-EAS-76-421.

FPEIS, Test Series Nos. 89 and 126, 1977, by J. P. Gooch and G. B. Nichols, SoRI Report No. SoRI-EAS-77-098 and EPRI-RP413-1.

FPEIS, Test Series No. 115, 1974, by J. D. McCain, et al., SoRI, Report No. SoRI-EAS-74-418.

FPEIS, Test Series No. 119, 1972, by J. B. Nichols, SoRI, SoRI Internal Correspondence No. A1402-3005-IF.

FPEIS, Test Series No. 120, 1975, by J. B. Nichols and J. D. McCain, SoRI, Report No. EPA-600/2-75-056.

FPEIS, Test Series No. 121, 1972, by G. B. Nichols and J. P. Gooch, SoRI, SoRI Internal Correspondence A1364-2975.

FPEIS, Test Series Nos. 122, 125, 132, 1977 by J. P. Gooch and G. M. Marchant, SoRI Report No. SoRI-EAS-77-476 and EPRI-RP413-1.

FPEIS, Test Series Nos. 127 and 128, 1975, by E. Dismukes, SoRI, Report Nos. SoRI-EAS-75-311, EPA-600/2-75-015.

FPEIS, Test Series No. 131, 1975, by J. P. Gooch, et al., SoRI, Report No. SoRI-EAS-76-622.

FPEIS, Test Series No. 133, 1976, by J. D. McCain, SoRI, Report No. SoRI-EAS-76-355.

FPEIS, Test Series No. 189, 1975, by J. Ondov, Lawrence Livermore Laboratory.

FPEIS References for Coal-Fired Utility Boilers Controlled by Scrubbers.

FPEIS, Test Series Nos. 15 and 16, 1975, by R. M. Statnick and D. C. Drehmel, CSL/EPA-RTP,NC.

FPEIS, Test Series Nos. 50 and 51, 1974, by S. Calvert, Air Pollution Technology, Inc., Report No. EPA-650/2-74-093.

FPEIS, Test Series Nos. 56 and 57, 1977, by Bechtel Corp., EPA Contract No. 68-02-1814.

FPEIS, Test Series No. 68, 1974, by D. S. Ensor, et al., Meteorology Research, Inc., Report No. EPA-600/2-75-074.

FPEIS, Test Series No. 116, 1973, by A. N. Bird, SoRI, Report No. SoRI-EAS-73-214.

FPEIS, Test Series No. 130, 1978, by SoRI, Report No. EPA-650/7-78-094.

FPEIS, Test Series No. 172, TRW, Inc. EPA Contract No. 68-02-2613, Task No. 8.

FPEIS References for Coal-Fired Utility Boilers with Baghouses.

FPEIS, Test Series No. 11, 1973, by D. B. Harris and J. A. Turner, EPA/CSL RTP,NC. Report: "Particulate and SO₂/SO₃ Measurements Around an Anthracite Steam Generator Baghouse", CSL Report, November 8, 1973.

FPEIS, Test Series No. 35, 1975, by R. M. Bradway and R. W. Cass. Report: EPA-600/2-75-013-A.

FPEIS, Test Series No. 71, 1977, by J. W. Snyder, Monsanto Research Corp., EPA Contract 68-02-1816, Report 5.

- Minicucci, D., Herther, M., Babb, L. and Kuby W., 1979 , Acurex Corp. Assessment of Control Technology for Stationary Sources , Final Report for California Air Resources Board, Contract A7-170-30.
- Monroe, G. S., 1973, Combustion of Liquid Fuels. In Section 9 of Perry J. H., Jr. and Chilton, C. H., editors, Chemical Engineer's Handbook, 5th Edition, McGraw Hill, New York, New York.
- Nimelstein, S. A., 1980. Texaco, Inc. Production Div., Bakersfield, California. Telephone Conversation.
- Oglesby, S., Jr. and Nichols, G. B., Southern Research Institute, 1970. A Manual of Electrostatic Precipitator Technology, Vol. II for NAPCA Contract CPA-22-69-73.
- Patkar, A. N. and Kothari, S. P., 1980, PEDCo Environmental, Inc. An Evaluation of Flue Gas Desulfurization Systems for Thermally Enhanced Oil Recovery Operations in California. Talk No. 80-13.3, 73rd Annual Air Pollution Control Association Meeting, Montreal, Quebec, June 22-27, 1980.
- San Diego County Air Pollution Control District (SDAPCD), 1978. Rules and Regulations, Rule 62.
- Shannon, L. J., P. G. Gorman, M. Reichel, 1971. Particulate Pollutant System Study, Vol. II, Fine Particle Emissions, EPA/APCD Contract CPA 22-69-109.
- Smith, M., M. Melia, and M. Gregory, 1980. EPA Utility FGD Survey, October-December 1979. EPA-600/7-80-029a, U. S. Environmental Protection Agency, Research Triangle Park, North Carolina.
- South Coast (California) Air Quality Management District (SCAQMD), 1977. "Rules and Regulations", Rule 431.2.
- Taback, H. J., 1980. Determination of Air Pollutant Emission Factors for Thermal Tertiary Oil Recovery Operations in California. Final Report California Air Resources Board Contract A7-075-30.
- Taback, H. J., A. R. Brienza, J. Marko, N. Brunetz, 1979. Fine Particle Emissions from Stationary and Miscellaneous Sources in the South Coast Air Basin. California Air Resources Board Contract A6-191-30, NTIS No. PB 293 922.

Vandegrift, A. E., L. J. Shannon, E. W. Lawless, P. G. Gorman, E. E. Sallee and M. Reichel, 1970. Handbook of Emissions Effluents and Control Properties for Stationary Particulate Pollution Sources. NAPCA Contract CPA 22-69-104.

Walsh, R. T. and Danielson, J. A., 1973. Boilers, Heaters and Steam Generators. In Chapter 9 of Danielson, J. A., editor, Air Pollution Engineering Manual, 2nd Edition. AP-40, U. S. Environmental Protection Agency, Washington, D.C.

Walsh, R. T. and N. R. Shaffer, 1973. Gaseous and Liquid Fuels. In Chapter 9 of Danielson, J. A., Editor, Air Pollution Engineering Manual, 2nd Edition. AP-40, U.S. Environmental Protection Agency, Washington, D. C.

